

UNIVERSITY OF CRETE

Πανεπιστήμιο Κρήτης

SCHOOL OF MEDICINE

Ιατρική Σχολή

PhD Thesis

Διαδακτορική Διατριβή

**Ex vivo visualization of megakaryocytic endomitosis and the role of Cyclin E in this process.**

**Ex vivo ΑΠΕΙΚΟΝΙΣΗ ΤΗΣ ΕΝΔΟΜΙΤΩΤΙΚΗΣ ΔΙΑΔΙΚΑΣΙΑΣ ΤΩΝ ΜΕΓΑΚΑΡΥΟΚΥΤΤΑΡΩΝ ΚΑΙ ΔΙΕΡΕΥΝΗΣΗ ΤΟΥ ΡΟΛΟΥ ΤΗΣ ΚΥΚΛΙΝΗΣ Ε ΣΤΗΝ ΔΙΑΔΙΚΑΣΙΑ ΑΥΤΗ.**

**NIKOLAOS PAPADANTONAKIS**

B.Sc (Hons), University of Glasgow, 1999

M.D, University of Crete, 2005

M.Sc, University of Crete, 2007

Submitted in partial fulfillment of the requirements for the degree of Doctor in Philosophy in the graduate program "Cellular and Genetic Etiology, Diagnosis and Treatment of Human Disease"

25/2/2013

Members of the advising/overseeing committee.

First Reader \_\_\_\_\_

Dr Helen Papadaki, MD, Ph.D

Professor of Hematology

Second Reader \_\_\_\_\_

Dr Dimitrios Boumpas, MD, MACP

Professor of Medicine

Third Reader \_\_\_\_\_

Dr Aristeides Eliopoulos Ph.D

Associate Professor

## **Acknowledgments**

*The whole PhD thesis was conducted in the Boston University School of Medicine (BUSM) at Dr Ravid's Laboratory. Dr. Ravid is professor of Biochemistry and Medicine, Scientific Director of BUSM Transgenic Core, Director of the EVANS Center for Interdisciplinary Biomedical Research at BUSM and American Heart Association (AHA) Established Investigator. Dr. Ravid has served in the editorial board of several Hematological journals including Blood.*

*Part of data were generated in collaboration with Dr Joseph E Italiano's laboratory. Dr Italiano's laboratory is part of Translational Medicine Division, Brigham and Women's Hospital, Boston, Massachusetts and the Vascular Biology Program, Department of Surgery, Children's Hospital, Boston, Massachusetts, USA.*

*My graduation from the University of Glasgow with a B.Sc (Hons) in molecular biology offered me with the opportunity to pursue research in many different and exciting fields. However, I decided to study medicine because I always wanted to expand the knowledge I gained in cellular level to that of the whole organism.*

*After graduation from the medical school I was privileged to be granted the opportunity through the program to join Dr. Ravid's laboratory.*

*Under Dr. Ravid's guidance I was exposed into the difficult and largely unexplored field of megakaryocytes. Dr. Ravid's lab is decorated with multiple Awards and Prizes including best teaching award and for mentorship. Dr. Ravid is one of the most dedicated, charismatic enthusiastic and with never ending will to explore new aspects of megakaryocytes.*

*Through her constant encouragement and mentorship I started exploring aspects of megakaryocyte physiology and I am very excited that I uncovered some of less known roles of platelets and Megakaryocytes in the pathophysiology of myeloproliferative neoplasms.*

*Dr Ravid always finds time, despite her very busy and hectic schedule, to listen, recommend solutions but above all explain proposed strategies and offer insights. I never saw Dr Ravid discouraged by negative results or experiments that did not work. Through her example I learned that experiments have always information to give us, things to teach us.*

*Carefully planned experiments, literature research and in depth rationale for proposed strategies are the highlights of my education with Dr. Ravid. These*

*principles served me well when I rejoined the clinical discipline and I am proud of my training.*

*Training I was privileged to share with a an exceptional team. Dr Hao Nguyen was a vibrant source of positive energy especially in times of arduous cloning adventures. Donald McCrann was a valuable coworker and a great teacher Maria Makitalo was also a great source for help.*

*I would like to express my greatest gratitude to Cindy St Hilaire, Milka Koupenova, Dan Yang for creating a friendly collaborative environment that research can flourish.*

*Shannon, Hillary and Alexia were a source of inspiration, constant stimulus for scientific discussions and great companions.*

*My journey to U.S and my joining in Dr Ravid's laboratory would not be possible without the help and the vision of several established researchers from university of Crete Medical school. Dr Zannis , Dr Papadaki and Dr. Boumpas were instrumental in my introduction to research and their passion serves as my guide.*

## Dedicatory Page

*To my parents with the deepest appreciation for what they have offered me throughout my life. Especially to my father that he is not alive to see the completion of this work.*

*To Elpida K. for her love and support. To Alex S., Katerina K., Maria V., Amalia K., Stayvro M. and Konstantino D. for their friendship and support.*

# **Ex vivo visualization of megakaryocytic endomitosis and the role of Cyclin E in this process**

**NIKOLAOS PAPADANTONAKIS**

University of Crete School of Medicine, 2013

## **Abstract**

The endomitotic cell cycle in Megakaryocytes, which is comprised by repeated cycles of abrogated mitosis is an integral part of Megakaryocytic development . By utilizing a unique transgenic mouse model where GFP-histone expression is limited to megakaryocytic lineage we demonstrated that endomitosis is different between Megakaryocytes of high and low ploidy. In the low ploidy Megakaryocytes the DNA is clearly segregated into two distinct regions before it rejoins into a single nucleus. In High ploidy Megakaryocytes distinct segregation of DNA is not observed prior to DNA content rejoining into a single nucleus. Our study was the first one to describe the chromosomal dynamics of endomitosis Ex vivo using live imaging.

In order to further characterize the endomitotic process efforts to generate transgenic mice that their microtubule network could be visualized were pursued. Several transgenic lines were generated without success and a novel approach is also outlined that may overcome the problems of previous transgenic mice attempts.

In addition, based on transgenic mouse model where human Cyclin E1 overexpression is restricted in the megakaryocytic lineage we demonstrate that a higher fraction of bone marrow transgenic Megakaryocytes are in the S phase compared to wild type Megakaryocytes indicating that Cyclin E overexpression is sufficient to drive Megakaryocytes to S phase. Furthermore, a method to rapidly identify homozygotes from heterozygotes in the founder lines of transgenic mice is also described.

Polo Like Kinase 3 is a protein that is implicated in the modulation of cell cycle and we detected its expression in Megakaryocytes but experiments using Knock out mice did not reveal an impact in polyploidization.

Lysyl Oxidase propeptide (LOX-PP) is a moiety that is part of the Pre Lysyl oxidase protein and is liberated when mature Lysyl oxidase is produced. It has been shown in multiple studies to exert a powerful anti- proliferation effect in cell lines and here we describe its effect in Megakaryocytic physiology and ploidy. Namely the Lysyl Oxidase Propeptide was able to inhibit Megakaryocytic polyploidization in bone marrow cultures without affecting viability. Importantly, Megakaryocytes expressing human Cyclin E1 were not able the inhibitory effect of LOX-PP.

## Ex vivo ΑΠΕΙΚΟΝΙΣΗ ΤΗΣ ΕΝΔΟΜΙΤΩΤΙΚΗΣ ΔΙΑΔΙΚΑΣΙΑΣ ΤΩΝ ΜΕΓΑΚΑΡΥΟΚΥΤΤΑΡΩΝ ΚΑΙ ΔΙΕΡΕΥΝΗΣΗ ΤΟΥ ΡΟΛΟΥ ΤΗΣ ΚΥΚΛΙΝΗΣ Ε ΣΤΗΝ ΔΙΑΔΙΚΑΣΙΑ ΑΥΤΗ.

ΝΙΚΟΛΑΟΣ ΠΑΠΑΔΑΝΤΩΝΑΚΗΣ

ΠΑΝΕΠΙΣΤΗΜΙΟ ΚΡΗΤΗΣ, ΙΑΤΡΙΚΗ ΣΧΟΛΗ, 2013

### Περίληψη

Ο ενδομιτωτικός κύκλος των μεγακαρυοκύτταρων, ο οποίος αποτελείται από επαναλαμβανόμενους μη ολοκληρωμένους κύκλους μίτωσης αποτελεί αναπόσπαστο μέρος της μεγακαρυοκυτταρικής ανάπτυξης. Με την χρησιμοποίηση ενός μοναδικού διαγονιδιακού μοντέλου ποντικού, όπου η έκφραση της GFP-ιστόνης περιορίζεται στην μεγακαρυοκυτταρική κυτταρική σειρά αποδείξαμε ότι ενδομίτωση είναι διαφορετική μεταξύ μεγακαρυοκύτταρων υψηλής και χαμηλής πλοειδίας. Στα χαμηλής πλοειδίας μεγακαρυοκύτταρα το DNA είναι σαφώς διαχωριζόμενο σε δύο διακριτές περιοχές πριν επανασυσταθεί σε ένα ενιαίο πυρήνα. Σε υψηλής πλοειδίας μεγακαρυοκύτταρα διαχωρισμός του DNA σε διακριτές περιοχές δεν παρατηρείται πριν από την επανασύνδεση του περιεχομένου του DNA σε ένα ενιαίο πυρήνα. Η μελέτη μας ήταν ο πρώτη που περιέγραψε την δυναμική των χρωμωσωματτών κατά την διάρκεια της ενδομίτωσης Ex-vivo χρησιμοποιώντας μικροσκοπία ζώντων κυττάρων. Προκειμένου να χαρακτηριστούν περαιτέρω οι διαδικασίες σχετιζόμενες με ενδομίτωση, έγιναν προσπάθειες για δημιουργία διαγονιδιακών ποντικών των οποίων το δίκτυο των μικροσωληνίσκων τους θα μπορούσε να παρατηρηθεί. Αρκετές διαγονιδιακές σειρές παρήχθησαν χωρίς επιτυχία και μια νέα προσέγγιση περιγράφεται που θα μπορούσε να ξεπεράσει τα προβλήματα των προηγούμενων διαγονιδιακών μοντέλων. Επιπλέον, με βάση ένα διαγονιδιακό μοντέλο ποντικού όπου η υπερέκφραση ανθρώπινης κυκλίνης E1 περιορίζεται στην μεγακαρυοκυτταρική κυτταρική σειρά έχουμε αποδείξει ότι ένας υψηλότερο κλάσμα των διαγονιδιακών μεγακαρυοκυτταρων του μυελού των οστών στην S φάση σε σύγκριση με το αγρίου τύπου μεγακαρυοκύτταρα υποδεικνύοντας ότι η υπερέκφραση της κυκλίνης E είναι επαρκής για να οδηγήσει μεγακαρυοκύτταρα στην S φάση. Περαιτέρω, μια μέθοδος για τον γηγόρο εντοπισμό ομοζυγώτων από τους ετεροζυγώτες στις ιδρυτικές γραμμές (founder lines) διαγονιδιακών ποντικών περιγράφεται επίσης. Polo Like Kinase 3 είναι μια πρωτεΐνη που εμπλέκεται στη ρύθμιση του κυτταρικού κύκλου και ανιχνεύσαμε την έκφραση της σε μεγακαρυοκύτταρα, όμως πειράματα χρησιμοποιώντας Knock out ποντικά δεν αποκαλύπτουν μια επίδραση στη πολυπλοειδία. Το προπεπτιδίο της λυσυλ οξειδάσης (LOX-PP) είναι ένα πρωτεϊνικό θραύσμα μέρος της πρωτεΐνης Προ- λυσυλ οξειδάσης και απελευθερώνεται όταν η ωριμη λυσυλ οξειδάση παράγεται. Έχει αποδειχθεί σε πολλές μελέτες ότι ασκεί μια ισχυρή αντι-αυξητική δράση σε κυτταρικές σειρές και εδώ περιγράφουμε την επίδρασή του στην φυσιολογία και στην πολυπλοειδία των μεγακαρυοκυτταρων. Δηλαδή το προπεπτιδίο της λυσυλ οξειδάσης ήταν ικανό να αναστείλει μεγακαρυοκυτταρική πολυπλοειδία σε καλλιέργειες μυελού των οστών χωρίς να επηρεάζει τη βιωσιμότητα. Ένα σημαντικό εύρημα ήταν ότι μεγακαρυοκύτταρα που εκφράζουν ανθρώπινη κυκλίνη E1 δεν ήταν σε θέση να αναστείλουν το αποτέλεσμα του LOX-PP.



## Table of Contents

Members of the Ph.D Committee .....	2
Acknowledgments.....	3
Dedicatory page.....	6
Abstract.....	7
Table of contents.....	9
List of Figures .....	11
Chapter I. Introduction	
Background.....	13
Megakaryopoiesis .....	15
TPO and its effect on Megakaryopoiesis .....	16
State of Ploidy.....	17
The role of cyclins in endomitosis.....	19
The role of PLK family in polyploidization .....	22
The importance of cytoskeleton in Endomitosis.....	25
Study of Megakaryopoiesis .....	26
PF4 promoter targets expression in Megakaryocytes.....	27
Immunofluorescence and live imaging of Megakaryocytes .....	27
Transgenic mouse models visualizing endomitosis .....	30
An introduction to Lysyl Oxidase and its propeptide (LOX-PP).....	35
Chapter II. Materials and Methods	
Generation of PF4-AcGFP1-tubulin construct .....	39
Generation of PF4-AcGFP1-tubulin transgenic mouse.....	39
Mouse genomic DNA isolation .....	39
Electrolution .....	39
Generation of PF4-AcGFP1-tubulin transgenic mouse.....	40
Mouse genomic DNA isolation .....	41
Bone marrow claming and cultures.....	42
Megakaryocyte enrichment by MACS® magnetic bead purification system .....	42
Imaging of living Megakaryocytes .....	43
Real time PCR Analysis .....	44
Cell Cultures .....	45
Hoechst Staining.....	45
Generation of the PF4-3XGFP-EMTB construct.....	45
Transfection assays of PF4 3XGFP-EMTB plasmid.....	46
Generation of the PF4 3XGFP-EMTB transgenic mouse model.....	48
FACS screening of PF4 3XGFP-EMTB founders platelets .....	49
Generation of the PF4 Cyclin E mouse .....	49
Identifying homozygotes of the PF4-Cyclin E transgenic mouse model.....	50
Brdu (Bromodeoxyuridine) assay .....	50
Bone marrow treatment with LOX-PP.....	52
FACS analysis of the LOX-PP samples.....	53
LOX-PP immunofluorescence .....	54
Chapter III. Results	
Part I. Visualization of Megakaryocytic endomitosis through the PF4-H2B-GFP model.....	56
Part II. Transgenic mouse models to visualize the microtubule network .....	66
Part III. The Cyclin E transgenic mouse .....	97
Part IV. The role of PLK3 in polyploidization.....	110
Part IV. The Lysyl Oxidase Propetide in the context of megakaryopoiesis .....	119

Chapter IV. Discussion	
AIM I. Visualizing endomitosis through PF4-H2B-GFP mouse .....	131
AIM II. Transgenic mouse models to visualized microtubules.....	137
AIM III. The Cyclin E transgenic mouse .....	147
AIM IV. PLK3 and MK endomitosis .....	148
AIM V. Lysyl oxidase propetide in the context of megakaryopoiesis .....	149
Acknowledgments.....	152
References.....	153

## List of Figures

Figure 1. Hoechst staining of the PF4-H2B-GFP Megakaryocytes .....	57
Figure 2. Low ploidy Megakaryocyte undergoing endomitosis .....	59
Figure 3. A high ploidy Megakaryocyte undergoing endomitosis.....	61
Figure 4. Measurements of chromosomal dynamics during endomitosis .....	63
Figure 5. The organization of the PF4 plasmid.....	68
Figure 6. The PF4 mcherry human tubulin construct and founders testing.....	70
Figure 7 . The PF4-AcGFP1-tubulin construct.....	73
Figure 8. The generation of the PF4-pAcGFP1-tubulin transgenic mouse.....	75
Figure 9. Screening for potential founders of PF4-AcGFP1-tubulin transgenic mouse model.....	77
Figure 10. Imaging of Megakaryocytes derived from cultured bone marrow of PF4- AcGFP1-tubulin transgenic mouse model.....	79
Figure 11. Schematic representation of PF4-3XGFP-EMTB .....	81
Figure 12. Maxi prep verification of PF4 3XGFP-EMTB using HpaI and ClaI. ....	83
Figure 13. Transfection expression of PF4 3XGFP-EMTB in Y-10/L8057 cell line. ....	85
Figure 14. Treatment of transfected Y-10/L8057 reveals that 3XGFP-EMTB decorates microtubules.....	87
Figure 15. Isolation of the PF4 3XGFP-EMTB sequence for injection. ....	89
Figure 16. Transfection experiments employing the human megakaryoblastic cell line CMK.....	91
Figure 17. Example of PF4-3XGFP-EMTB founder screening. ....	93
Figure 18. Screening of PF4 3XGFP-EMTB for expression of the transgene in platelets isolated form whole blood. ....	95

Figure 19. Isolation of transgene for injection for the generation of the PF4 Cyclin E mouse.....	98
Figure 20. Titration of the isolated PF4 Cyclin E transgene for injection in male pronuclei of FVB mice.....	100
Figure 21. Identification of homozygotes based on real time PCR using tail genomic DNA as template.....	102
Figure 22 . Titration and specificity testing of Brdu assay.....	104
Figure 23. Brdu assay of transgenic and wild type to determine fraction of Megakaryocytes that are in S phase. ....	108
Figure 24. Comparison of PLK3 expression post TPO injection. ....	111
Figure 25. PLK3 is expressed in Y-10 cells and vascular smooth muscle cells. ....	113
Figure 26. Expression of PLK3 in CD41 enriched fractions of the bone marrow cultures in the presence of TPO at 12 hr and 72 hr.....	115
Figure 27. PLK3 KO ploidy profile is not significantly different of that of the wild type mice.....	117
Figure 28. The sequence and characteristics of the recombinant LOX-PP.....	120
Figure 29. LOX-PP inhibits polyploidization of murine Megakaryocytes in a dose related manner .....	122
Figure 30. LOX-PP inhibits polyploidization of Cyclin E transgenic mouse model bone cultures .....	125
Figure 31. Immunofluorescence studies of Bone marrow cells focusing on Megalaryocytes using anti LOX-PP and anti tubulin antibodies.....	127
Figure 32. Schematic representation of the CAG-CAT-EGFP plasmid.....	142
Figure 33. Overview of the strategy to generate transgenic mice that expresses Tubulin –eGFP only on Megakaryocytes using a Cre recombinase approach.....	145

## Background

Platelets and their precursors the Megakaryocytes were considered for many years to as only the key mediators of thrombosis and hemostasis<sup>1</sup>. Megakaryocytes although they are the largest cells of bone marrow under physiological condition comprise only a small fraction of the total bone marrow cell population. For example, in a study<sup>2</sup> human Megakaryocytes averaged 0.37% of all cells in marrow cell suspensions with a range of 10 to 48 micrometers with other studies estimating that Megakaryocytes constitute approximately 0.05% of nucleated cells of human bone marrow<sup>3</sup>. Nevertheless, Megakaryocytes are responsible for the production of almost a trillion platelets in human adults<sup>4</sup> and production can further accelerated in stages of increased demand<sup>5</sup>.

A key characteristic of Megakaryocytes are their ability to attain states of highly ploidy through a process called endomitosis<sup>6</sup>. Megakaryocytes can attain levels up to 256 N through this elaborate process which key molecular steps are not yet elucidated<sup>7,8</sup>.

By contrast to other cells such as lymphocytes, Megakaryocytes have some common progenitors with another lineage that of erythrocytes<sup>9</sup>. The mechanisms that dictate commitment to the megakaryocytic lineage or govern endomitosis have been gradually elucidated, and several transcription factors<sup>10</sup>, cyclins<sup>11,12</sup>, oxidases<sup>13</sup> and signaling pathways<sup>14</sup> appear to play a key role. Thrombopoietin (TPO) is the key growth factor of megakaryopoiesis<sup>15</sup>, while the contribution of other growth factors is evident too<sup>16</sup>. TPO interaction with its receptor activates several signaling pathways, including RAS, MAPK, JAK / STAT that lead to Megakaryocytic endomitosis and maturation<sup>17-23</sup>. The JAK2 protein is instrumental in relaying TPO receptor signaling to downstream signaling pathways and

suppressor of cytokine signaling (SOCS) family of proteins can inhibit JAK2 activity<sup>24</sup>, preventing unrestrained megakaryopoiesis. The JAK2 is an important element of TPO receptor signaling as a mutation rendering the JAK2 constitutively active is implicated in the development of Myeloproliferative neoplasms<sup>25-28</sup>. The role of Mammalian Target Of Rapamycin mTOR<sup>29</sup> and Focal Adhesion Kinase (FAK)<sup>30</sup> has also attracted interest in the context of megakaryopoiesis.

Intriguingly, while Megakaryocytes are consummated in the production of anucleate platelets in the erythroid lineage the nucleus is expelled to give rise to erythrocytes that they do not have also nucleus<sup>31,32</sup>. A recent provocative discovery is that the protein Survivin may have a role in the latest stages of erythroid lineage maturation<sup>33,34</sup>.

The reason behind this programming is not well understood but it is hypothesized that by polyploidization Megakaryocytes increase their volume and produce more platelets<sup>35</sup>. This maybe energy beneficial than producing more diploid Megakaryocytes.

Another example of the complexity of megakaryopoiesis involves the biogenesis of platelets. Namely, platelets are generated by the DMS of Megakaryocytes and hence carry proteins and mRNA of Megakaryocytes. However, the proteins and the mRNA are not a random assortment of what is found on Megakaryocytic cytoplasm. Studies from Italiano and coworkers demonstrated that platelets selectively target factors to granules<sup>36</sup>. For example, angiogenic and anti-angiogenic factors are packaged into different granules.

Microtubules are an important component of the platelet and the structure of a tightly coiled bundle of microtubules called marginal band was recently visualized through a lentiviral expression of fluorescently tagged tubulin<sup>37</sup>. A mouse model that express fluorescently

labeled microtubules would be a unique tool for the study of microtubule architecture in platelets, alleviating concerns for toxicity or artifacts due to excessive accumulation of tubulin.

### **Megakaryopoiesis**

Fetal liver followed by bone marrow (in the later stages) are the main organ of megakaryopoiesis during embryonic life and human platelets can be detected at approximately 5 weeks of gestation<sup>38</sup>. Bone marrow is the main organ of megakaryopoiesis in adults under non pathological stages. Human Stem Cells (HSC) that reside in specialized areas of bone marrow –the niche- are differentiated through a series of intermediate cells to Megakaryocytes. This elaborate process can be outlined and summarized as follows; A key cell is the Megakaryocyte/Erythrocyte Progenitor (MEP)<sup>39</sup> that can contribute both to the megakaryocytic and erythroid lineages. Successively more differentiated populations derived from MEP are the high proliferation potential-colony-forming unit-megakaryocyte<sup>40,41</sup>, the burst-forming unit-megakaryocyte (BFU-MK) and the colony-forming unit-megakaryocyte (CFU-MK)<sup>42</sup>.

The next cell population of cells to arise is the Megakaryoblast; these cells are large and basophilic with a high nucleus/cytoplasm ratio.

Immature megakaryocytes are derived from megakaryoblast and characterized by a polylobated nucleus and contain a large population of mitochondria. The final stage is the mature megakaryocytes which can give birth to platelets through an elaborate process that requires reshaping of the microtubule network to create forms called proplatelets. Study of the different stages of megakaryopoiesis can be achieved using markers such as integrin GPIIIa (CD61), receptor of von Willebrand factor (CD42), GPIV receptor, GPVI receptor, GPIIb/IIIa alternatively designated as integrin  $\alpha_{IIb} \beta_3$  (CD41a), GPIb (CD41b) that can identify

megakaryocytes in different developmental stages<sup>43 5,44</sup> . However, not all progenitors of megakaryocytes have a determined immunophenotypic signature. For example, murine Megakaryocyte progenitors representing 0.01% of nucleated cells have been determined to be Lin-,C-Kit+,Sca1-, CD150+, CD41+<sup>45</sup> but a similar signature has not been determined for their human counterpart .

The CD41 (GPIIb) is expressed in Megakaryocytes but is also expressed by mast cells and bone marrow and fetal liver progenitors<sup>43</sup>. CD 42 is expressed latter than CD41 and has a more restricted repertoire of expression.

### **TPO and its effects on Megakaryopoiesis**

The key growth factors of Megakaryocytes is undoubtedly the thrombopoietin (TPO) (reviewed in<sup>15,46,47</sup>). TPO is produced constitutively mainly from the liver and smaller amounts can also produced in the bone marrow or kidneys. TPO dynamics are complex<sup>48,49</sup>and production can be augmented by inflammation<sup>50</sup> and its level can be diminished in advanced liver disease<sup>51</sup>. Human and murine TPO share extensive homology especially in the regions that interact with TPO receptor<sup>52-54</sup>. The human TPO is a 353 amino acid precursor protein that contains a 21 amino acid signal peptide and its results in a final protein of 95 KDa<sup>55</sup>. TPO protein can be divided into the receptor binding domain (residues 1 to 153) and the COOH terminal domain that is consisted of 179 aminoacid residues (reviewed in<sup>56</sup>). The receptor interacting domain is characterized by two binding sites with different affinity for the receptor<sup>57</sup>. Binding of TPO with its receptor augments growth of cells committed to megakaryocytic lineage by increasing ploidy and subsequently platelet levels. Although, TPO receptors are



carried by HSC and pluripotent cells and its effect in these cell populations is potent<sup>58</sup>, it does not affect commitment to megakaryocytic lineage<sup>59</sup>. Interestingly, TPO does not affect the last steps of megakaryocytic life cycle as it does not influence the terminal events leading to the biogenesis of platelets<sup>60</sup>.

A key component of the TPO signaling cascade is the TPO receptor which is composed by an extracellular domain, a 25 amino acid transmembrane domain and an approximately 120 amino acids intracellular domain<sup>46</sup>. TPO interaction with its receptor liberates the latter from signaling suppression<sup>47</sup>.

TPO exerts its action through several signaling pathways that include the PI3K-AKT (phosphoinositol-3-Kinase/AKT), MAPK (Mitogen Activated Protein Kinase) and JAK-STAT (Janus Kinase-Signal Transducers and Activators of Transcription).

### **The state of polyploidy**

One of the characteristics of Megakaryocytes is that they can accumulate under non pathological conditions DNA content that is higher than 2N (up to 128 N - 256 N) which is the case with most somatic cells<sup>6</sup>. Both in humans and most mice strains modal ploidy of Megakaryocytes is 16 N<sup>61</sup>.

Polyploidy has been described in invertebrates (e.g *Pontoporeia Affinis*), plants, yeast and vertebrates (especially fish species- e.g *Carassius*, *Barbus*) and recently reviewed extensively in<sup>62</sup>. However, higher vertebrates do not tolerate global polyploidy<sup>63</sup>.

In humans cells that can attain polyploidy status apart from Megakaryocytes are the giant cell of trophoblast<sup>64</sup>, vascular smooth muscle cells<sup>65</sup> or liver cells<sup>6,66</sup>. Some advantages of polyploidy could include the masking by dominant alleles of the recessives one's and gain of

asexual reproduction with disadvantages being changes in cell signaling pathways, constrains of large amount of DNA that needs to be replicated/segreated faithfully<sup>63</sup> .

Polyploidy can be reached by different mechanisms. Megakaryocytes accumulate the chromosomal content through the process of endomitosis<sup>67</sup>. During endomitosis, Megakaryocytes undergo all parts of cell cycle but late stages of mitosis are aborted resulting in a single cell with increased chromosomal content. Of note, the term endomitosis was devised to describe accumulation of DNA without disturbance of nuclear membrane; latter studies have confirmed that nuclear membrane does not remain intact during polyploidization.

During megakaryocytic endomitosis cells enter S-phase and then mitosis with nuclear membrane dismantle and formation of multiple spindle poles<sup>68</sup> . However, late anaphase and events related to telophase such as formation of daughter cells are not observed and cells commence a subsequent endomitic cycle<sup>69</sup> through a variable time window. A long standing view was that endomitosis departs from mitosis at the stage of anaphase B<sup>68</sup>. Based on studies of fixed cells it was thought that Anaphase B and subsequent furrowing<sup>70</sup> did not occur during mitosis.

Studies to explore the timing and kinetics of endomitosis are limited. For example, Bromodeoxyuridine (BrdU) studies pursued in Megakaryocytes are scant; Odell and coworkers used radio-labelled thymidine to study kinetics of rat megakaryocytes<sup>71</sup>. Their conclusion was that endomitosis duration is approximately 9 hours with the larger time devoted in S phase. Another pioneering study by Wang and coworkers<sup>12</sup> used murine Megakaryocytes that were incubated with BrdU in a medium that was shown previously to support endomitosis. Megakaryocytes were determined by morphology and it was shown that in the first hour of incubation 10% of megakaryocytes were stained positive with BrdU. The highest percentage

of megakaryocytes that Brdu incorporation was detected was 15% and included incubation up to 24 hours. The larger megakaryocytes were almost invariably not incorporating Brdu. In the same study the G1 phase was estimated to be less than 90 minutes.

Taken together, these data suggest the majority of polyploid Megakaryocytes are arrested at G1, while the rest at Go. However, cell cycle-arrested Megakaryocytes may be recruited into endomitotic cycles by TPO treatment. Another seminal study<sup>72</sup> using purified murine Megakaryocytes cultured in the presence of TPO indicated that after 2-3 days of culture almost half of diploid Megakaryocytes were in G1 phase with approximately 25% in S phase and the remaining in the G2/M phase. However, as the ploidy class increased up to 32 N megakaryocytes were mostly in S phase followed by G2/M phase and the least percentage being in G1 phase. An exemption was megakaryocytes with 32N content which again half of them were in G1 phase with slightly more than 1 / 3 in S phase and only a fraction as G2/M phase.

The prevailing theory is that TPO can recruit both Megakaryocytes that are arrested in Go as well as stimulating diploid Megakaryocytes to enter active cyclining.

### **The role of Cyclins in endomitosis.**

The endomitotic process is tightly controlled although it deviates from mitosis and abrogates several check points that evolved to prevent aneuploidy<sup>73-75</sup>. Cyclins have an important role in modulating entry and exit from S phase and mitosis<sup>76-79</sup>. Cyclin D3 and in lesser extent D1 was shown to be important for endomitosis (reviewed in <sup>12,80,81</sup>), while levels of Cyclin B are reduced in polyploidizing cell line y-10<sup>82</sup>. Recently, PLK-1, a protein with multiple roles

(reviewed in <sup>83-85</sup>), was reported to be absent in polyploid Megakaryocytes<sup>86</sup>. Finally, although an array of proteins was implicated in endomitosis in recent publications<sup>70,87</sup>, evidence apart from reduction in RhoA protein levels<sup>88</sup> is lacking.

Proteins that act in G1 / Go transition to S phase or are involved in the late stage of mitosis were considered as potential mediators of endomitosis. In this context, cyclins that promote transition from G1 to S phase (Cyclins D1-3 and Cyclins E1-2) have attracted attention as mediators of endomitosis<sup>6</sup>. Ablation of cyclin D3, the predominant cyclin D in Megakaryocytes, in vitro reduces megakaryocytic ploidy levels<sup>12</sup>. On the other hand, transgenic mouse models of Cyclin D exhibit increased Megakaryocyte ploidy levels<sup>81,89</sup>. Cyclin E1 and E2 are highly homologous and they have a key role in the transition from G1 to S phase<sup>90-92</sup>. Cyclin E hyperphosphorylate retinoblastoma protein causing the E2F mediated enhanced expression of S phase modulators. Regulation of Cyclin E occurs both in transcriptional and posttranslational level highlighting the importance of this protein in regulation of cell cycle<sup>93,94</sup>. Furthermore, cultured megakaryocytes of Cyclin E double knock out mice exhibited reduced ploidy compared to wild type<sup>95</sup>.

The construction of the Cyclin E double knock out mouse involved multiple steps<sup>95</sup>. The Cyclin E1 knock out mouse model did not have decreased life span and did not exhibit any overt morphological abnormalities. The Cyclin E2 knock mouse model exhibited decreased spermatogenesis and decrease in testicular size and about 50% of males were infertile. Crossing of the knock out mice indicated Cyclin E1<sup>+/-</sup>CyclinE2<sup>-/-</sup> had also defects in spermatogenesis and fertility while CyclinE1<sup>-/-</sup>CyclinE2<sup>+/-</sup> was indistinguishable from wild type. However, the double Cyclin E knockout mouse model (Cyclin E1<sup>-/-</sup>CyclinE2<sup>-/-</sup>) was embryonic lethal due to defects of the placenta, especially affecting the giant cells of

trophoblasts that can reach ploidy levels up to 1000 N. In the double Cyclin E knock out mice examination of placentas demonstrated that giant trophoblasts had a modal ploidy less than 30 N with few cells having ploidy above 300. By comparison, almost half of the wild type giant cells of trophoblast had ploidy above 100N with 20% reaching ploidy between 300-900 N. However, when wild type placenta was provided through complementation knock out mice were born and were viable. Almost half of the Cyclin E double knock out mice died between E.15.5 and E18.5 due to extensive embryonic abnormalities associated with the cardiovascular system. Megakaryocytes that were retrieved from E14.5 livers of the Cyclin E double knock out mice were cultured in the presence of TPO and exhibited reduced ploidy compared to wild type megakaryocytes cultured under similar conditions. More specifically, the modal ploidy of Cyclin E double knock out mice derived megakaryocytes was 8N while the modal ploidy of the wild type Megakaryocytes was 32 N. In this study, the percentage of megakaryocytes in bone marrow or in cultures as well as the megakaryocytic ploidy profile of fresh bone marrow preparations was not performed.

Other studies, in cell lines involving overexpression of Cyclin E through adenoviral constructs demonstrated that mitotic failure and polyploidy can occur and cells were delayed in early mitosis<sup>96</sup>. Furthermore, in a mouse model where Cyclin E overexpression was restricted on mammary epithelium hyperplasia of the aforementioned organ was noted<sup>97</sup>. In another mouse model where Surfactant C promoter drove expression of wild type or non degradable human Cyclin E demonstrated early onset carcinogenesis with the majority of homozygote mice having premalignancy or malignancy by 6 months of age associated also with aneuploidy<sup>98</sup>.

The chromosomal passenger complex (CPC) proteins that include Survivin, Aurora-B and INCENP attracted attention in the context of endomitosis because their localization correlates

with specific stages of mitosis<sup>99,100</sup>. It was recently shown that megakaryocytic targeted overexpression or ablation of Survivin does not affect ploidy in vivo<sup>101,102</sup>, although ex vivo mediated ablation of Survivin using retrovirally expressed Cre had as result increased levels of high ( $\geq 8N$ ) ploidy Megakaryocytes<sup>102</sup>. As the search for mediators of endomitosis expanded the effect of other cellular processes became apparent. For example, Reactive Oxygen Species (ROS) were recently to exert potent control on megakaryocytic polyploidisation<sup>13</sup>, implicating regulation of cyclin E levels by NADPH oxidase-mediated changes in ROS. A potential role for RhoA/ Rock pathway and the contractile ring in Megakaryocytic polyploidization was the focus of another recent publication, with inhibition of RhoA or Rock increasing ploidy by a yet unexplored mechanism<sup>88</sup>. Furthermore, the Megakaryocytic specific ablation of the Focal Adhesion Kinase (FAK), which has a major role in integrin signaling-mediated cell migration<sup>103</sup>, augmented megakaryopoiesis and increased ploidy levels<sup>30</sup>.

Under physiological conditions, megakaryocytic ploidy increase parallels that of cytoplasmatic volume and components<sup>44</sup>. At the last stages of Megakaryocyte life cycle, cytoplasm of megakaryocytes is consumed during biogenesis of platelets<sup>104</sup>.

A key question at hand is if targeted overexpression of Cyclin E in Megakaryocytes could lead to higher ploidy levels. To this end, our lab engineered a transgenic mouse model that the rat PF4 promoter drives expression of the human Cyclin E1 cDNA followed by an intron and polyA tail.

### **The role of PLK family in polyploidization**

The most studied member of the family of Polo-Like-Kinase (PLK) proteins is PLK1<sup>84,105</sup>. Interestingly, PLK1 has attracted attention in the context of megakaryocytic endomitosis based on a study which demonstrated that PLK1 expression was decreased in mouse primary polyploid Megakaryocytes<sup>86</sup>. Based on the role of PLK1 in Megakaryocytic endomitosis<sup>86</sup>, we decided to study the potential role of another PLK family member, PLK3.

PLK3 has multiple roles<sup>106</sup> and it was cloned by different teams. PLK3 was identified by Wei Dai group by cloning transcripts that were expressed on the megakaryocytic line Dami using oligodeoxynucleotides targeted to cyclin-dependent kinases<sup>107</sup>. In the same study PLK3 expression was detected also in the megakaryoblastic line MO7e. In addition, TPO caused a moderate increase in PLK3 expression in Dami cell line<sup>107</sup>. A smaller increase in PLK3 was also reported by IL3 induction<sup>107</sup>.

PLK3 is not detected in the erythroleukemic cell line K562 at base line. However, addition of phorbol 12-myristate 13-acetate (PMA) that induces differentiation of K562 towards the megakaryocytic lineage (as exhibited by increase in CD41 levels) also upregulates PLK3 protein levels<sup>108</sup>. Northern blot analysis of various human tissues indicated that PLK3 is moderately expressed on the placenta<sup>107</sup>. It was also detected in lungs<sup>109</sup> but in most other tissues its expression is low or undetectable<sup>107,109</sup>. In blood cells PLK3 was reported to be strongly expressed in macrophages and it was undetectable in resting leucocytes<sup>109</sup>. PLK3 was also found to be an immediately early gene and its expression was significantly upregulated in the addition of fibroblast growth factor.

Microarray data indicated that PLK3 is modestly increased (2 fold) during murine Megakaryocytic polyploidization in the presence of TPO (derived from European Bioinformatics Institute; (<http://www.ebi.ac.uk>)).

There is no consensus regarding localization of PLK3 protein. It has been reported to localized to actin focal plates<sup>109</sup> and to co-localize with CIB (calcium and integrin binding) protein<sup>110</sup>. The CIB binds GPIIb/IIIa protein and interestingly, a recently reported Megakaryocytic specific KO mouse model of Focal Adhesion Kinase (FAK) protein that also binds CIB exhibited increased ploidy<sup>30</sup>. PLK3 was also reported to localize at centrosomes and around spindle poles and interact with Aurora A and BubR1 kinases<sup>108</sup>.

By contrast, recent studies could detect PLK3 only on nucleolus<sup>111,112</sup> and linked PLK3 with Cyclin E pathway<sup>112</sup>. Namely, Cyclin E degradation occurs via two pathways; Cdk2 associated Cyclin E is degraded by Fbw7 ubiquitin ligase (F-box and WD repeat domain-containing 7 protein; reviewed in <sup>113,114</sup>), while free Cyclin E is degraded by Cullin-3<sup>115</sup>.

Studies in MC10A cell line<sup>112</sup> indicated that depletion of PLK3 through RNAi led to significantly reduced levels of Cyclin E possibly through a mechanism involving the cdc25A. In addition PLK3 depleted cells that were serum starved failed to enter S phase upon reintroduction of serum.

Based on the above studies, and the findings of microarray data (described above) we envision that PLK3 may be an important factor for the transition of Megakaryocytes to S phase. In addition, PLK3 ability to post transitionally regulate levels of Cyclin E may have an important role in modulating endomitosis.

At the time of our experiments there were no published studies regarding PLK3 in primary Megakaryocytes, apart from microarray data deposited on EBI website (<http://www.ebi.ac.uk>). PLK3 KO mice were reported to be viable, but they have a propensity to develop tumors at lung, kidney and liver after the first year of life<sup>116</sup>. PLK3 was shown in the same publication to act as tumor suppressor.



## **The importance of cytoskeleton in Endomitosis**

In the diploid cells the main element governing cell division is the mitotic spindle which is composed by microtubules<sup>117</sup>. The first step involves duplication of the centrosome and migration to the opposite pole of the cell<sup>118</sup>. The next step involves the organization and subsequently the assembly of emanating microtubules towards the chromosomes of the cells. Microtubules elongate only in the plus (+) end of the assembly and they attach in the kinetochores of chromosomes<sup>119</sup>. However, some of the microtubules do not attach in the chromosomes but rather intermingle in the equator of the cell creating the central spindle assembly. Several proteins have been identified that have a key role in the formation of the central spindle including the centralspindlin, MKLP-1, and the role of Rho/Rac pathway has been elucidated recently<sup>120</sup>. The spindle midzone is crucial for proper division of cells since ablation of that area has been shown to result in disruption of the proper chromosomal dynamics and impairment of the cytokinesis related functions control of midzone<sup>121</sup>. The Cdk1/Cyclin B is a key regulator of cell progression. SAC keeps Cdk1/Cyclin B complex protected from degradation until all kinetochores have microtubules attached to them<sup>122</sup>.

Once proper attachment and alignment of chromosomes is achieved then a critical function of cell mechanisms –the spindle checkpoint - guarding against aneuploidy/polyploidy is switched off. Then separase is liberated and dissolves the cohesin inducing sister chromatids separation. Cdc14 has a pivotal role in this process as its activation is required for this step with Ase1 to play an instrumental role.

## *Study of Megakaryopoiesis*

Studies focused on Megakaryocytes are difficult because Megakaryocytic population is very scarce; typically comprising less than 1 % of murine bone marrow. Although most freshly isolated Megakaryocytes are cell cycle arrested, they respond to stimulation by thrombopoietin (TPO). Megakaryocytes return to cell cycling and form mature Megakaryocytes that ultimately give rise to platelets. TPO is the main growth factor associated with megakaryopoiesis<sup>123</sup>.

Studies of Megakaryocytes are based on isolation from murine bone marrow or from CD34 cells that are stimulated with a combination of factors that typically include TPO. An advantage of murine Megakaryocytes is that the ploidy distribution resembles that of humans (modal ploidy 16N)<sup>124</sup>, while Megakaryocytes derived from CD34 cells are of lower ploidy<sup>125</sup>.

There is not currently available a unique marker to identify Megakaryocytes. This is particularly important when trying to detect Megakaryocytes at different levels of maturation. Potential markers (reviewed in<sup>5,44</sup>) include integrin GPIIIa (CD61), receptor of von Willebrand factor (CD42), GPIIb/IIIa alternatively designated as integrin  $\alpha_{IIb}\beta_3$ (CD41a), GPIb (CD41b).

The most widely used in the literature is CD41 and in less extent CD42 or CD61. Although, CD41 is expressed on Megakaryocytic progenitors or Hemopoietic Stem Cells (HSC) its expression appears to be weak in this cells based on a Knock-in mouse model that expressed YFP under CD41 promoter<sup>126</sup>. Moreover, CD41 staining combined with DNA staining can identify polyploid Megakaryocytes and permits comparison of ploidy levels under different experimental conditions (examples<sup>89,101</sup>). Other approaches, especially for studies that involve fixed cells is the apparent larger size of polyploid Megakaryocytes compared to diploid cells and the presence of multiple spindle poles that characterize polyploidy.

## **PF4 promoter targets expression in Megakaryocytes**

Platelet Factor 4 is a component of alpha granules of Megakaryocytes and plays a key role in neutralizing anticoagulant activity of heparin sulfate and is a powerful chemotactic agent<sup>127,128</sup>. Importantly, its expression is considered to be limited to Megakaryocytic lineage<sup>129</sup>. A fragment of The Rat platelet Factor 4 promoter of approximately 1.1 Kb (containing the 1104 bases of 5' upstream sequence as well as the cap site to + 20) was shown in seminal experiments<sup>130</sup> with transgenic mouse lines using B galactosidase as reporter gene that drives expression of transgenes predominantly in Megakaryocytes. In non hematopoietic tissues weak expression of B galactosidase (compared to Megakaryocytes) was detected only adrenal cortex. Many transgenic mouse lines were generated<sup>81,89,131,132</sup> utilizing the Rat PF4 promoter and even today there is no other promoter that can target exclusively the Megakaryocytic lineage.

## **Immunofluorescence and live imaging studies of Megakaryocytes**

Studies of endomitosis related phenomena are based predominantly on immunocytochemistry data of fixed cells. Seminal studies were hampered with many problems; for example only a minority of Megakaryocytes are undergoing endomitosis in the bone marrow<sup>12</sup> and prior to discovery of TPO culture media have only limited success in promoting endomitosis. Another approach would be to use one of several megakaryocytic lines<sup>133,134</sup> that are available. However, this approach is the least favorable as these cell lines are not recapitulating faithfully the endomitosis of primary Megakaryocytes due to their aberrant cell cycle. In addition, these cell lines frequently require the use of potent

chemicals<sup>135,136</sup> such as phorbol esters<sup>137</sup> which could further compromise the validity of studies.

The characterization of TPO and its production in large amount by recombinant DNA technology had a dramatic impact on the study of endomitosis<sup>138-140</sup>. TPO not only drives Megakaryocytes back to cell cycle but also promotes their maturation. Nagata and coworkers<sup>141</sup> using TPO to stimulate bone marrow cultures and immunofluorescence described that multiple mitotic spindle poles formed during polyploidization of Megakaryocytes accompanied by the presence of multiple centrosomes. In addition, they described that the nuclear membrane dissociates during endomitosis. Using an anti centromere antibody they discerned that in interphase centromeres were not located in a particular area of the nucleus. However, in prophase as well as prometaphase chromosomes were clearly visible and during metaphase the chromosomes aligned. However, late stages of mitosis such as Anaphase B or Telophase were not observed. Studies of Roy<sup>68</sup> and coworkers utilized CD34+ derived Megakaryocytes and by employing microtubule staining coupled with PRINS technique to visualize centrosomes demonstrated that polyploid Megakaryocytes have multiple spindle poles that correlate with their ploidy and that the segregation of chromosomes was not synchronous. In this study also by utilizing Nocodazole Roy and coworkers observed that chromosomes segregate during Anaphase. Another study, employing immunofluorescence of fixed Megakaryocytes examined furrowing during endomitosis<sup>70</sup>. In this study<sup>70</sup> using both murine and human Megakaryocytes researchers demonstrated by using partial synchronization of Megakaryocytes that a midzone area is formed but furrowing was not observed. Authors attributed the lack of furrowing in the localization of a crucial protein for Midzone formation RhoA.

The same group however, using lentiviral constructs to perform live imaging of Megakaryocytes demonstrated that furrowing occurs<sup>87</sup>. In this pioneering study that CD 34 human cells were lentivirally transduced to express YFP-tubulin and then live imaging was performed. In this study, Megakaryocytes were purified by immunomagnetic beads and were imaged both in brightfield and fluorescence. This study documented diploid MKs undergoing mitosis and MKs undergoing endomitosis. Low ploidy Megakaryocytes, exhibited pronounced furrowing resembling that of diploid Megakaryocytes before they rejoin in a single Megakaryocyte cell . By contrast, high ploidy Megakaryocytes exhibited only attenuated and transient furrowing<sup>87</sup>. This study demonstrated that the lack of furrowing of fixed polyploid Megakaryocytes reported on the previous study from that group<sup>70</sup> was an artifact of fixation method. Of note, in this study only the cytoskeleton was visualized and not the chromosomes as the study was mostly focused on the furrowing.

However, in this study the Megakaryocytes were column purified and the degree of purity was not accessed. Hence, the percentage of non Megakaryocyte cells in the sample was not determined and hence cells documented to undergo mitosis are not with certainty Megakaryocytes. Furthermore, lentiviral transduction and the expression of YFP fused to tubulin may be lethal to cells, alter mitotic index or microtubule network architecture as was demonstrated in cell lines (also in our results).

The results from these studies were important but also highlighted the weakness associated with immunofluorescence studies. For example, Immunofluorescence studies of fixed cells may be prone to fixation artifacts and can not capture the dynamic choreography of chromosomes during endomitosis. For example a cell with 4N DNA content can be either undergoing regular mitosis or undergoing endomitosis that would result in a polyploidy

megakaryocyte. In our experience and reported elsewhere<sup>68</sup> obtaining fixed megakaryocytes at anaphase for immunocytochemistry studies may require screening of a large number of samples.

### **Transgenic mouse models visualizing endomitosis**

We decided to study endomitosis by devising a strategy of in vivo cell imaging based on fetal liver or bone marrow derived Megakaryocytes. For the in vivo imaging studies we took advantage of a mouse model in which Rat PF-4 promoter is driving expression of Green Fluorescent Protein (GFP) fused to Histone 2B. Histone 2B is an essential component of the chromosomal scaffold<sup>142</sup> and constructs based on the PF-4 promoter have already successfully utilized in previous studies to drive expression of genes of interest only in megakaryocytes<sup>143, 130</sup>. It has been previously demonstrated that fluorochrome tagging of Histones does not affect cell viability<sup>144</sup> and has been used for the visualization studies in murine embryos<sup>145</sup>. Histone tagging is particularly useful in studies of endomitosis because Megakaryocytes are readily identified by fluorescence circumventing purification procedures. Furthermore, DNA can be visualized during all phases of cell cycle regardless of nuclear envelope integrity. This aspect is particularly useful since it alleviates potential problems related to fixation methods commonly faced on immunocytochemistry studies.

We described the preliminary results of our initial studies in the master thesis, and here we present additional data.

Visualization of proteins is based on their tagging with a fluorescent protein that can permit fluorescence upon excitation<sup>144,146</sup>. Transgenic models that offer visualization of

microtubules are very few<sup>147</sup>, and currently there is none targeted only to hematopoietic system.

A transgenic mouse model has some key advantages compared to lentiviral approaches. Namely, a potential drawback of a lentiviral approach is that overexpression of microtubule constructs, at least in some cell lines, was associated with abnormal mitotic index or microtubule dynamics. In addition identification with certainty of diploid Megakaryocytes is difficult due to ubiquitous mode of lentiviral expression.

The construct that would allow visualization of Megakaryocyte microtubules must satisfy several requirements. It must emit a bright signal upon excitation for prolonged periods (associated with imaging of such phenomena); however It is very difficult to predict brightness of the fluorescent proteins that belong to different spectral class as the brightness is depended on many different variables such as the intrinsic properties of the protein, the imaging set up and the optical equipment used in a given experiment.

In addition, the fluorescent protein must be folded optimally at 37 C and this is not only dependent on the intrinsic protein characteristics but also on the mammalian chaperones that must recognize the protein (protein folding in the natural host may require assistance of bacterial chaperones.) Most of enhanced versions of GFP have been shown to fold particularly well in 37 C.

Another crucial element of fluorescent protein that will be utilized for live imaging is that it must be resistant to degradation of the emission when excitation is performed (photobleaching) especially for long term experiments. mCherry a monomer that emits in the red spectrum has superior resistance to photobleaching.

A favorable property of the fluorescent protein is to be emitting in a narrow spectral window allowing by this way the potential use of multiple fluorescent proteins in the same experiment. Apart from the GFP variants red fluorescent proteins are under intense research as due to their longer wavelength excitation and emission spectrum could be linked to reduced cellular toxicity and furthermore allow colocalization experiments with GFP tagged proteins<sup>148</sup>.

The optimized fluorescent proteins are monomers or weakly dimmers and tetramers might be toxic to the cells. Another concern for toxicity is the that overproduction per se of fluorescent protein may be lethal to the cells.

The importance of these requirements were exemplified by the tau-GFP mouse model. In this mouse model, tau (a protein associating with microtubules-especially in neurons) was fused to GFP and was expressed under the CAG ubiquitous promoter<sup>149</sup>. tissues of this transgenic mouse model were visualized efficiently by GFP-tau and microtubules were decorated by the fluorescent tau. However, subsequent studies of this mouse model indicated lethality problems.

We generated several transgenic models in an attempt to visualize Megakaryocytic microtubule network.

The first two mouse models were based on transgenic constructs that Rat Platelet Factor 4 (PF4) promoter drives expression of tubulin linked to a fluorescent protein (mCherry or AcGFP1). PF4 promoter has been used to develop other transgenic mouse models<sup>89,101,150</sup> and is the only known promoter to confer Megakaryocytic only specific expression. The third mouse model is based on a transgenic construct that PF4 drives expression of microtubule associated protein (EMTB) fused to three GFP moieties (3XGFP-EMTB).



Data presented here are related to our second and third attempt at which we employed pAcGFP1-tubulin and 3XGFP-EMTB. The first attempt was based on mCherry human alpha tubulin which its expression was driven by the PF4 promoter and will be described briefly here. The mCherry is a monomeric photostable, non toxic protein that emits on the red spectrum (reviewed in<sup>146</sup>). Transgenic mice have been reported where mCherry was utilized as reporter gene<sup>151,152</sup>. The mcherry-tubulin construct was obtained by Chen lab through a collaborator. The mCherry human alpha tubulin was digested with Apal restriction enzyme and blunt ends were treated using T4 klenow enzyme. NheI digestion was performed to create the fragment of interest containing the mCherry human alpha tubulin with one blunt end and with an end with NheI restriction site sequence. PF4 plasmid was cut with NotI that recognize a unique sequence in the polylinker preceding the intron and the polyA tail. T4 klenow was used again to create blunt ends and digestion with NheI was performed to create compatible ends with mCherry human alpha tubulin. Ligation was then performed and a plasmid that PF4 promoter drives expression of mCherry human alpha tubulin followed by intron and poly A tail. Functional expression of the mCherry was confirmed with transfection experiments involving cell lines and visualization under the microscope. The sequence that contained the PF4 promoter the mCherry human alpha tubulin followed by intron and poly A tail was isolated by restriction enzyme digestion (AatII and SwaI) and electroelution, and was used to generate founders. Potential founders were screened with PCR of genomic (tail DNA). Founders were bred and mice carrying the transgene were sacrificed and bone marrow expression was checked under the microscope. However, mCherry protein is inherently dim and our transgenic mouse model was not suitable for living imaging of Megakaryocytes.

The pAcGFP1-tubulin vector was obtained from Clontech and is based on a fusion of a variant of GFP to human  $\alpha$ -tubulin cDNA sequence<sup>153</sup>. The pAcGFP1-tubulin is a chimeric protein that is composed of monomeric green fluorescent protein of AcGFP1 and the gene encoding human alpha tubulin. The AcGFP1-Tubulin<sup>153</sup> is derived by *Aequorea Coerulescens* but has been engineered to have brighter fluorescence and higher excitation (Excitation maximum = 475 nm and the emission maximum= 505 nm). The pAcGFP-tubulin construct has some favorable attributes for imaging Megakaryocyte microtubules. It's a true monomer with satisfactory brightness, good solubility and can be used for prolonged imaging. This transgenic mouse model will offer significant information regarding endomitosis, platelet biogenesis and ultrastructure and could be useful for in vivo imaging or even ontogeny studies. The 3XGFP-EMTB construct<sup>154</sup> that was kindly provided by Dr. Cloe Bulinski. In this construct, the microtubule associated domain of Enscosin protein (EMTB) is fused to 3 GFP moieties. This construct was successfully utilized to visualize microtubules of skin cells in a recently reported transgenic mouse model<sup>147</sup>.

Enscosin is a large basic protein (~84 KDa) with a unique N terminal microtubule binding domain that is found in non neural tissues<sup>155,156</sup>. Experiments<sup>157</sup> where the Microtubule binding domain was conjugated to GFP showed that association with microtubules occurs immediately both in steady state or during polymerization. In addition, microtubular depolymerization was not affected by the binding of EMTB-GFP and low level expression of the chimeric protein did not perturb cellular function. Variable amounts of GFP moieties were attached to EMTB with the maximum being 5 (discussed in<sup>154</sup>). The 5XGFP-EMTB appears to be the upper limit as the protein has an apparent size of more than 205 KDa and furthermore the addition of another

GFP moiety to EMTB decreased expression by 25%-60%. The 3xGFP appears to be the optimum balance between expression and brightness<sup>158</sup>.

The 3XGFP-EMTB was subcloned into the PF4  $\beta$ -globin vector and the resulting PF4-3XGFP-EMTB construct was transfected into the megakaryocytic cell lines Y-10/L8057 and CMK. Expression was confirmed in both cell lines and proper localization to microtubule network was verified upon taxol treatment.

The PF4-3XGFP-EMTB plasmid was then digested and the transgene composed by the 1.1 Kb sequence of the Rat PF4 promoter, the EMTB fused in frame with 3 GFP moieties the  $\beta$ -intron and the poly A tail was isolated. Injection in male pronuclei was performed and founders are now screened for the expression of EMTB 3XGFP.

### **An introduction to Lysyl Oxidase and its Propeptide (LOX-PP)**

LOX is a copper-dependent enzyme that cross-links collagen or elastin and contributes to the accumulation of extracellular matrix<sup>159</sup>. LOX oxidizes lysine or hydroxylysine residues of collagen telopeptides promoting intermolecular cross-linking. LOX is produced by fibrogenic cells and is secreted as a 52 kDa glycosylated pro-enzyme. Bone morphogenic protein 1 (BMP-1), which is also expressed in Megakaryocytes, cleaves the pro-enzyme extracellularly to release a 18 kDa propeptide (LOXPP) and the mature 32 kDa LOX. The Mammalian Tolloid protein and the Mammalian Tolloid like proteins 1 and 3 can also cleave the pro-enzyme albeit with lower efficiency<sup>160</sup>. The LOX catalytic domain is highly conserved between species including that of human and mouse. The LOX enzymatic activity is inhibited irreversibly by  $\beta$ -aminopropionitrile (BAPN) which has been used in mouse and rat models in the context of fibrosis or metastasis<sup>161,162</sup>. At very high doses BAPN can cause lathyrism<sup>163</sup>.

The LOX gene expression is closely linked to that of collagen. For example, a putative binding site has been recognized for the CCAAT binding factor, an inducer of collagen synthesis in the Rat LOX promoter<sup>164</sup>. On the other hand, putative binding sites for inhibitors of collagen synthesis including C-Krox A, C-Krox B and SP1 like factor have been described in the same study. Of note, NF1 transcription factor, with a role in the response to oxidative stress, has several binding sites clustered in the Rat LOX promoter.

Growth factors such as PDGF, TGF-B1 and the cytokine interleukin 1b increase expression of LOX. However, FGF-2 and IFN-γ have an opposite effect. Furthermore, at least in c-H-Ras transformed fibroblasts an autocrine pathway involving FGF-2 keeps expression of LOX in low levels. Intriguingly, LOX can oxidize FGF-2 receptor and attenuate emanating signaling cascades underscoring the complex transcriptional control of LOX expression.

The functions attributed to LOX have recently expanded; our studies show that LOX oxidizes the PDGF receptor on smooth muscle cells and fibroblasts and enhances proliferation signaling<sup>165</sup>. LOX has a key role in the development of cardiovascular and respiratory system and defects manifest towards the end of gestation. Namely, LOX Knock Out (KO) Mice succumb perinatally to vascular and respiratory developmental aberrations which include rupture of aorta. In addition, LOX has been detected in the murine CNS and in a murine model of Amyotrophic Lateral Sclerosis (ALS) its expression in the CNS had an aberrant pattern during late stages of the disease<sup>166</sup>.

LOX is currently the focus of cancer research<sup>167</sup>. LOX was originally identified as repressor of RAS transformation in 3T3 cells, and its gene expression is downregulated in several carcinomas<sup>168</sup>. On the other hand, LOX has attracted attention in the context of metastasis<sup>161 168</sup>. Namely, breast cancer cell lines with high metastatic potential have

upregulated LOX gene expression (Discussed in <sup>168</sup>). A potential mechanism is based on the production of H<sub>2</sub>O<sub>2</sub> by LOX<sup>169</sup> but whether mature LOX acts extracellularly or intracellularly (by entering the cell and translocating to the nucleus) remains controversial<sup>159,168,170</sup>. Studies from our group and others have shown that LOX mobilizes monocytes, fibroblasts and vascular smooth muscle cells.

Intriguingly, the 141 aminoacid LOXPP moiety appears to be biologically active and have tumor suppressing activity<sup>171</sup>. LOXPP primary sequence has little resemblance with the propeptide of LOXL1 and no similarity with the domains of the rest of LOXL proteins<sup>172,173</sup>. LOXPP is a powerful inhibitor of proliferation or migration of several cancer cell lines and exerts its action through multiple pathways. These pathways involve RAS signaling in transformed cell lines or malignant cells harboring RAS mutations<sup>174</sup>. Recently, LOXPP was found to suppress FAK activation<sup>175</sup> and interferes with FGF-2 binding to its receptor and hence attenuates FGF receptor emanating RAS signaling<sup>176</sup>. A LOXPP mutation at Arg158Gln residue could not suppressed Ras signaling in the same extent as LOXPP in breast cancer lines<sup>174</sup>. Importantly, LOXPP activity is not inhibited by the BAPN.

Of note, LOX-like proteins (LOXL 1-4) have been described that share the LOX catalytic site. The LOXL-1 is structurally more closely related to LOX and their pattern of expression overlap in many tissues but is different in kidney and neural tissues such as cerebellum or cerebral cortex<sup>177</sup>. LOXL1 KO mice are viable and display defects predominantly in tissues with high elastin content including lungs, skin and uterus<sup>178</sup>. By contrast, the LOXL-2,3 and 4 have a different, less diverse, gene expression pattern and they share four Scavenger Receptor Cysteine Rich (SRCR) regions. Their function remains largely unexplored but LOXL-2 may modulate, in conjunction with LOXL-3, E-cadherin expression through interaction with SNAIL

<sup>179</sup>. Furthermore, LOXL2 is associated with liver fibrosis and development aneurysms and LOXL3 expression was detected on placenta, heart and breast and importantly in highly malignant breast cells.<sup>180</sup> In the context of megakaryopoiesis, upregulated LOXL-3 gene expression has been reported during endomitosis<sup>181</sup>, and LOXL-3 protein was detected in human platelets<sup>182</sup>. LOX-PP has not been studied in the context of Megakaryopoiesis and we sought to explore its potential role.

## **CHAPTER II.**

### **Materials and methods**

#### **Generation of PF4-AcGFP1-tubulin construct**

The PF4- $\beta$ -globin vector contains 1.1 Kb of the rat PF4 promoter sequence and a fragment of the human  $\beta$ -globin intron followed by polyA tail sequence. The PF4- $\beta$ -globin plasmid was digested with NotI followed by blunting using NEB large T Klenow fragment enzyme. The linearized PF4- $\beta$ -globin vector was subsequently digested with NheI-HF followed by gel purification to isolate the PF4- $\beta$ -globin with a blunt end and a NheI compatible end.

The pAcGFP1-tubulin vector was obtained from Clontech (Clontech, cat# 632488) and is based on a fusion of a variant of GFP to human  $\alpha$ -tubulin. The pAcGFP1-tubulin vector was digested with NheI-HF and HpaI restriction enzymes in order to isolate a 2241 bp fragment that contained pAcGFP1-tubulin cDNA. The pAcGFP1-tubulin fragment was ligated to the PF4- $\beta$ -globin vector that was prepared as described above.

The resulting PF4-pAcGFP1-tubulin plasmid was verified both with restriction enzyme digestions and by sequencing.

#### **Electroelution**

PF4-pAcGFP1 tubulin maxiprep were digested with AatII and KpnI and the fragment of interest was isolated by gel purification in 1% agarose gel at 4 C and 96 volts for 4 hours. The gel band of interested was excised under UV visualization and was placed on electroelution tubes followed by electrophoresis at room temperature and 96 volts for approximately 1 hr followed by reversing of polarity for 40 Sec. The electrophoresis buffer within the

electroelution tube was collected and of 1/10 volume NaHCO<sub>3</sub> and 1 volume of Isopropanol were added. The mixture was incubated overnight at -20 °C to promote precipitation. The next day centrifugation of the mixture at 16,000 g and 4 °C for 15 Min was performed. The pellet was air dried and reconstituted on injection buffer. Gel electrophoresis was then performed to estimate DNA content.

Electroelution tubes (Spectra/POR Molecularporous membrane tubing (Catalog #132650) prior to use are boiled in TAE buffer for 5 minutes to destroy DNases. A similar approach was utilized for isolation of the rest of the transgenic DNA constructs.

-

### **Generation of PF4-AcGFP1-tubulin transgenic mouse**

The PF4-AcGFP1-tubulin vector was digested with NheI and KpnI and the PF4-AcGFP1-tubulin fragment was isolated by electroelution and it was provided to the Boston University Transgenic Core for injection into pronuclei of FVB mouse strain oocytes.

Founders were identified based on PCR detection of a transgenic specific sequence using 100 ng genomic mouse tail DNA. The PCR primers were designated to amplify a 594 bp sequence spanning the PF4 promoter and the GFP of the transgenic sequence; forward primer 5'-GTTCCACAAGTGTCATTGCTTCTG-3' and reverse primer 5'-GTATCGCCCTCGAACTTCAC-3'. The PCR reaction was performed at 58 °C for 30 cycles and the fragment was visualized by gel electrophoresis and ethidium bromide staining.



In order to minimize false negative results a PCR reaction of the mouse tail genomic DNA was also performed using GAPDH primers forward 5'-TCACCATCTTCCAGGAG-3' and reverse 5'-GCTTCACCACCTTCTTG-3' at 56 °C for 30 cycles that amplified a fragment of 554 bp.

### **Mouse genomic DNA isolation**

A small amount of mouse tail tissue of every potential founder was digested using 1 µg proteinase K (American Bioanalytical, cat# AB00925) and 300 µl tail digestion buffer (100 mM NaCl, 10 mM Tris pH 7.6, 25 mM EDTA pH 8.0, 0.5% SDS) overnight at 55 °C.

The mouse tissue samples were then centrifuged at 16,000g for 10 minutes. The supernatants were claimed and were treated with 100 µl Protein Precipitation Solution (Qiagen, cat# 1045697) and incubation for 5 minutes on ice after 20 seconds of vortex. The samples were then centrifuged at 16,000 g for 10 minutes and the supernatants were collected. In the next step 300 µl of isopropanol were added and thorough mixing was performed. The samples were centrifuged at 16,000 g for 15 minutes and the supernatant was discarded. The DNA pellets were washed with 500 µl of 70% ethanol followed by centrifugation at 16,000 g for 5 minutes. The supernatant of each sample was discarded and the DNA pellet was allowed to air dry. Finally, 50 µl of ddH<sub>2</sub>O was added to each sample followed by incubation at 65 C to facilitate DNA rehydration. The DNA of mouse tails was stored at -20 C.

## **Bone marrow claiming and cultures**

Mice were euthanized according to Boston University School of Medicine policy and guidelines. Bone marrow cells were claimed from murine femurs and tibias as described previously. Briefly, the epiphyses of femurs and tibias were perforated with a 23 G needle and bone cutter and then the bone marrow was flushed using CATCH buffer (10xHBSS, 3.8% Na3Citrate, 10 mM Adenosine, 10 mM Theophylline, 5% Bovine Calf Serum (BCS)). Bone marrow cell suspension was then centrifuged at 500 g for 5 minutes at 4 C. The supernatant was discarded and the bone marrow pellet was resuspended in 8-12 ml of erythrocyte lysis buffer (17 mM Tris, 14 mM NH<sub>4</sub>Cl) followed with incubation at 37 C for 10 minutes. The bone marrow suspension was then centrifuged at 500 g for 5 minutes at 4 C and the supernatant was decanted. The bone marrow cells were then resuspended in CATCH buffer and centrifuged at 500 g for 5 minutes at 4 C and the supernatant was decanted. The bone marrow cells were resuspended in IMDM media (Gibco, cat# 21056) containing 10% bovine calf serum and 1% penicillin/streptomycin (Gibco, cat# 15070-063) and filtered through a 250 µm mesh to remove tissue debris and clots. Bone marrow cells were then counted and incubated with a concentration of 5-10 X 10<sup>6</sup> cells per ml of medium at 37 C and 5 % CO<sub>2</sub> humidified conditions. Bone marrow cultures were supplemented with TPO 25 ng/ml to promote megakaryopoiesis.

## **Megakaryocyte enrichment by MACS® magnetic bead purification system**

Bone marrow cells were washed with PBS followed with an additional wash using degassed staining buffer (0.5% BSA, 2 mM EDTA, and PBS, pH 7.2) at 500 g for 5 minutes at 4 C .

Bone marrow cells were incubated with anti-CD41-FITC (BD Pharmingen, Franklin Lakes, NJ, cat# 553848) at 4 °C for 30 minutes. Staining buffer was added followed by a centrifugation at 500 g for 5 minutes at 4 °C to remove unbound anti-CD41-FITC antibody. The bone marrow pellet was resuspended in staining buffer and microbeads followed by 15 minutes incubation at 4 °C. Cells were washed and then resuspended in 500 µl staining buffer. The bone marrow suspension was loaded on equilibrated large cell separation column (Miltenyi Biotech, cat# 130-042-202). A 25G needle was assembled in the column to provide flow resistance according to manufacturer's instructions. Two cell fractions were collected, the first one included unlabelled cells which were not retained on the column and the second fraction (obtained after the removal of the magnet) that was consisted of the labeled CD41 positive cells.

### **Imaging of living Megakaryocytes**

Bone marrow cells were washed with PBS at 500g for 5 minutes at 4 °C and then resuspended in IMDM without phenol red (Gibco, cat#21056) supplemented with 1% P/S, 10% BCS and 20% Leibowitz's medium (Gibco, Cat# 21083). Bone marrow cells were subsequently placed on Delta T micro-observation chambers (Optecs, cat# 04200415B) and mounted on Olympus IX70 microscope while the temperature was kept at 37 C. Images were obtained at 600X using 60X lens with 0.9 Numerical Aperture (N.A) and a C4742-95 CCD camera (Hamamatsu,Japan). Images were captured, compiled and analyzed using ImagePro software (Media Cybernetics,Inc).

## Real time PCR Analysis

Cells derived from bone marrow cultures of cell lines were used to isolate RNA. The RNeasy kit (Qiagen, Cat# 74104 ) or RNeasy plus kit (Qiagen, Cat# 74134) were used according to manufacturer instructions, The difference between the two kits is that RNeasy kit employs DNase enzyme to eliminate genomic DNA while RNeasy plus kit employs a gDNA eliminator column.

RNA was quantified and RT-PCR was performed using Applied biosystems High Capacity cDNA Reverse Transcription kit. (Applied biosystems, cat# 4368814) according to manufacturer instructions. We used a mixture of 1:1 oligo dt and 18s primers<sup>183</sup>.

Real time PCR was performed using taqman gene expression assay primers obtained from Applied Biosystems Inc.. We used mouse Emi1 (Cat# Mm 00650195\_m1), PLK3 (Cat# Mm 00457348\_m1 ) and 18s rRNA endogenous control (Cat#4319413E) primers. The reaction mixture included: 10 µl Taqman Gene expression master mix (cat # 4369016), 1 µl cDNA as template, 8 µl dH<sub>2</sub>O and 1 µ of the appropriate assay primer. For 18s the cDNA was diluted 100 times due to is abundant amount.

Real time PCR assay was performed on Applied Biosystems sequence detection system 7300 at the recommended conditions. Briefly, the reaction mixture was subject to 5 minutes hold at 60 C, 10 minutes hold at 95 C followed by 40 cycles of 15 seconds at 95 C and 60 seconds at 60 C. Analysis of data was based on the ddCt method.

## **Cell Cultures**

Y1-10 cell line was maintained in F-12 medium supplemented with 1% P/S and 10% BCS. Ploidy induction of Y-10 cells can be performed using IMDM medium supplemented with 1% P/S and 10% BCS plus 25 ng / ml TPO.

## **Hoechst Staining**

Bone marrow cells of PF4-H2B –GFP mice was incubated with Hoechst stain under conditions similar to live imaging.

## **Generation of the PF4-3XGFP-EMTB construct.**

PF4-  $\beta$  globin vector was digested with NheI-HF (NEB, #R3131) restriction enzyme and the linearized vector was isolated using Gene Clean Turbo kit (MP Biomedicals,#1001-200). In the next step the linearized vector was blunted using DNA Polymerase I, Large (Klenow) Fragment (NEB,#M0210). The blunted vector was isolated using Gene Clean turbo kit. The vector then was digested with NotI (NEB, # R0189) followed by gel purification and elution of the vector utilizing Gene clean turbo kit.

The 3XGFP-EMTB plasmid was obtained from Dr. Niels Galjart (Netherlands) after Dr. Chloe Bulinski (Columbia University, New York) permission. The plasmid was digested with HindIII (NEB, # R0104) and the linearized plasmid was isolated using Gene Clean turbo kit. The plasmid was then subject to blunting using DNA Polymerase I, Large (Klenow) Fragment. The blunted plasmid was isolated using Gene Clean turbo kit followed by NotI digestion. The

fragment of interest containing the 3XGFP-EMTB sequence was isolated by gel purification and elution using Gene Clean turbo kit.

The PF4  $\beta$ -globin vector and the plasmid fragment containing 3XGFP-EMTB were ligated overnight at 16 °C using T4 DNA Ligase (NEB, #M0202) Transformation was done on Dh5a subcloning efficiency competent cells (Invitrogen,# 18265-017) and selection of colonies was based on ampicillin (American Bioanalytical,#AB00115) resistance. Colonies were picked up and mini preps were screened for the presence of PF4 3XGFP-EMTB using a combination of a)HindIII (NEB,#R0104) and XhoI (NEB,# R0146) b) ClaI (NEB,#R0197) and HpaI (NEB,# R0105).

The generation of the PF4-3XGFP-EMTB plasmid was then verified by restriction enzyme digestions and sequencing.

### **Transfection assays of PF4 3XGFP-EMTB plasmid**

The Y-10/L8057 mouse megakaryocytic cell line and the human megakaryoblastic cell line CMK were utilized to perform transfections using the PF4-3XGFP-EMTB plasmid or the transgene used for injections.

Approximately, 600,000 Y-10/L8057 cells were incubated in a 2 ml volume of IMDM (Gibco,#12440) supplemented with 10% BCS, 1% Pen & Strep (Cellgro,#300-002-CI) and 50 nM TPA (Phorbol 12-Myristate 13-Acetate) (Sigma,# P 1585) to induce polyploidization for 3 days. The cells were then washed two times with PBS and plated with IMDM supplemented with 10% BCS but without Pen & Strep or TPA. Few hours later, transfection using Fugene 6

(Roche, ref number 11814443001) was performed. Briefly, 2 µg of PF4-3XGFP-EMTB plasmid and 10 µl of Fugene 6 were mixed in a final volume of 110 µl of transfection mixture. Addition of transfection mixture was performed dropwise with gentle swirling. Cells were incubated overnight at 37 °C and the next day medium was replaced with IMDM without phenol red (Gibco,#21056) supplemented with 10% BCS and 1% Pen & Strep and 50 nM TPA. Medium was replaced again the next day with IMDM without phenol red supplemented with 10% BCS and 1% Pen & Strep and 50 nM TPA. Three days post transfection pictures were obtained with Olympus IX70 microscope in Brightfield as well as using red and green filters. Y-10/L8057 cells that express bright GFP signal were documented, verifying expression 3XGFP-EMTB.

In order to demonstrate that 3XGFP-EMTB localizes with microtubules, transfected Y-10/L8057 cells were fed with fresh IMDM without phenol red supplemented with 10% BCS and 1% Pen & Strep and 10 µM Taxol. Pictures were obtained the next day in an Olympus IX70 microscope, in Brightfield as well as using red and green filters.

CMK cell line was grown in RPMI-1640 without L-Glutamine (Lonza, #12-702E) supplemented with BCS, 2 mM L-Glutamine (Gibco,#25030-081) and 10 nM TPA for two days. Cells were then washed with PBS and approximately 1,200,000 cells were plated in 1 ml of RPMI-1640 without L-Glutamine, supplemented to 2 mM L-Glutamine and 10% BCS without antibiotics. Transfection was performed with 800 ng PF4 3XGFP-EMTB plasmid or transgene preparation for injection. Pictures were obtained the next day in the IX70 olympus microscope. In the next step, cells were washed and those transfected with the PF4 3XGFP-EMTB transgene were fed with 2 ml RPMI-1640 without L-glutamine supplemented to 2mM L-

glutamine, 10 % BCS, 1% Pen Strep and 10 mM taxol. Pictures were obtained 24 hours later as described previously demonstrating that 3XGFP-EMTB decorates microtubules.

Transfection of transgene was also based on manufacturer recommendations for maximum DNA concentration.

### **Generation of the PF4 3XGFP-EMTB transgenic mouse model**

The PF4-3XGFP-EMTB plasmid was digested with AatII (NEB, # R0117) and XhoI restriction enzymes to release a fragment that contains the PF4 promoter, the 3XGFP-EMTB sequence, the  $\beta$ -globin intron and a poly A tail. The digestion mixture was run on a 0.8% gel at 4 C. The gel band containing the fragment of interest was excised and the fragment was eluted using either a) electroelution or Gene clean kit (based on silica beads-MP Biomedicals,# 1001-200)). Serial dilutions of the isolated fragment confirmed the presence of a single band corresponding to the anticipated molecular weight. In addition, estimation of the DNA amount was performed by comparing the band intensity with that of the 1Kb marker (NEB,# N0468G). The transgene was provided to the Boston University Transgenic Core for injection in male pronuclei of FVB mice.

Founders screening was based on PCR approach as was previously described. Two different PCR primer pairs were used. SCRI screening pair was composed by a) forward: GTTCCACAAGTGTCATTGCTTCTG and reverse: ACCTCTTCTTCCGCTCTTCC and the SCRIII by forward: TGGATCTAGCAGCACCTCT and reverse: ACGACCAACGGTTATGCTTC. In addition, GAPDH primers were used to check DNA quality and exclude false negatives.



## **FACS screening of PF4 3XGFP-EMTB founders platelets**

Screening for expression was based on detection of fluorescent platelets. Blood samples of potential founders, wild type mice (negative control) and GFP (positive control) were obtained using retroorbital bleeding. Blood samples were mixed with Aster Jandl anti-coagulant (85 mM Sodium Citrate, 69 mM Citric Acid, 2 % (w/v) Glucose, with the final pH titrated to 4.6). Samples were centrifuged at room temperature at 500g for 10 minutes. Plasma rich in platelets was collected and subject to FACS for the detection of GFP fluorescence using FACScan (BD Dictinson). Gating of platelets was based on size and events were acquired in linear scale. FACS analysis was based on BD Cellquest Pro v5.2 software.

## **Generation of the PF4 Cyclin E mouse**

The PF4 Cyclin E plasmid was generated by a former lab member Dr. Kenian Lieu. This plasmid is based on the PF4  $\beta$ -globin backbone and the human Cyclin E1 cDNA was subcloned between the rat PF4 promoter and the  $\beta$ - globin intron. Hence, PF4 promoter drives expression of the human Cyclin E1 followed by the  $\beta$ - globin intron and a poly A tail.

The plasmid was digested with AatII and XhoI restriction enzymes and the fragment of interest was purified by gel electrophoresis at a 0.8% agarose gel run at 4 C. The fragment of interest was excised and its elution was based on electroelution. Serial dilutions indicated that the concentration was 125 ng/ $\mu$ l. The transgene composed by the rat PF4 promoter, human Cyclin E1 cDNA the intron and poly A tail was provided to Boston University School of Medicine transgenic core for injection in FVB male pronuclei. Identification of founders and

biochemical analysis was assigned to Alexia Eliades (graduate student of Department of Biochemistry Ph.D program).

### **Identifying homozygotes of the PF4-Cyclin E transgenic mouse model**

The generation of PF4 Cyclin E homozygotes was based on a real time PCR using genomic DNA as template. The rationale was that comparison of transgene number between mice using an murine gene for normalization would reveal homozygotes from heterozygotes. Namely, homozygotes have twice the copy number of transgenes compared to heterozygotes.

Breedings were set between PF4 Cyclin E heterozygotes and tail tissue was claimed from mouse progeny that were carrying the transgene (based on conventional PCR screening). Processing of tail tissue to claim genomic DNA was previously described.. Approximately 100 ng genomic DNA were used per assay and transgene copy amount was assayed using CCNE1 Taqman primer (Applied Biosystems,#Hs0023356\_m1). Normalization was based on a Taqman primer set that recognize a genomic sequence of the mouse Adenosine A<sub>2</sub>B receptor gene (Adora2b) (Applied biosystems,#Mm0128529\_S1) and reaction was carried in the Taqman gene expression master mix (Applied Biosystems). Estimation of transgene amounts was based on the delta delta C method.

### **BrdU (Bromodeoxyuridine) assay**

Cyclin E mice and gender and age matched wild type (FVB) mice were injected intraperitoneally with BrdU (BD pharmingen, material # 550891) solution. Namely, 100 µl (1 mg) BrdU were diluted with 300 µl DPBS and 2 hours post injection mice were sacrificed and bone marrow was claimed. An age and gender matched wild type mice (non exposed to BrdU)

was also sacrificed in order to discern non specific binding of the anti-BrdU antibody. All bone marrow samples were processed at the same time.

Bone marrow cells were washed twice with 1% BSA in PBS and the pellet was resuspended in 1% BSA in PBS held in ice. Cells were added dropwise in 3 ml EtOH pre-chilled at -20 C. Cells were suspended several times followed by vortexing in order to obtain single cells suspensions. Fixed cells were kept at -20 C for 1 hr. In the next step fixed cells were centrifuged at 400g for 10 minutes at 10 °C. The cell pellet was resuspended at 1 ml 2N HCl in 0.5% Triton X-100 solution for 30 minutes in room temperature. This step is necessary to create single stranded DNA and expose incorporated BrdU.

Cells were then centrifuged at 500g for 10 min and the cell pellet was resuspended in 1 ml Sodium tetraborate decahydrate (Borax) (Sigma, #71999) pH adjusted to 8.5. Cells are centrifuged at 500g for 10 min.

Cells then were resuspended in 0.5% Tween 20, 1% BSA in PBS. After cell counting,  $10^6$  cells were placed in 1 ml of 0.5% Tween 20, 1% BSA in PBS and 50 µl FITC conjugated anti-BrdU antibody (Becton Dickinson, #347580) was added. Incubation is performed for 30 minutes under dark conditions in room temperature.

The cells were centrifuged at 500g for 10 min and then resuspended in 450 µl PBS. 3 slides are cytospan per sample each with 150 µl of cell suspension. The cells are mounted with DAPI.

Cells were observed in an Olympus IX70 microscope and megakaryocyte identification was determined by morphology and size. The threshold for identifying megakaryocytes was set at 20 µm. Pictures were obtained in brightfield and phase. Bone marrow samples of the

untreated mouse that were incubated with Fitc- anti Brdu antibody did not reveal significant staining.

### **Bone marrow treatment with LOX-PP**

Bone marrow was claimed from FVB mice and it was plated for 3 days under 5% serum conditions in the presence of LOX-PP or vehicle. Briefly, the epiphyses of femurs and tibias were perforated with a 23 G needle and bone cutter and then the bone marrow was flushed using CATCH buffer (10xHBSS, 3.8% Na<sub>3</sub>Citrate, 10 mM Adenosine, 10 mM Theophylline, 5% Bovine Calf Serum (BCS)). Bone marrow cell suspension was then centrifuged at 400 g for 5 minutes at 4 C. The supernatant was discarded and the bone marrow pellet was resuspended in 8-12 ml of erythrocyte lysis buffer (17 mMTris, 14 mM NH<sub>4</sub>Cl) followed with incubation at 37 °C for 10 minutes. The bone marrow suspension was then centrifuged at 400 g for 5 minutes at 4 °C and the supernatant was decanted. The bone marrow cells were then resuspended in CATCH buffer and centrifuged at 400 g for 5 minutes at 4 C and the supernatant was decanted. The bone marrow cells were resuspended in PBS, filtered through a 250 µm mesh to remove tissue debris and clots and centrifuged at 400g for 5 minutes at 4 C. Supernatant was decanted and Bone marrow cells were resuspended in plain IMDM and centrifuged at 400g for 5 minutes at 4C. Bone marrow cells were then resuspended in a small volume of plain IMDM and cell counting was performed. Equal number of cells was plated in 1 ml plain IMDM in the presence of 10 µg LOX-PP or equal volume dH<sub>2</sub>O (vehicle). 15 minutes post plating 50 ng TPO was added in all samples and cells were incubated for another 45 minutes. Bone marrow cultures were supplemented with IMDM with 10% BCS and Penicillin/Streptomycin (P/S) to obtain a final volume of 2 ml IMDM with 5% BCS,1% P/S,25 ng/ml TPO. 10 µg LOX-

PP or vehicle were also added and cells were cultured for 3 days at 37 °C and 5 % CO<sub>2</sub> humidified conditions.

A similar approach was employed for the analysis of PF4 Cyclin E transgenic mouse bone marrow cultures. More specifically, 3 male seven week old heterozygote Cyclin E mice were sacrificed and  $13 \times 10^6$  cells were treated with 10 µg/ml LOX-PP or vehicle and cells were fixed 3 days later. No wild type mice were included.

### **FACS analysis of the LOX-PP samples**

Bone marrow cultures were washed and centrifuged twice with PBS at 400g for 5 minutes at 4 C. Bone marrow cells were then suspended in approximately 150 µl PBS and added dropwise in 3 ml of Ethanol (-20 C). Cells were vortexed for 30 seconds and resuspended by pipeting to obtain single cell suspensions. Fixed cells were stored at -20 C.

Fixed cells were washed twice with PBS at 400g for 10 minutes at 4 C. Cells were resuspended in 450 µl 10% BCS in PBS (blocking solution) and cells were counted. The number of cells of each sample was adjusted to obtain equal number of cells across all samples in a final volume of 450 µl blocking solution. Samples were incubated with 3 µl FITC Rat CD41 (BD Biosciences, # 553848) or FITC Rat IgG (isotype) (BD Biosciences, # 554684) for 30 minutes in ice under dark conditions. Cells were then washed with PBS at 400g for 5 minutes at 4 C. Cells were then resuspended in 600 – 800 µl staining solution and incubated at 37 C for at least 45 minutes. Staining solution is consisted of 0.05 mg/ml Propidium Iodine and 100 µg/ml Rnase A in PBS.

Samples were filtered through a mesh filter into flow cytometry tubes and subject to FACS analysis in FACSscan (Becton Dickinson). Data were analyzed using CellQuest software (Becton Dickinson).

The PF4 Cyclin E mouse bone marrow cultures cells were fixed and analyzed with the same manner as described above.

### **LOX-PP immunofluorescence**

Bone marrow culture cells were washed two times with PBS and centrifuged for 5 minutes at 400g at 4C (or at room temperature for double immunofluorescence experiments). Cells were then cytospan using the following settings speed: 480 rpm, acceleration: low and time:5 minutes. Slides were then placed in a 4% formaldehyde solution in PBS kept in room temperature for 30 minutes. Two washes with PBS for a total of 10 minutes were then performed to remove residual formaldehyde. Cells were permeabilized with ice cold 0.2% Triton X-100 in PBS for 20 minutes. Followed by two washes with PBS for a total of 10 minutes.

Slides were then incubated at room temperature with 2% donkey serum in PBS (Blocking Solution-BS). Rabbit polyclonal LOX-PP antibody provided by Dr Trackman's laboratory (concentration 2.69  $\mu\text{g}/\mu\text{l}$ ) was used in a dilution (1.68  $\mu\text{l}$  in 1200  $\mu\text{l}$  of BS). The rabbit normal IgG serving as isotype was provided by Dr Trackman's lab and is produced by Vector labs (Cat#I-1000, concentration 5 mg/ml).

Three washes were performed with PBS (30 minutes total) followed by addition of secondary donkey anti rabbit Alexa 594 antibody 1:200 dilution in BS and incubation was performed for 1 hr at RT. Followed by three washes performed with PBS (30 minutes total). Slides were mounted with Vectrashield mounting medium with DAPI

For experiments visualizing microtubules the same protocol was followed with the addition of primary mouse monoclonal anti tubulin (Santa Cruz) at 1:200 dilution and secondary goat anti mouse Alexa 488 at 1:800 dilution for visualizing microtubules.

## **CHAPTER III.**

### **RESULTS**

#### **Part I. Visualization of Megakaryocytic endomitosis through the PF4-H2B-GFP model.**

Here, GFP is shown to localize with Hoechst staining (figure 1) and a high ploidy Megakaryocyte is undergoing endomitosis exhibiting an annular arrangements of chromosomes (figure 2).

Colocalization of GFP and chromosomes (visualized by Hoechst staining) precludes a non specific pattern of staining of GFP.

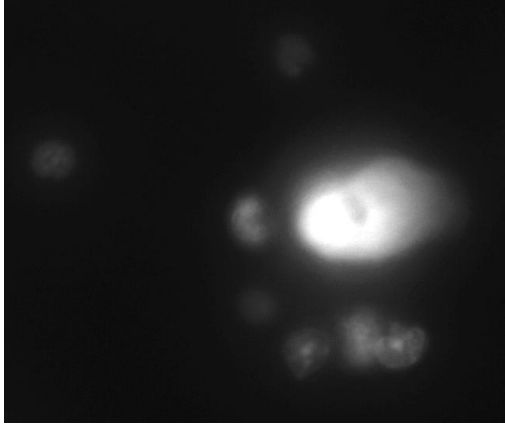
A low ploidy megakaryocyte is shown to have a midzone formed which disappears as the chromosomes are rejoined into a single group. By contrast, the high ploidy Megakaryocytes were initially had a tight chromosomal formation which then expanded without a clear midzone formation.

Finally, chromosomal measurements are included to denote low ploidy megakaryocytes are initially separated in two groups with smaller size chromosomal content prior to rejoining to one group. The high ploidy Megakaryocytes have a larger dimension of chromosomal content which occupies more space once expansion occurs.

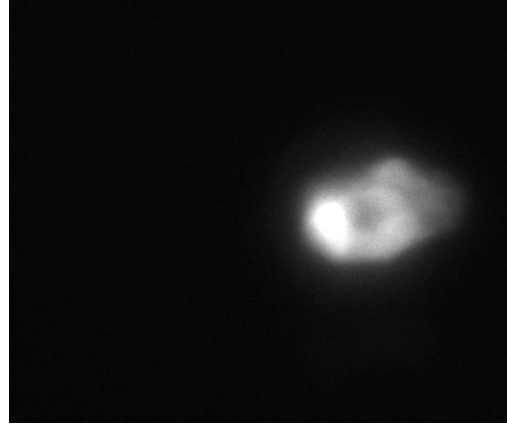


**Figure 1. Hoechst staining of the PF4-H2B-GFP Megakaryocytes.**

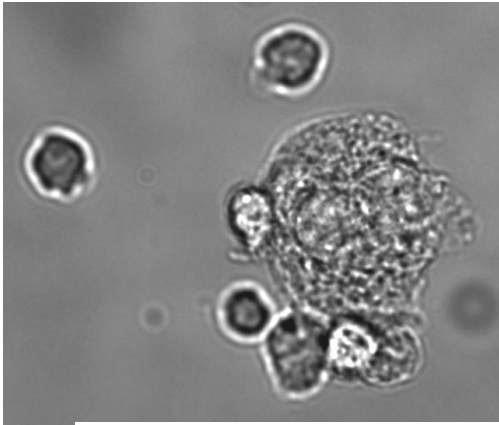
Bone marrow cells derived from bone marrow of PF4-H2B-GFP mice were incubated with IMDM with 10% BCS and 1% P/S in the presence of Hoechst. The bone marrow cells were then mounted on biopetecs optical dish and were viewed using brightfield, GFP and UV filter. The GFP signal co localize with Hoechst staining (viewed in UV filter) in a PF4-H2B-GFP derived Megakaryocyte. Original magnification 60X.



Hoechst



GFP



Brightfield

**Figure 2. Low ploidy Megakaryocyte undergoing endomitosis.**

A low ploidy Megakaryocyte (as compared in size to neighboring cells) undergoing endomitosis with a clear midzone formed between the chromosomal groups.

The arrow denotes the midzone formation. Original magnification 60X.

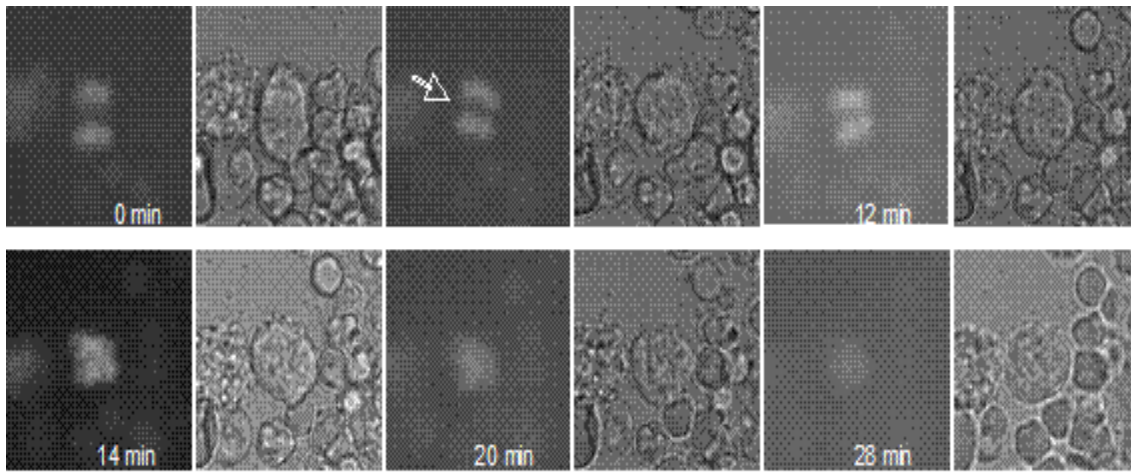


**Figure 3. A high ploidy Megakaryocyte undergoing endomitosis.**

A Megakaryocyte derived from bone marrow of PF4-H2B-GFP mouse model was followed undergoing endomitosis. The chromosomes initially were spread but at 10 minutes of observation form a tight cluster. At 20 minutes chromosomes have separated to at least 4 groups in an annular formation. The chromosomal groups begin delineation at 44 minutes. Original magnification 60X.

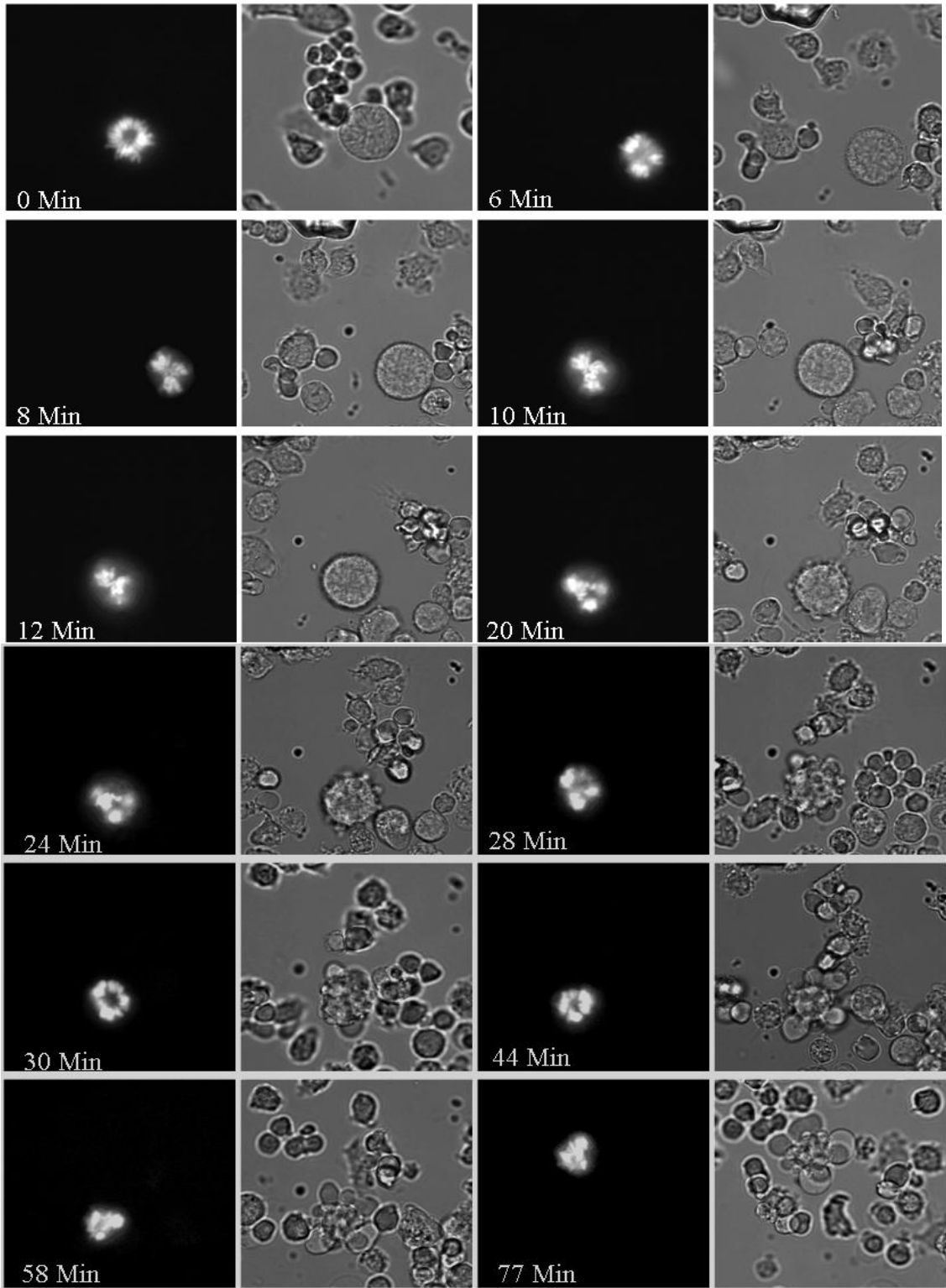
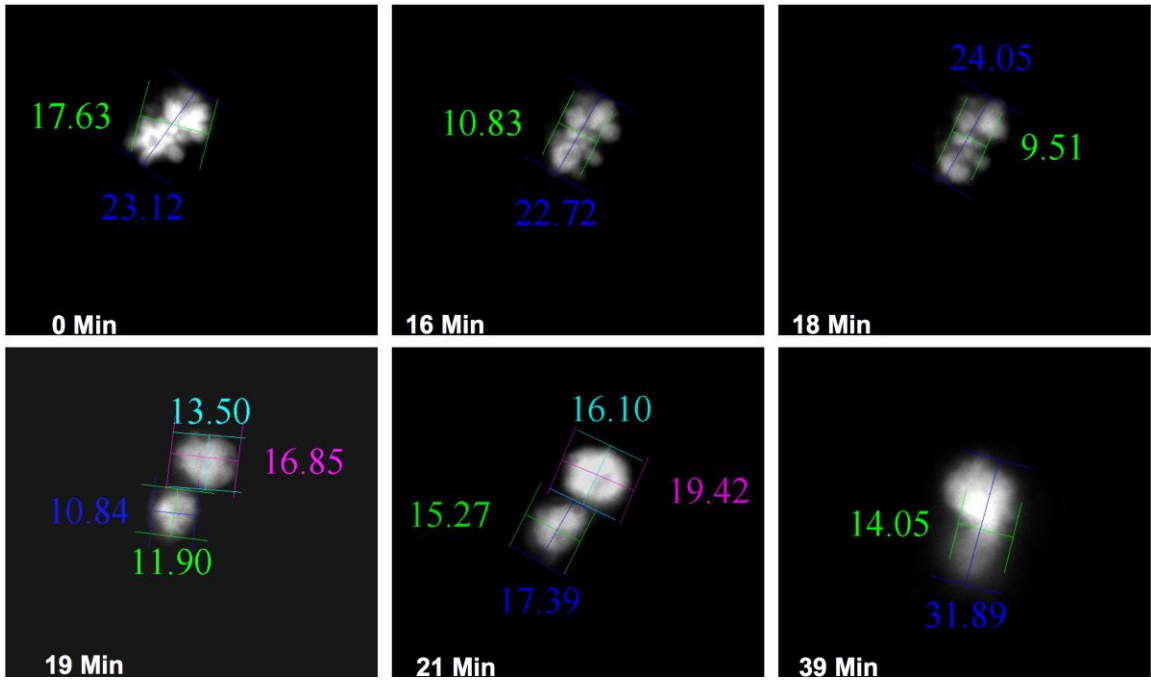
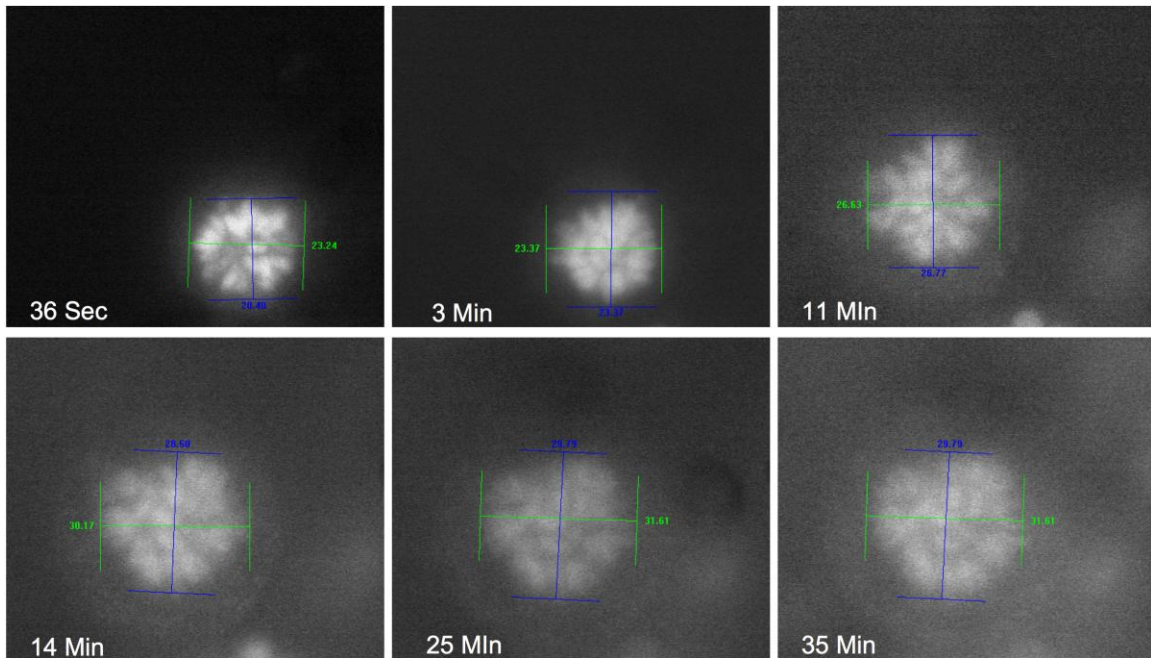


**Figure 4. Measurements of chromosomal dynamics during endomitosis.**

In Panel A the chromosomes are originally aggregated but then dissociated to two groups with smaller diameter before they rejoin in a single group with slightly larger dimensions compared to the original assembly. In Panel B and C high ploidy megakaryocytes are depicted initially to have a multi lobar aggregation of chromosomes which then expands to significantly larger proportion compared to initial aggregation.

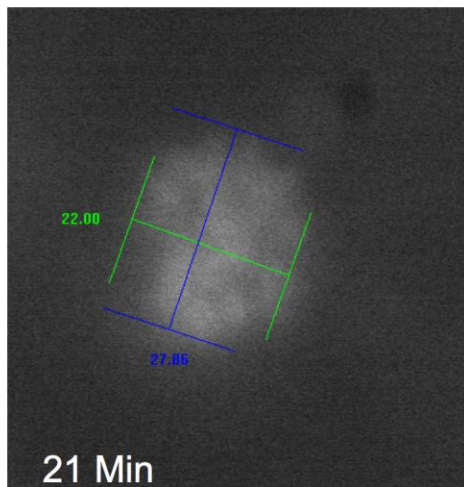
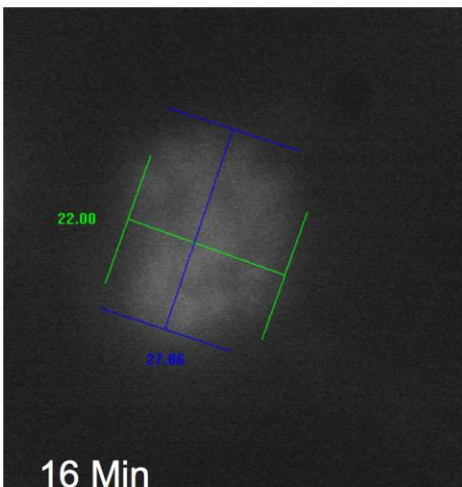
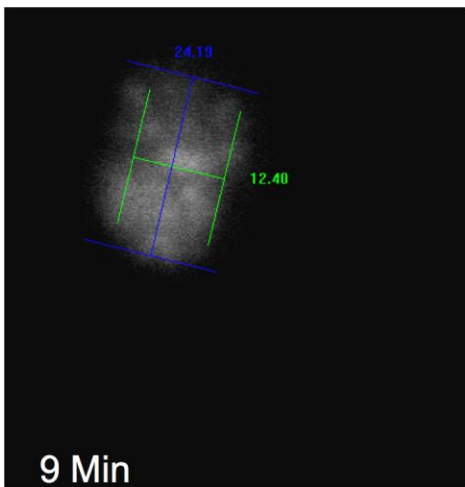
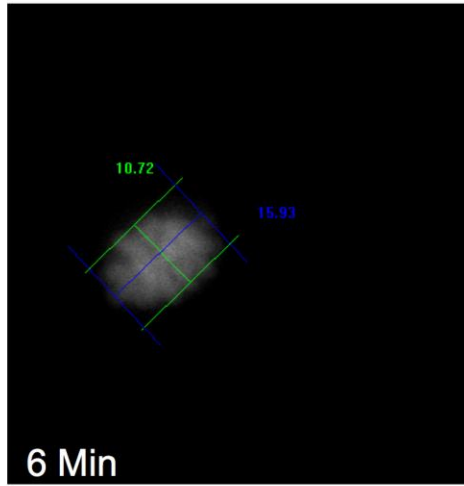
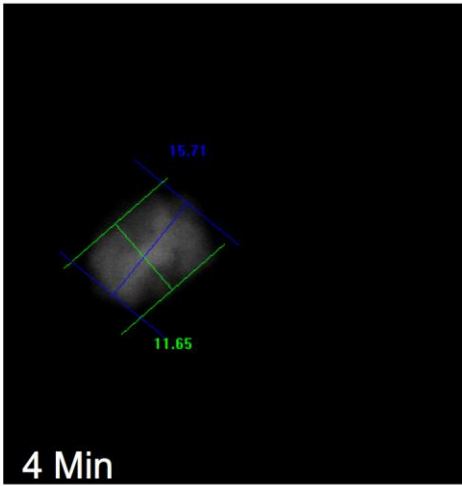
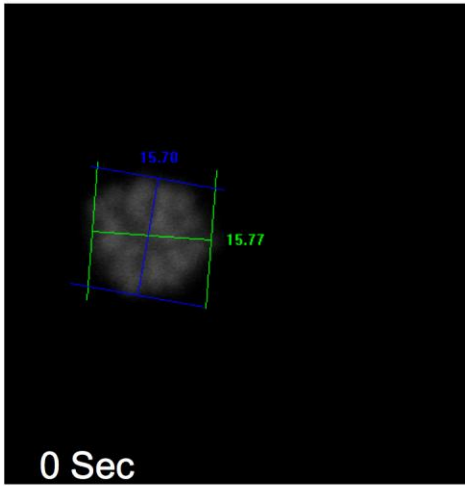


A



B





C

## **Part II. Transgenic mouse models to visualize the microtubule network.**

We sought to generate a transgenic mouse model that the microtubules of Megakaryocytes would be visualized. Visualization of microtubules could elucidate many aspects of the Megakaryocytic physiology. For example, coupled with fluorescently tagged proteins could reveal associations and dynamics of proteins crucial for endomitosis that are difficult to be discerned on fixed cells. In addition, it would be helpful to study proplatelet formations or platelet cytoskeleton and may also elucidate aspects of syndromes that animal models are lacking.

### **Results**

Our first attempt involved the generation of a transgenic mouse model where PF4 promoter drives expression of the mCherry human alpha tubulin. This transgenic mouse line would be expected to have microtubules that could be visualized in the red spectrum and would be ideal to create a double transgenic mouse by crossing with the PF4-H2B GFP transgenic line.. However, expression in several founders lines of the mCherry human alpha tubulin was not optimal for live imaging.

The second attempt involved the generation of the PF4-AcGFP1-tubulin transgenic mouse. The AcGFP1 tubulin plasmid is commercially available and the sequence encoding the chimeric protein of AcGFP1 human tubulin was excised and subcloned in PF4 plasmid. Although transfection experiments in cell lines were promising founders showed diminished expression which was not suitable for live imaging.

The last attempt involved the construction of the PF4 3XGFP-EMTB transgenic mouse line. In this transgenic mice the 3XGFP-EMTB sequence was subcloned in the PF4 plasmid. The plasmid containing the 3XGFP-EMTB sequence was obtained through collaboration. The PF4 3XGFP-EMTB has a size of 8520 bp and a sit was the case with previous constructs its generation was confirmed by restriction enzyme digestions and sequencing. Furthermore, transfection experiments using the whole plasmid and cell lines confirmed its expression.

Plasmid was digested with AatII and XhoI to release the fragment we would use for injection in male pronuclei in order to generate transgenic mice. The fragment released for injection was further confirmed by digestion using the restriction enzyme.

Founders were identified and platelet screening by FACS for GFP fluorescence was performed. The initial group of founders did not reveal expression by FACS which was further confirmed by imaging of bone marrow cultures in the presence of TPO (to stimulate megakaryopoiesis).

**Figure 5. The organization of the PF4 plasmid.**

The PF4 plasmid is composed by the Rat PF4 promoter sequence followed by a polylinker site (that contains several restriction sites) and an intron sequence and a poly A tail. The intron sequence has been shown to stabilize expression levels.

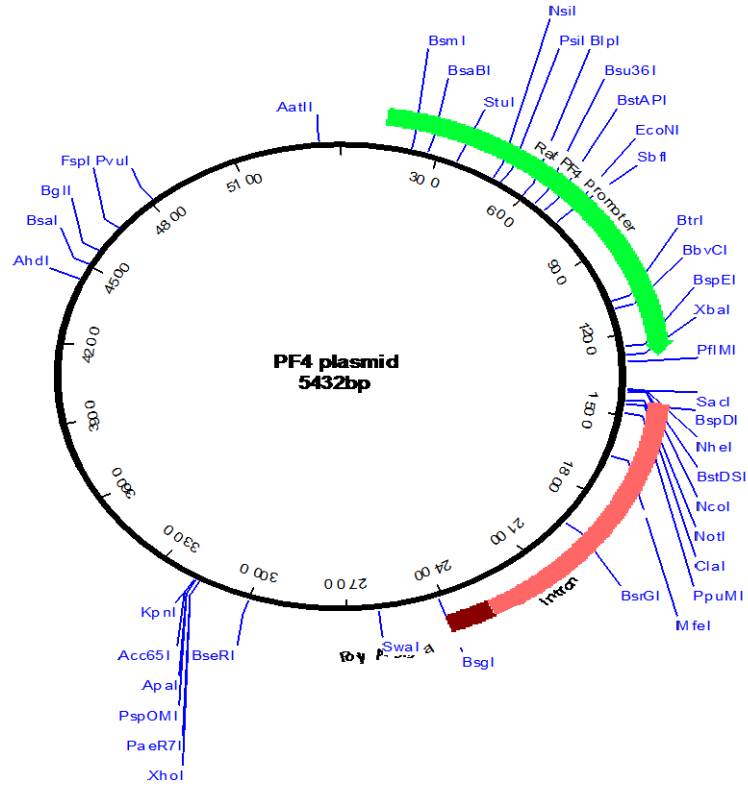


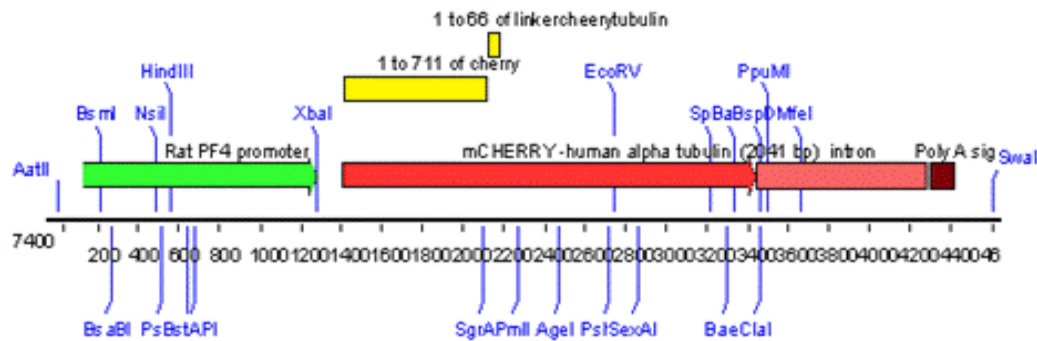
**Figure 6. The PF4 mcherry human tubulin construct and founders testing.**

A schematic description of the first transgenic mouse that was constructed to visualize the microtubules of Megakaryocytes (Panel A). A plasmid designated as PF4 mCherry human tubulin was generated by subcloning the mCherry Human tubulin sequence to the PF4 plasmid polylinker area. The plasmid containing the mCherry human tubulin was obtained by Chen lab through a collaborator. PCR primers were designated to recognize a unique sequence of 500 bp between the PF4 promoter sequence and mCherry human tubulin. The PCR primers were Forward 5'- GTTCCACAAGTGTCATTGCTTCTG- 3' and reverse 5' - CTTCAAGTAGTCGGGGATGTTCG -3'.

An example of Potential founders testing. A batch of founders is tested using PCR approach and at the same time genomic DNA of a non founder and a previously recognized founder are used for controls. Furthermore, the PF4 mCherry human tubulin plasmid was used as a further positive control (Panel B).

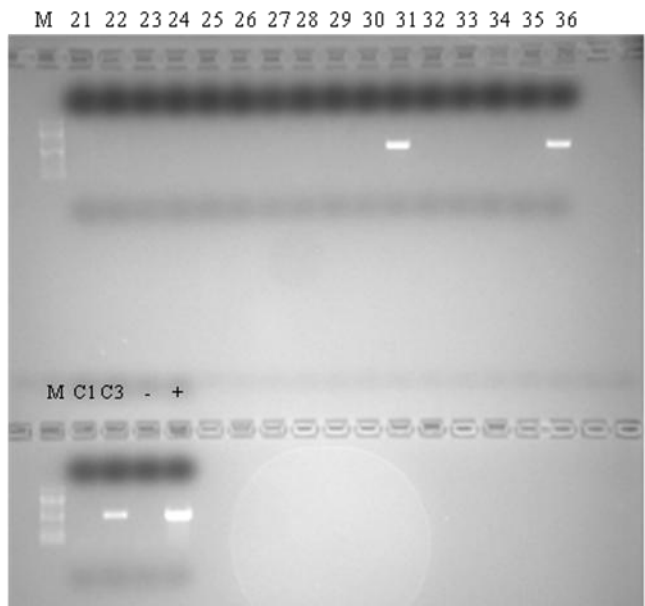
Unfortunately, expression of Megakaryocytes derived from founders was dim and hence unsuitable for live imaging. In panel C bone marrow cells were cultured in the presence of TPO for 3 days and megakaryocytes were observed with red and bright field filters. Few megakaryocytes were noted to have red fluorescence and in those observed the level was very dim (Panel C). Original magnification 60X.

## PF4-mcherry human tubulin

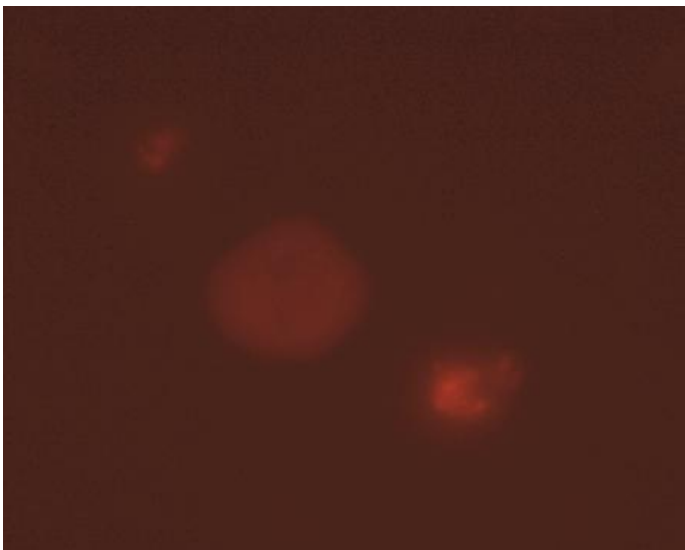


**A**

- Potential founders 21-36 were tested with PF4-mcherry primers @ 57 C.
- M= 100 bp DNA ladder
- 21-36= potential founders
- C1= DNA from mouse #1 (non founder)
- C3 = DNA from mouse #3 (founder)
- - = no DNA template
- + = PF4-mcherry Plasmid

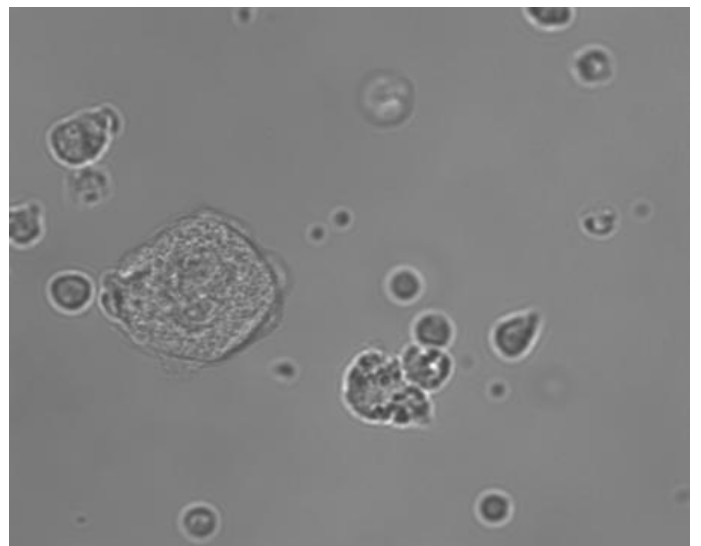


**B**



**Red filter**

**C**



**Brightfield**



**Figure 7 . The PF4-AcGFP1-tubulin construct.**

The PF4 plasmid was used to subclone the AcGFP1 human alpha tubulin sequence. The fragment containing the sequence of AcGFP1 human alpha tubulin sequence was retrieved from a commercially available plasmid – the pAcGFP1 human alpha tubulin. In the PF4-AcGFP1-tubulin the rat PF4 promoter 1.1 Kb fragment drives the expression of AcGFP1-human alpha tubulin cDNA. The intron sequence serve to stabilize transgene mRNA levels. The plasmid can be propagated in bacteria using the antibiotic ampicillin as a resistance marker. The PCR primers used for screening of potential founders were designated to amplify a sequence that spans both the PF4 promoter and AcGFP1-tubulin region and is denoted by a shaded box. The restriction sites of some commonly used restriction enzymes are also shown.

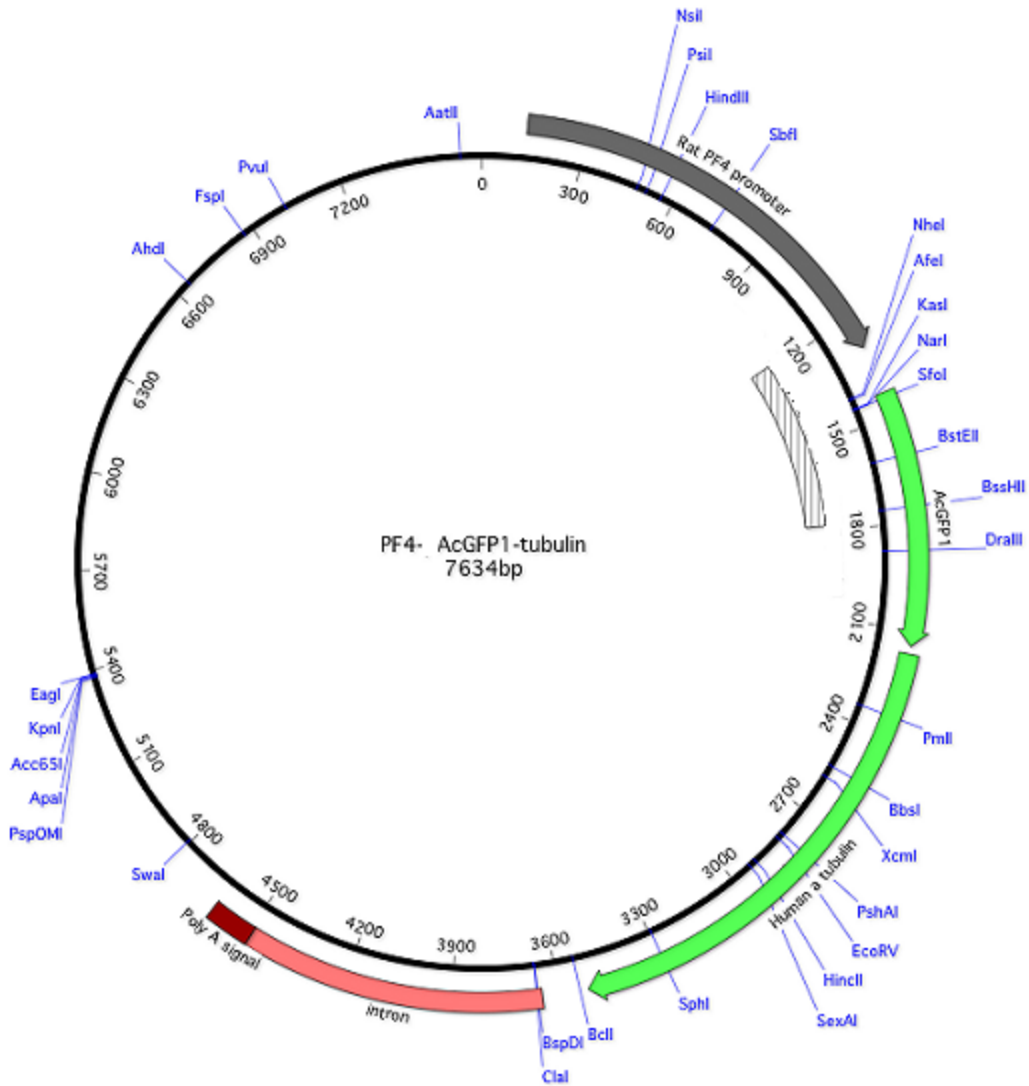
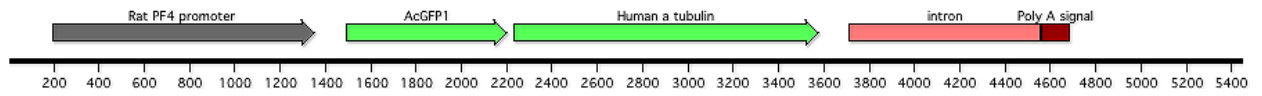
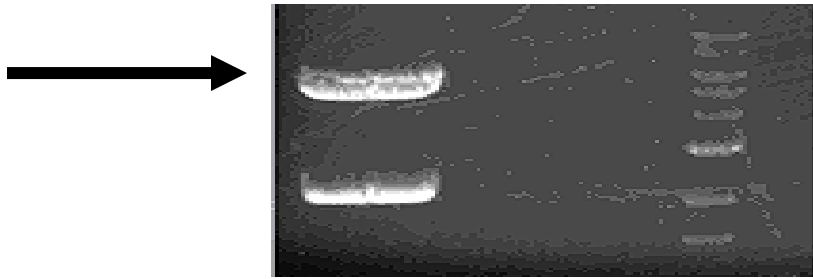


**Figure 8. The generation of the PF4-pAcGFP1-tubulin transgenic mouse.**

(A) schematic representation of the DNA fragment that was used for microinjection in male pronuclei of fertilized oocytes of FVB strain. (B) gel microphotograph displaying the fragment of interest (denoted by an arrow) prior to excision and electroelution. The fragment was released by digestion with the restriction enzymes AatII and KpnI. The black arrow indicates the fragment that was claimed with a predicted size of 5450 bp. The lower band had a size of 2150 bp.



(A)

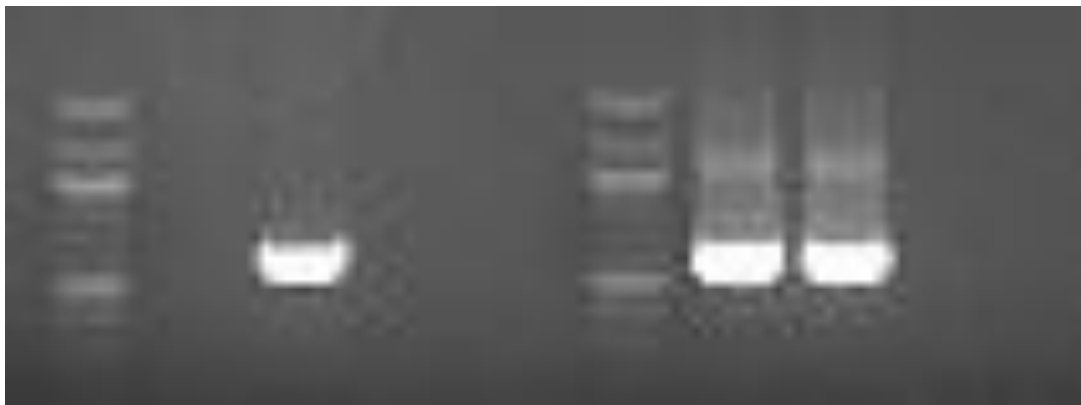


(B)

**Figure 9. Screening for potential founders of PF4-AcGFP1-tubulin transgenic mouse model.**

100 ng of genomic mouse tail DNA of the potential founders were used for PCR reactions using primers that a) recognize a sequence of PF4-AcGFP1-tubulin transgene construct and b) GAPDH genomic sequence. In the transgenic mice (Tg) a band was detected using the primers that recognize the sequence of PF4-AcGFP1-tubulin transgene construct. This band is absent on wild type (wt) mice. Every potential founder was verified with PCR screening of a second -separate - tail DNA preparation. NEB 100 bp Ladder was used (M) to provide an estimate of the band sizes.

M Wt Tg Neg. control M Wt Tg Neg. control

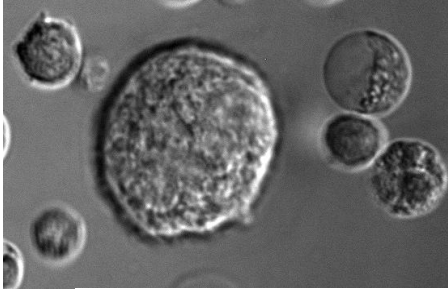


PF4-AcGFP1-tubulin primers

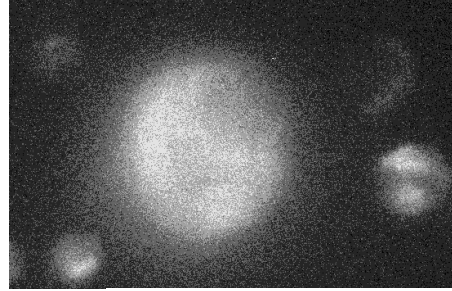
GAPDH Primers

**Figure 10. Imaging of Megakaryocytes derived from cultured bone marrow of PF4-AcGFP1-tubulin transgenic mouse model.**

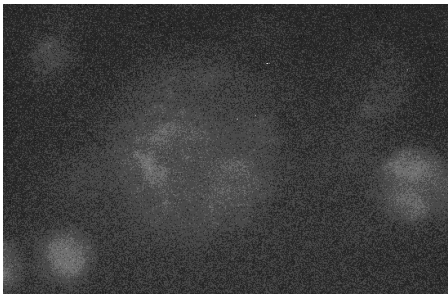
Bone marrow of PF4-AcGFP1-tubulin transgenic mice was cultured in the presence of TPO followed by mounting on microscope to obtain pictures in brightfield, and also GFP and Red filters. The exposure time of pictures obtained using GFP and Red filters was the same. Megakaryocytes were recognized based on their size compared to surrounding bone marrow cells. Megakaryocytes derived from two different founders are shown in panels A and B. Original magnification 60X.



Brightfield

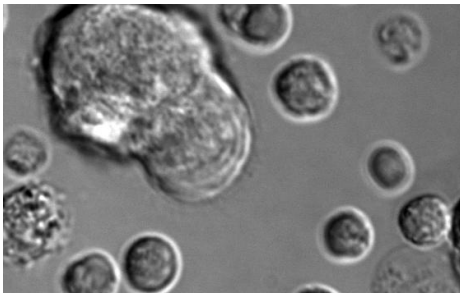


GFP

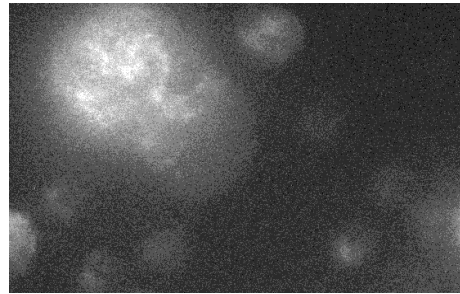


Red

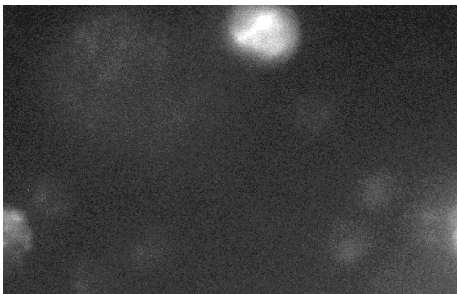
(A)



Brightfield



GFP



Red

(B)



**Figure 11. Schematic representation of PF4-3XGFP-EMTB.**

The PF4-3XGFP-EMTB plasmid is composed by the Rat PF4 promoter driving expression of EMTB fused in frame with 3 GFP moieties followed by the b-globin intron and a polyA tail. The PF4-3XGFP-EMTB carries the ampicillin resistance gene. The restriction sites of the XbaI and ClaI restriction enzymes sites that were used for verification of maxi prep are displayed. In addition, the restriction sites of AatII and XhoI that were used for isolation of the transgene for injection are also depicted.

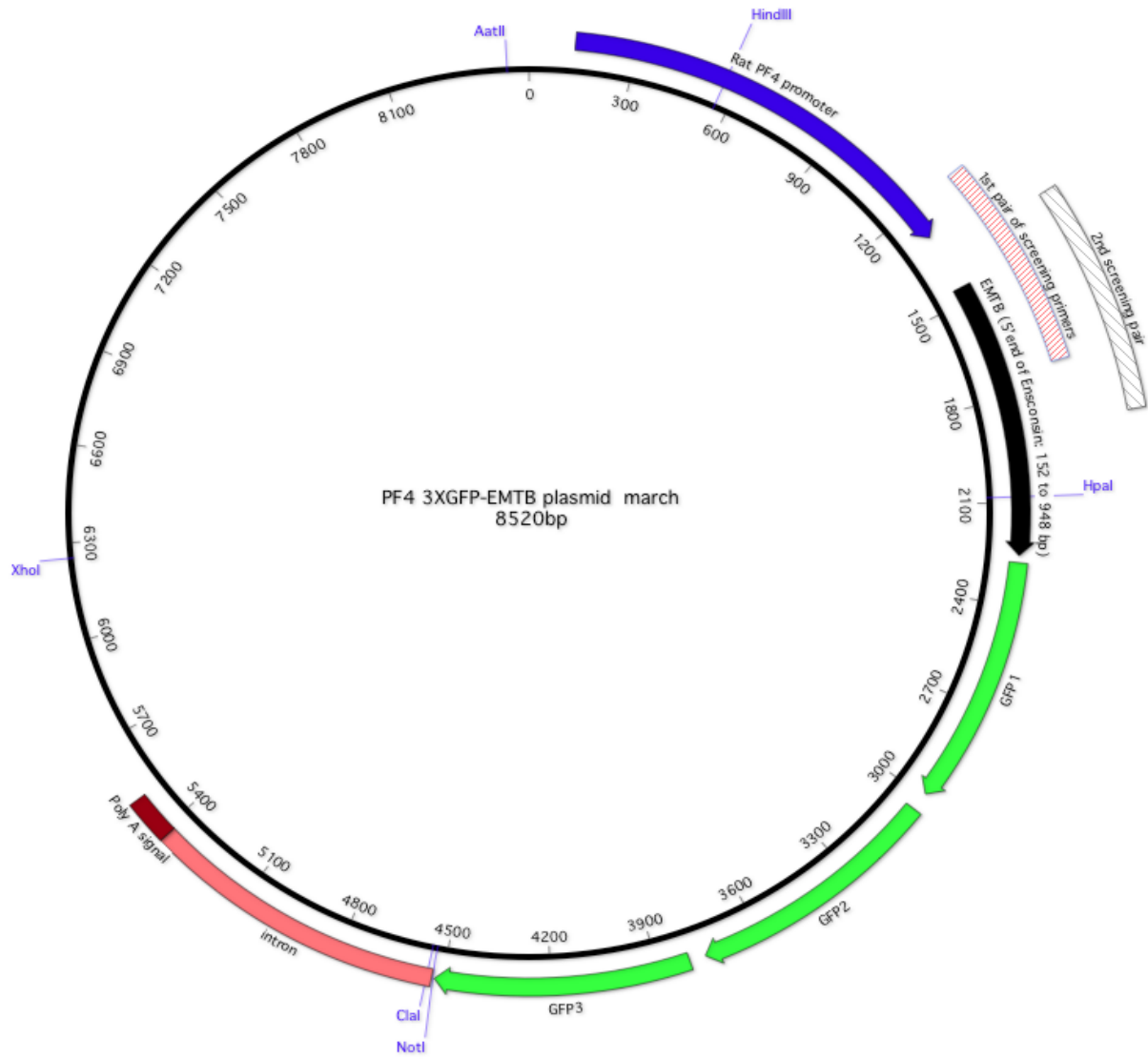
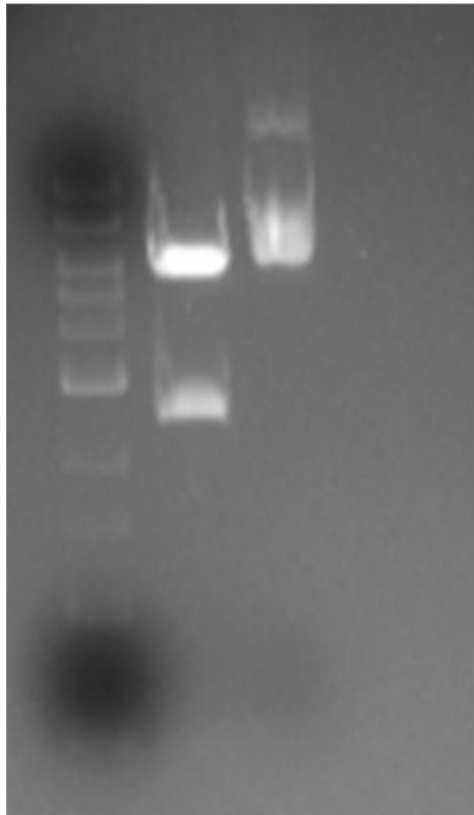


**Figure 12. Maxi prep verification of PF4 3XGFP-EMTB using HpaI and ClaI.**

Simultaneous digestion with HpaI and ClaI release two fragments with predicted size of approximately 6 Kb and 2.5 Kb. Undigested PF4 3XGFP-EMTB plasmid was also run simultaneously as control.

M 1 2



M = 1 Kb marker

1 = PF4-3XGFP-EMTB digested with ClaI + HpaI

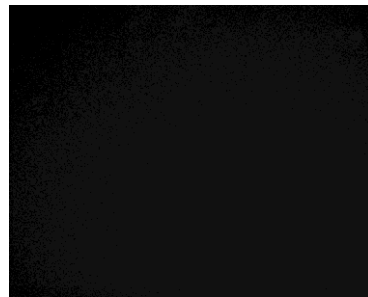
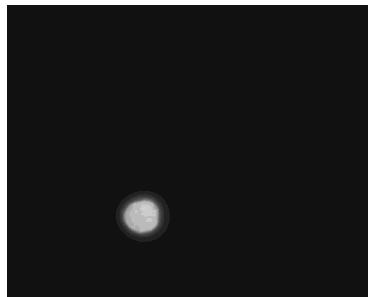
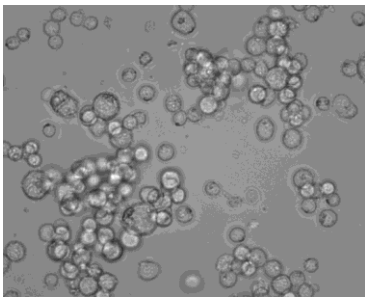
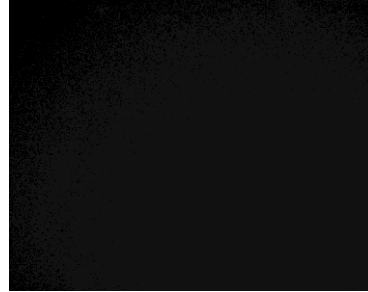
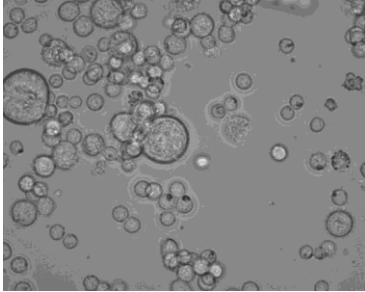
2 = PF4-3XGFP-EMTB uncut

← 6 Kb

← 2.5 Kb

**Figure 13. Transfection expression of PF4 3XGFP-EMTB in Y-10/L8057 cell line.**

The PF4-3XGFP-EMTB plasmid was transfected in Y-10s that were induced to polyploidize using TPA for 3 days. Pictures were taken 3 days post transfection. Images were obtained in 40X and in brightfield and using green and red filters to verify expression of the plasmid. Red filter was used to rule out autofluorescence.



Brightfield

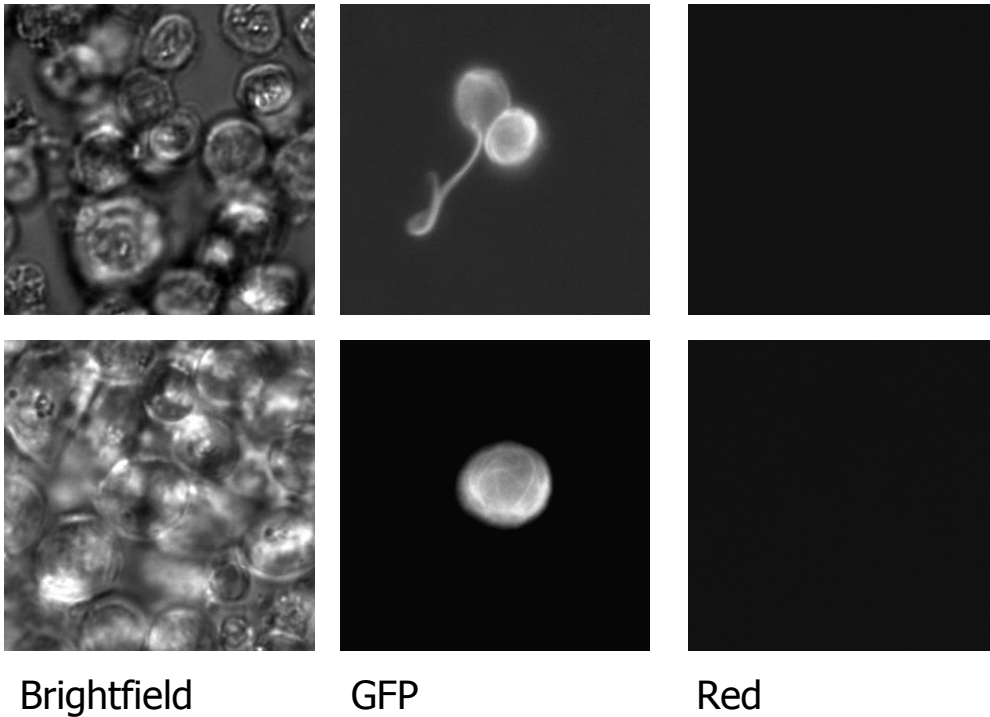
GFP

Red

40X. Approx 500 msec exposure time.

**Figure 14. Treatment of transfected Y-10/L8057 reveals that 3XGFP-EMTB decorates microtubules.**

Transfected Y-10/L8057 cells were treated with taxol –to stabilize microtubules in a metaphase stage- and pictures were taken with green filter to visualize decorated microtubules and with red filter to rule out autofluorescence. Brightfield was also included to visualize the morphology of cells.



Original magnification 40X.

Overnight incubation with Taxol 10  $\mu$ M.

Approx 120 hr post transfection with PF4-3xGFP-EMTB



**Figure 15. Isolation of the PF4 3XGFP-EMTB sequence for injection.**

The PF4 3XGFP-EMTB plasmid was digested with AatII and XhoI and the fragment of interest was gel purified. Serial dilutions were performed and a estimation of the concentration was based on the relative intensity of the 1 Kb molecular marker as recommended by the manufacturer. The arrow points in the 6Kb marker of the gel.

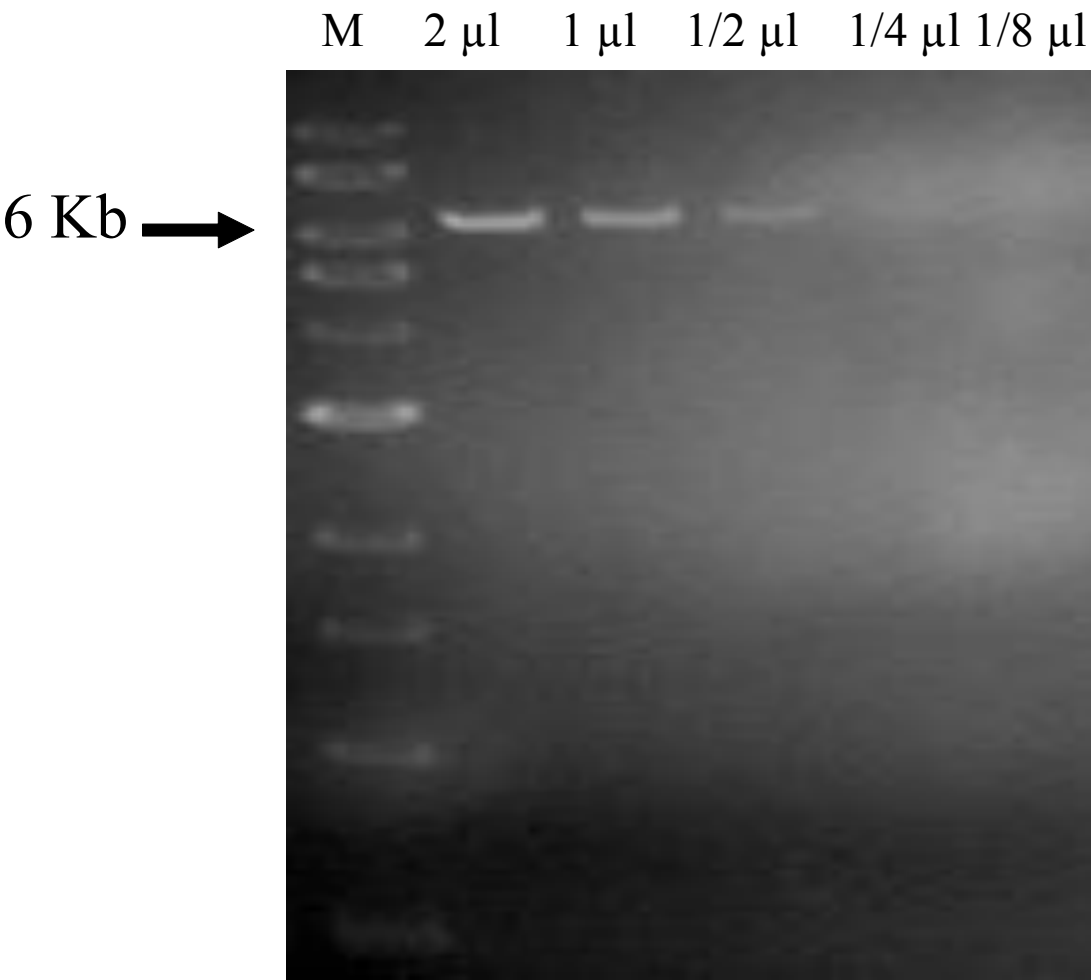
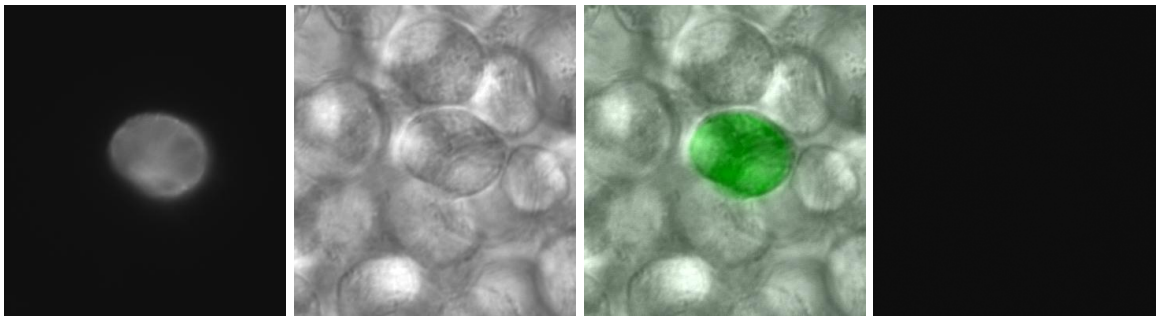


**Figure 16. Transfection experiments employing the human megakaryoblastic cell line**

**CMK.**

The CMK cells were induced to polyploidize using TPA and were transfected with isolated DNA fragment composed by the PF4 promoter the 3XGFP-EMTB the  $\beta$ -globin intron and the poly A tail that will be used for microinjection in ovaries to generate the transgenic mouse. Pictures were acquired at 40X.

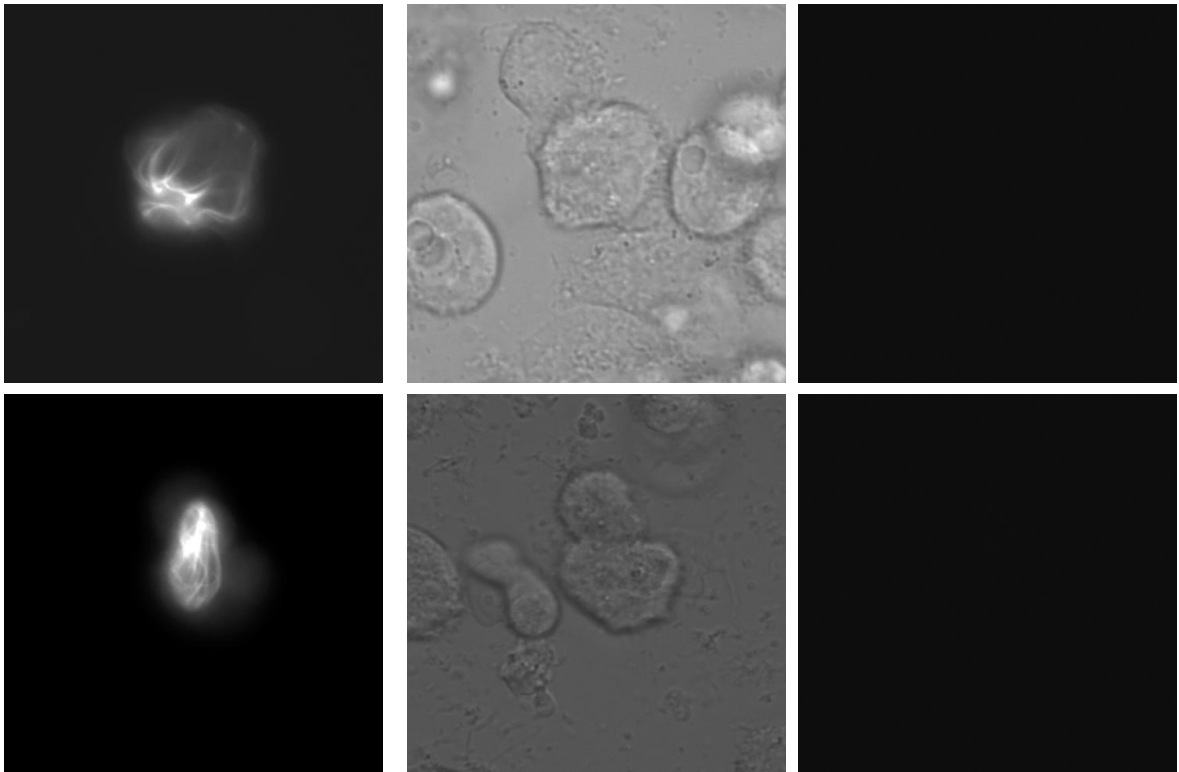


GFP

Brightfield

Composite

Red



GFP

Brightfield

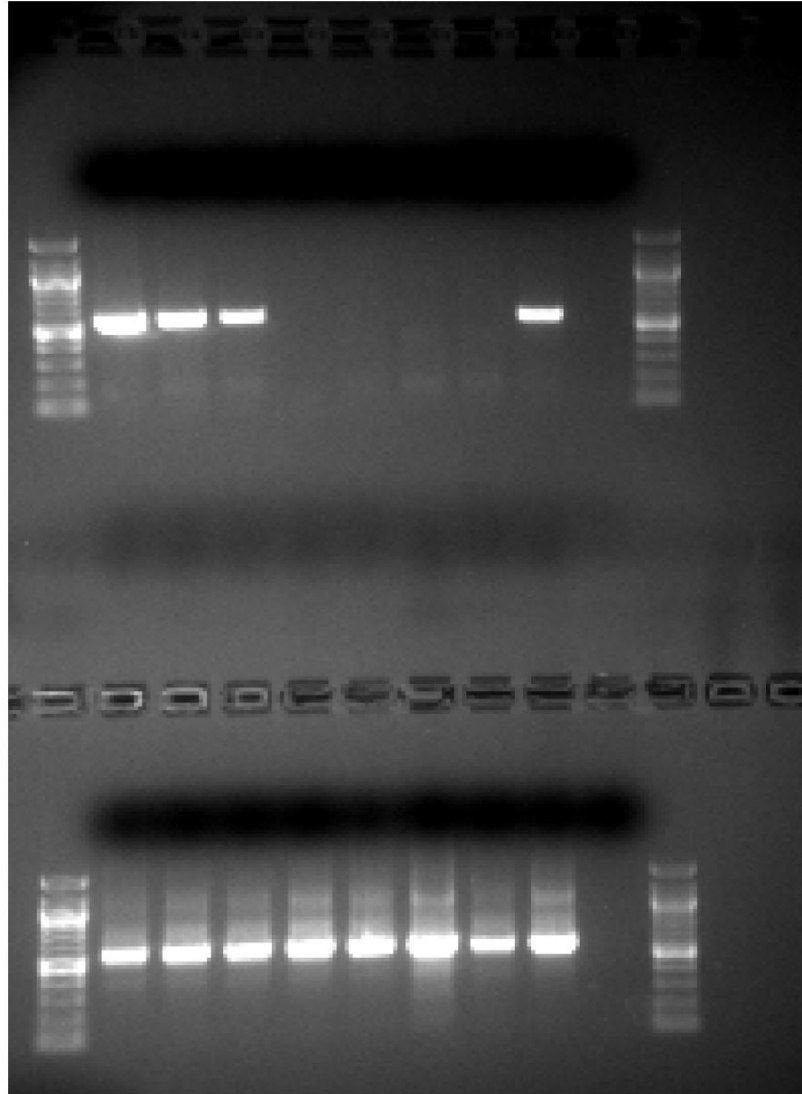
Red

**Figure 17. Example of PF4-3XGFP-EMTB founder screening.**

Tail genomic DNA was isolated and it was screened using two different screening pairs (denoted as SCRI and SCRIII) as described on materials and methods. GAPDH was used to exclude any false negative results genomic DNA samples. In this example here, PCR products of SCRI and GAPDH primers pair are depicted. The size of PCR products of a group of potential founders (denoted by numbers) were discerned using 100 bp NEB marker (M). The negative control contained reaction mixture without DNA template (Neg).

M 7 17 18 19 20 21 23 24 Neg

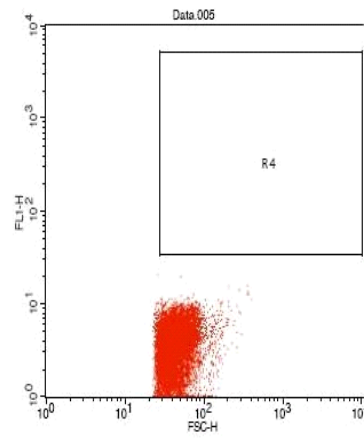
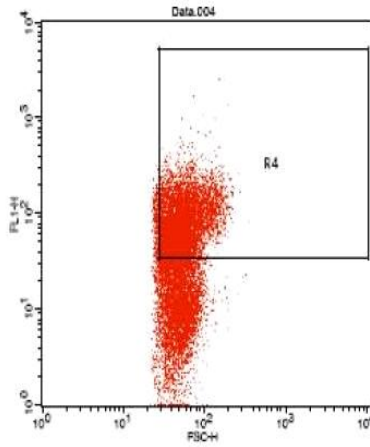
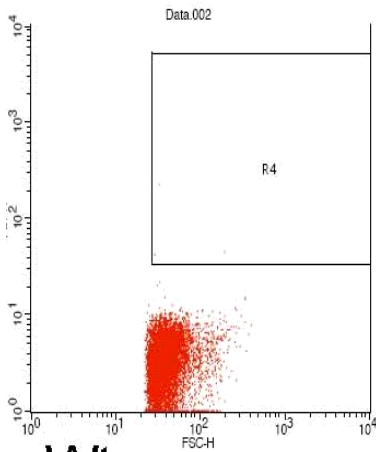
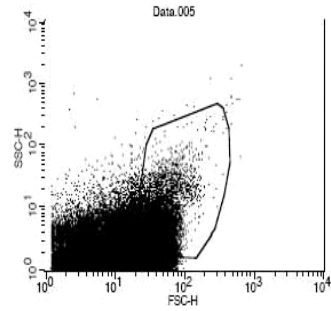
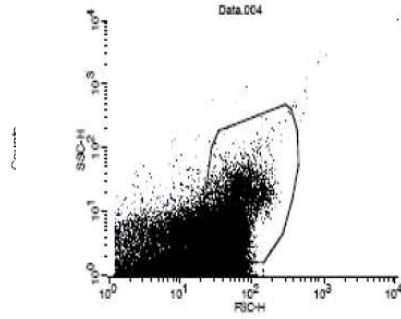
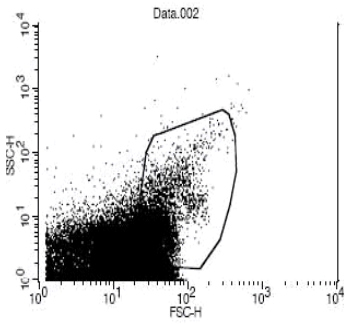
PF4-  
3xGFP-  
EMTB



GAPDH

**Figure 18. Screening of PF4 3XGFP-EMTB for expression of the transgene in platelets isolated from whole blood.**

Blood was collected by retroorbital bleeding and was mixed with Aster Jondl anti coagulant and kept in room temperature. The samples were centrifuged at 500 g for 10 minutes at room temperature to allow separation of platelets from erythrocytes that could mask GFP fluorescence. The enriched in platelets plasma was collected and it was used for FACS analysis. Gating was based on a) relative size of platelets and b) on the fluorescence of wild type (negative control) and GFP mouse (positive control). Samples of wt, founders and a transgenic mouse that GFP is expressed in all tissues were collected and processed concomitantly. Here is depicted the GFP mouse (GFP) the wild type (wt) and the founder 17.



Wt

GFP

Founder 17



### **Part III. The Cyclin E transgenic mouse .**

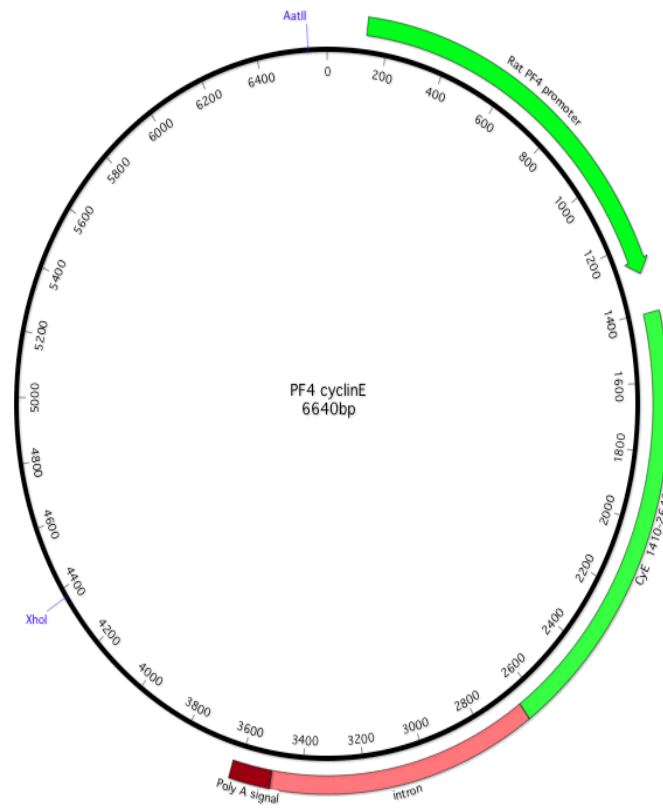
The PF4 Cyclin E plasmid was previously generated and encompass the Rat PF4 promoter driving expression of the human Cyclin E1 gene followed by an Intron and a Poly A tail. The fragment containing the above elements was isolated using restriction enzymes and gel purification followed by electroelution was used to isolated it in sufficient purity for injection.

Founders were crossed to generated homozygotes. A rapid screening method was devised where the tail genomic DNA was used for Real time PCR. In this approach the ratio of human Cyclin E1 to a mouse gene was used to discern homozygotes for heterozygotes. This approach that was latter expended to the screening of other transgenic mouse lines proved to be an effective alternative to the time consuming southern blotting.

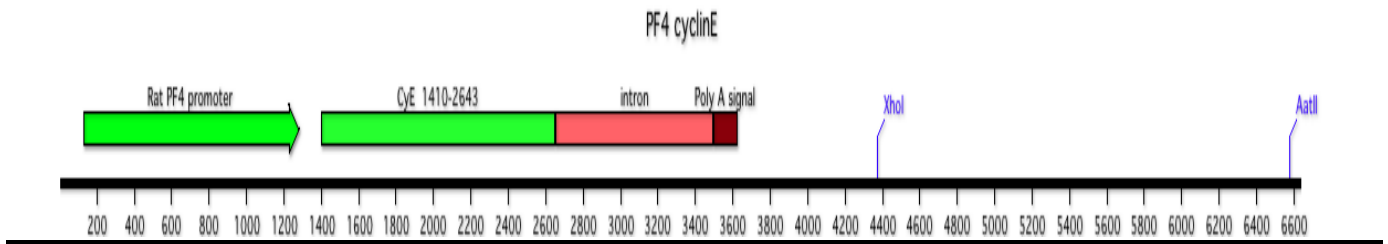
To determine the number of cells that are in the S phase Brdu assay was performed. Brdu was injected intraperitoneally in mice (transgenic for Cyclin E and wild type controls) which were sacrificed 2 hours later and an Anti Brdu antibody was used to determine the percentage of megakaryocytes of bone marrow that were stained. Concomitantly, bone marrow of a mouse that was not injected with Brdu was used as negative control. A higher fraction of Megakaryocytes of the Cyclin E1 transgenic mouse are in S phase compared to wild type megakaryocytes.

**Figure 19. Isolation of transgene for injection for the generation of the PF4 Cyclin E mouse.**

The PF4 Cyclin E plasmid was generated previously by Dr. Kenian Lieu, a former member of Ravid's laboratory. Panel A) In this construct, the rat PF4 promoter drives expression of the human Cyclin E1 cDNA followed by a intron and a polyA tail. The restriction enzymes AatII and XhoI were used to release the fragment of interest that contains the promoter, the Cyclin E cDNA, intron and polyA tail. Panel B) schematic representation of the transgene injected in male pronuclei. Isolation of the transgene was based on electroelution .



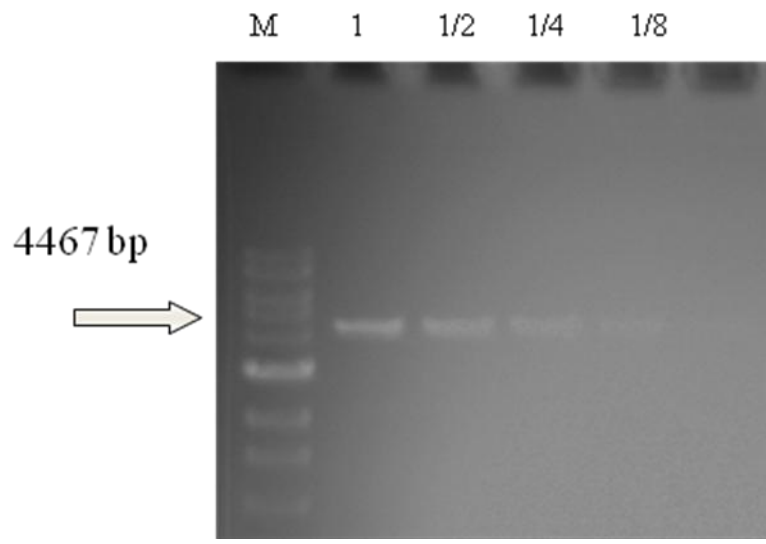
A



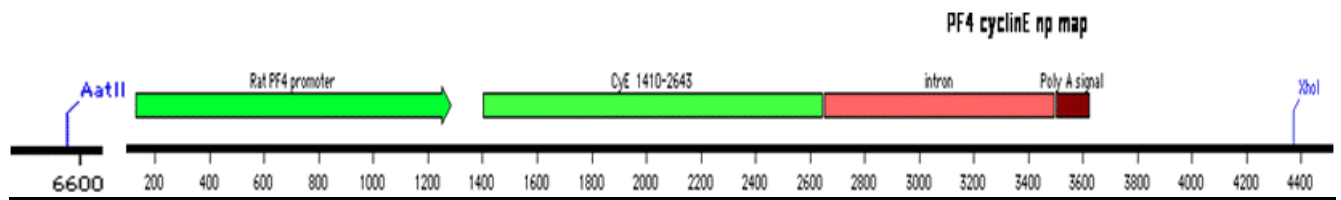
B

**Figure 20. Titration of the isolated PF4 Cyclin E transgene for injection in male pronuclei of FVB mice.**

Serial dilutions of the PF4 Cyclin E transgene that were used to estimate amount of DNA obtained after purification and also access purity.



**A**



**B**

**Figure 21. Identification of homozygotes based on real time PCR using tail genomic DNA as template.**

Genomic DNA was obtained from the tails of litter (denoted as F2#1-15) born by crossing two heterozygotes. 100 ng of genomic DNA was used as template to run real time PCR using Taqman primers recognizing a) a sequence spanning exon 4 and 5 of Human Cyclin E1 gene and b) a genomic sequence of Adenosine A2B receptor. In this example mice F2#6-9 and F2#10 have double the amount of Human Cyclin E1 transgene compared to F2#1, F2#3, F2#5, F2#10, F2#12, F2#14. Hence, F2#6-9 and F2#10 were designed as homozygotes, while F2#1, F2#3, F2#5, F2#10, F2#12, F2#14 as heterozygotes. On the other hand, F2#2, F2#4, F2#13 and F2#15 do not contain human Cyclin E1 cDNA sequences and were designated wild type mice. Designation of litter as wild type and transgenic was also vindicated with conventional PCR.

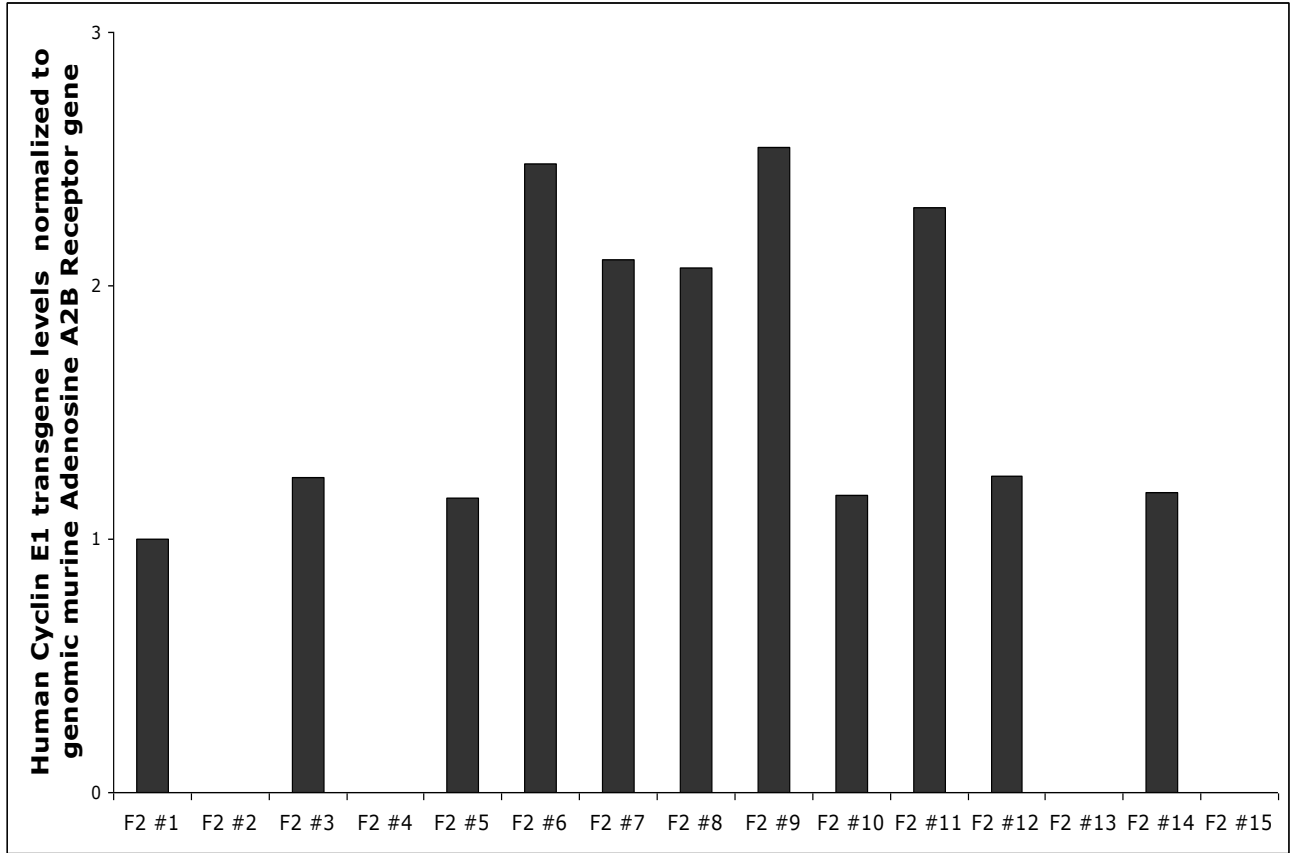


**Figure 22 . Titration and specificity testing of Brdu assay.**

Bone marrow cells were used to test the specificity of the Anti-Brdu FITC antibody that was used for the Brdu assay experiments. **In Panel A** bone marrow cells were cytopun and DNA content was visualized with DAPI stain. Slides were viewed under GFP filter and red filters. The GFP filter will be used to visualize cells with Anti-Brdu FITC antibody. Experiment of Panel demonstrates that there is minimal background autofluorence in both fields . This is essential for the interpretation of slides.

**Panel B)** Bone marrow cells of Mice not treated with intraperiotneal injection of Brdu were cytopun and fixed and Anti Brdu FITC antibody was used. As expected the antibody did not visualize any cells as there was no Brdu incorporated in the cells. Panel B demonstrates the excellent specificity of the antibody.

**Panel C)** provides an example of Bone marrow cells that were derived from mice treated with Brdu intraperitoneally prior to the fixation of cells. Anti Brdu FITC detected cells with Brdu incorporation with minimal autofluorescence.

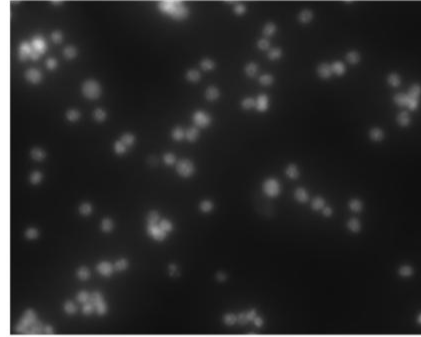
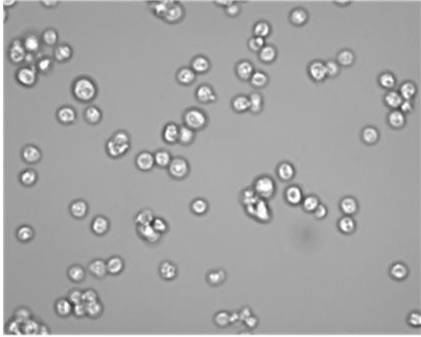


**Panel A**

Control (no Anti Brdu-FITC added)

Brightfield

Dapi



GFP (green) filter

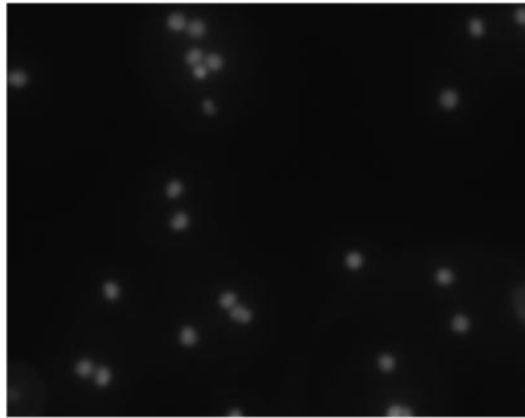
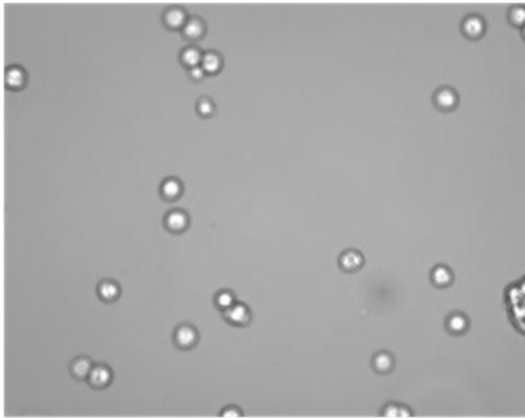
Red filter (autofluorescence)

**Panel B**

Cells without Brdu treatment + Anti Brdu-FITC (20  $\mu$ l / 10<sup>6</sup> cells)

Brightfield

Dapi



Anti-Brdu FITC

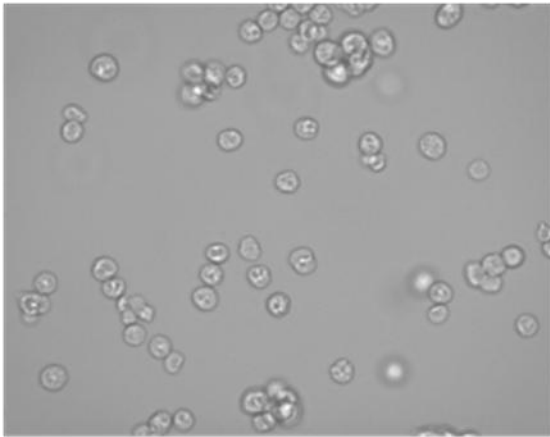
Red filter (autofluorescence)

---

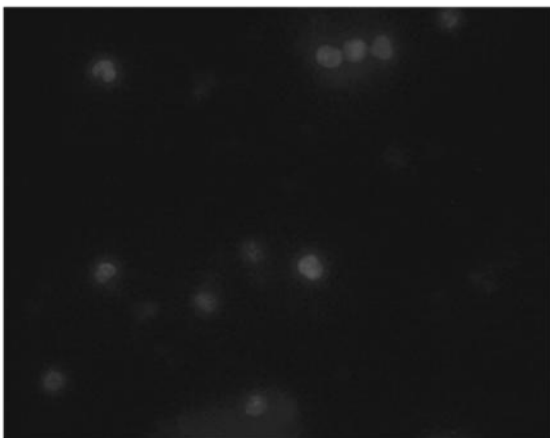
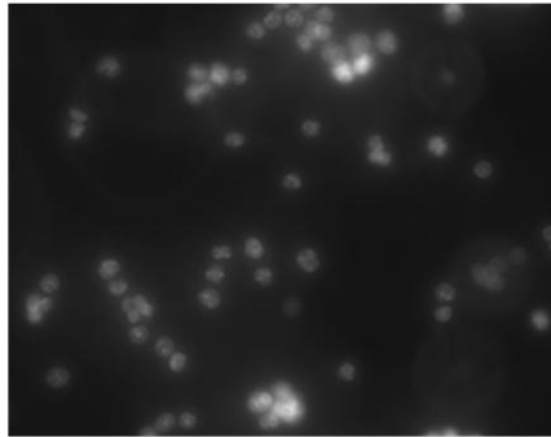
**Panel C**

Brdu labelled cells + Anti Brdu-FITC (20  $\mu$ l /  $10^6$  cells)

Brightfield



Dapi



Anti-Brdu FITC

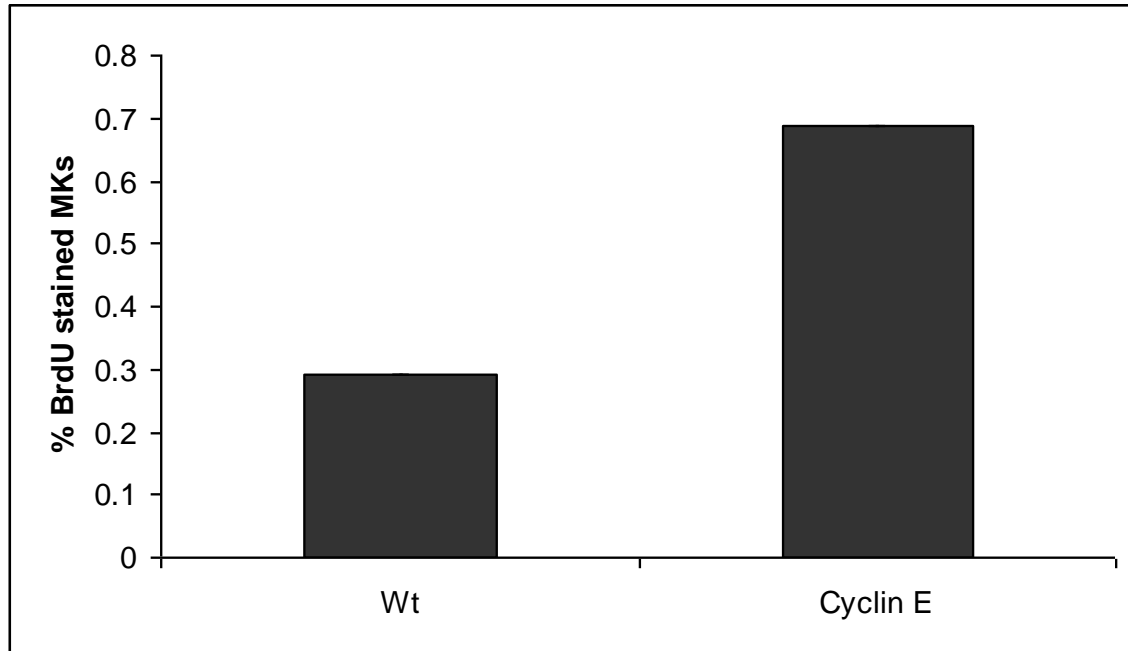


Red filter (autofluorescence)

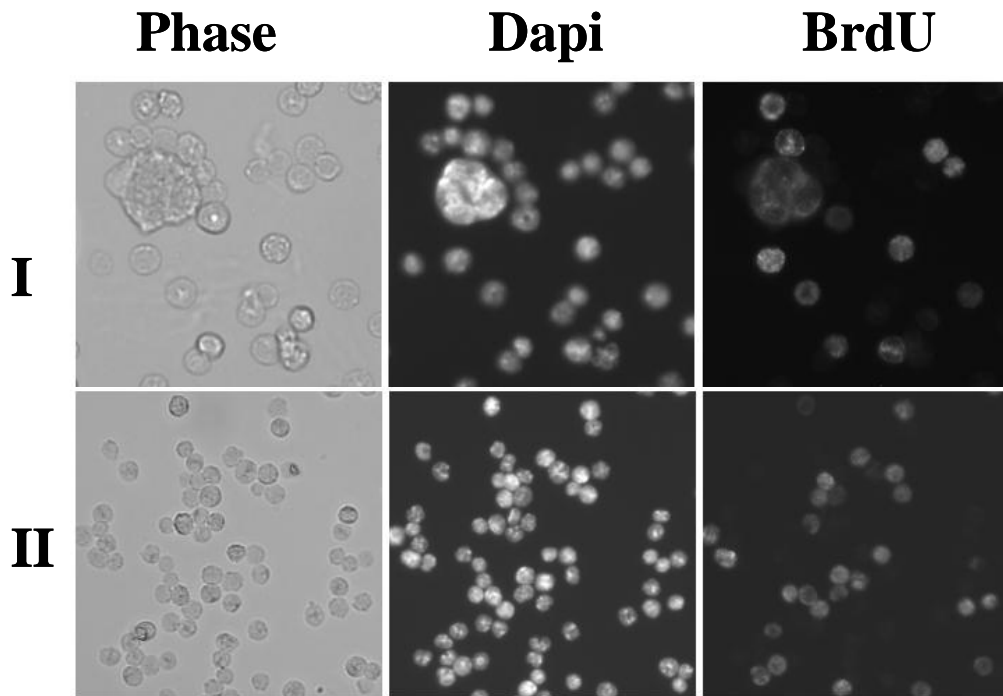
---

**Figure 23. Brdu assay of transgenic and wild type to determine fraction of Megakaryocytes that are in S phase.**

Panel A) A higher percentage of Megakaryocytes derived from the PF4 Cyclin E transgenic mouse model are in S phase compared to wild type mice. Panel BI) example of Brdu staining of Megakaryocytes (denoted by arrow) and example of staining in other diploid Megakaryocytes (Panel BII).



**A**



**B**

#### **Part IV. The role of PLK3 in polyploidization.**

Based on the role of PLK1 in the megakaryocytic polyploidization and the fact that PLK3 can modulate Cyclin E<sup>112,184</sup> we seek to explore the role of another member of the PLK family that of PLK3. We detected PLK3 gene expression in Megakaryocytic enriched fractions of bone marrow and in an experiment that involved injection with TPO. We also detected PLK3 in Y-10 megakaryocytic cell line and vascular smooth muscle cells. We used the latter because they are polyploid and would be also useful to study PLK3 in this system too.

Preliminary experiments of PLK3 Knock out mice (in 2009) kindly provided by Dr. Dai from New York University did not show a significant difference in ploidy which was further confirmed by studies of other groups<sup>185</sup>. Therefore, Although PLK3 is expressed in Megakaryocytes its absence does not appear to affect polyploidization significantly.

**Figure 24. Comparison of PLK3 expression post TPO injection.**

Mice were injected with TPO and after 3 days post injection bone marrow was claimed and Megakaryocytes were obtained through column purification. As control, we used wt mice that were not injected with TPO. TPO increased levels of PLK3 gene expression. Data shown from 2 experiments.

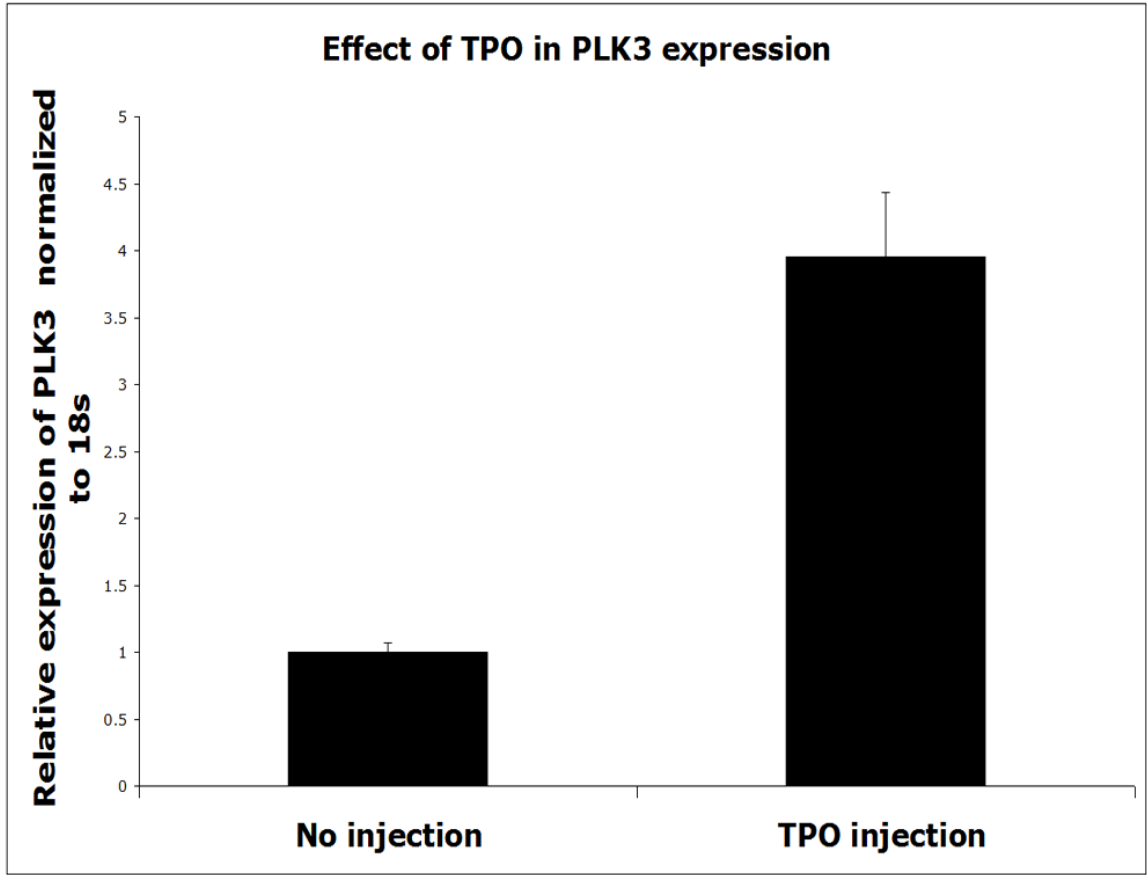




**Figure 25. PLK3 is expressed in Y-10 cells and vascular smooth muscle cells.**

Y-10 cells and vascular smooth muscle cells were used to obtain cDNA and real time PCR was performed using PLK3 and 18s primer. The levels of expression in Y-10 cells are much higher than in vascular smooth muscle cells. Data shown are derived from one experiment.

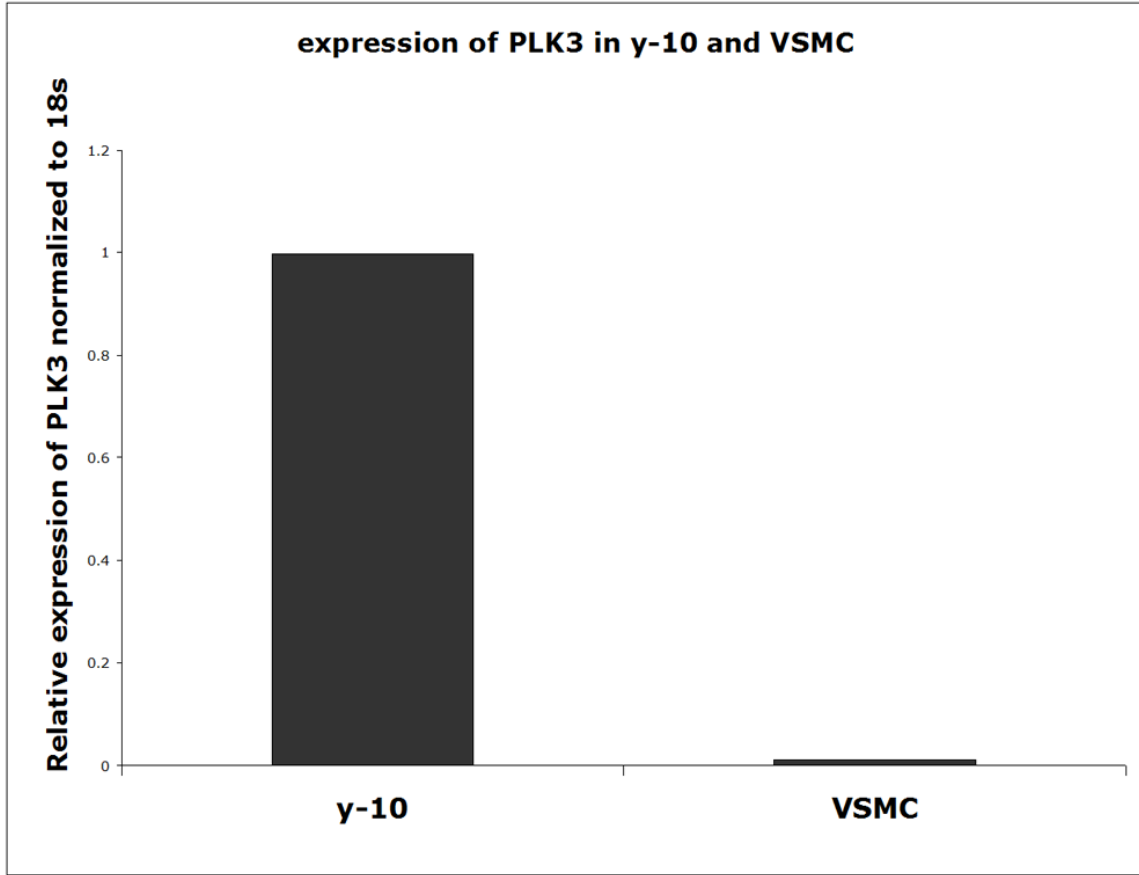


**Figure 26. Expression of PLK3 in CD41 enriched fractions of the bone marrow cultures in the presence of TPO at 12 hr and 72 hr.**

Bone marrow was cultured in the presence of TPO and CD41 positive cells were column purified after 12 hr or 72 hr. In the presence of TPO Megakaryocytes that are cell cycle arrested are induced to commence cycling and endomitosis. In addition, in this experiment CD41 expression was also measured in order to compensate for potential differences in Megakaryocytic fractions purities. The expression of PLK3 was subsequently normalized to CD41 and 18s. Data collected from two independent experiments.

**PLK3 gene expression in CD41 enriched fractions cultured in the presence of TPO**

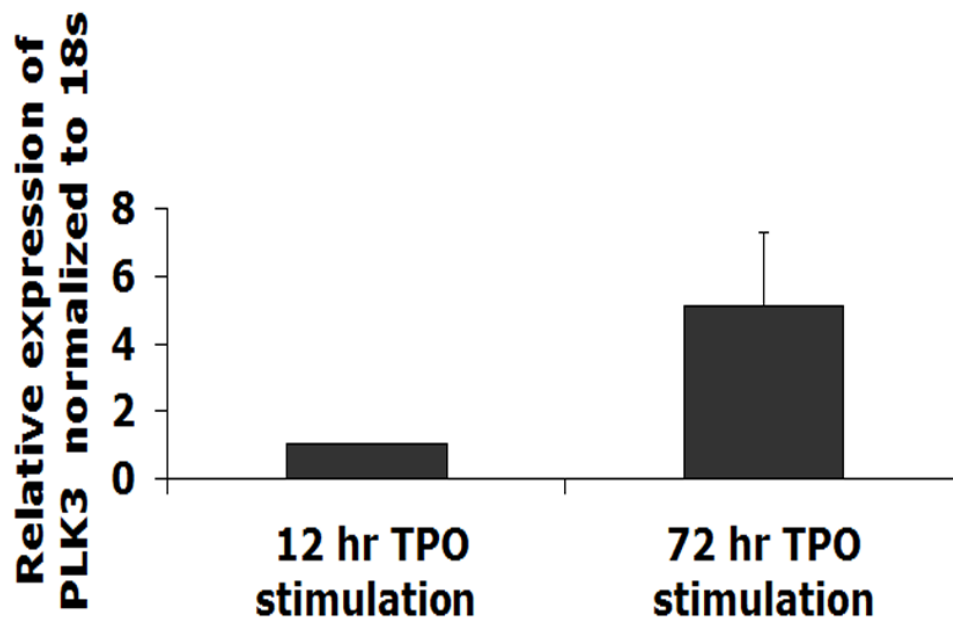
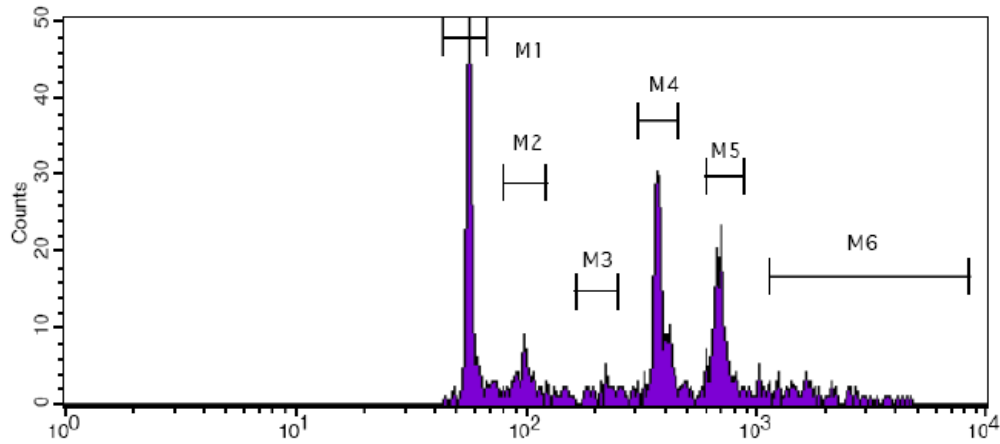
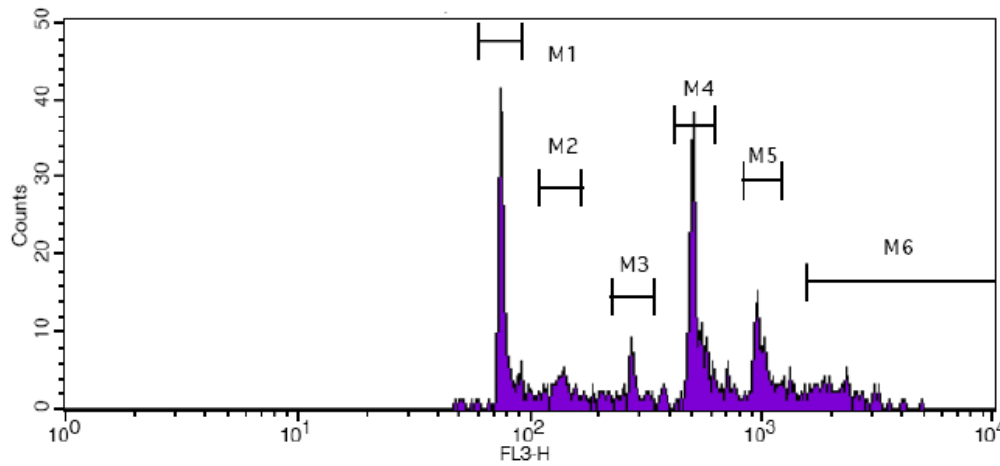


**Figure 27. PLK3 KO ploidy profile is not significantly different of that of the wild type mice.**

Ploidy analysis was performed on PLK3 KO male mice and their respective age and gender matched wild type controls. Ploidy profile was not significantly different. Example of ploidy analysis between a PLK3 KO mouse and a wild type is presented here. Ploidy classes are also shown. Panel A represents a wild type mouse ploidy profile while panel B a PLK3 KO mouse. Panel C represents the percentage of Megakaryocytes per ploidy class. 1200 Megakaryocytes were analysed to compile the ploidy profile.



**A**



**B**

plk3 KO					
2N	4N	8N	16N	32N	<32 N
22.42	7.75	4.75	27.33	15.08	9.75
WT					
2N	4N	8N	16N	32N	<32 N
25.92	8.17	3.67	26.42	18.25	7.17

**C**

## **Part V. The Lysyl Oxidase Propetide in the context of megakaryopoiesis**

The Lysyl Oxidase propeptide has been shown to exert a profound inhibitory effect in several cancer cell lines as well as primary cells (osteoblasts). We utilized a recombinant LOX-PP and we demonstrate that it has a significant impact on the Megakaryocytic ploidy. LOX-PP reduced ploidy and Megakaryocyte size and we demonstrate that its effect is also pronounced in Megakaryocytes that are derived from the Cyclin E transgenic mouse line.


Furthermore, immunofluorescence studies pursued with an antibody recognizing the LOX-PP moiety indicate that LOX-PP is present in Megakaryocytes. The source of LOX-PP (endogenous or exogenous) was not investigated in this study. Our lab has determined through sorting of Megakaryocytes based on ploidy that LOX is expressed in low ploidy Megakaryocytes but its expression is scant in polyploid Megakaryocytes. Therefore, the LOX-PP detected in Megakaryocytes could be exogenous that has entered the cytoplasm of Megakaryocytes.


**Figure 28. The sequence and characteristics of the recombinant LOX-PP.**


Schematic representation of the LOX-PP including glycozylation sites. A detailed description of the LOX-PP and its production through recombinant techniques was recently published<sup>186</sup>.




MRAWIFFLLCLAGRALAAPLAAPQAPREPPAAPGAWRQTIQ  
WENNGQVFSLLSLGAQYQPQRRRDSSATAPRADGNAAAQP  
RTPIILLRDNRTASARARTPSGVAAGRPRPAARHWFQVG  
FSPSGAGDGASRRANRTASPPQLSNLRPPSHVDRMVG  
LESRGPFQKLISEEDLNMHTEHHHHH

 Osteonectin Signal peptide

 c-myc 6xHis tag

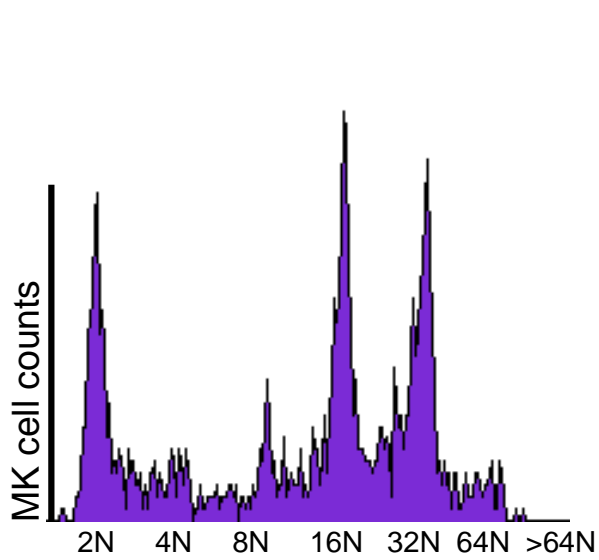
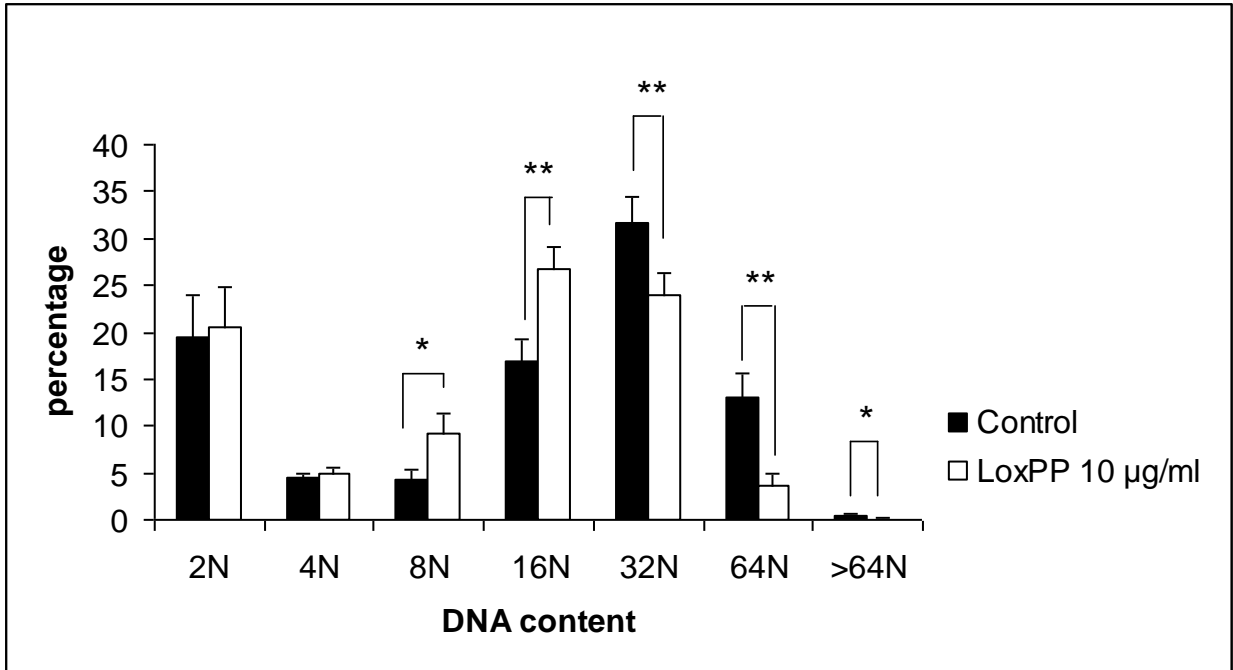
 Predicted N-linked glycosylation sites

 Predicted O-linked glycosylation sites

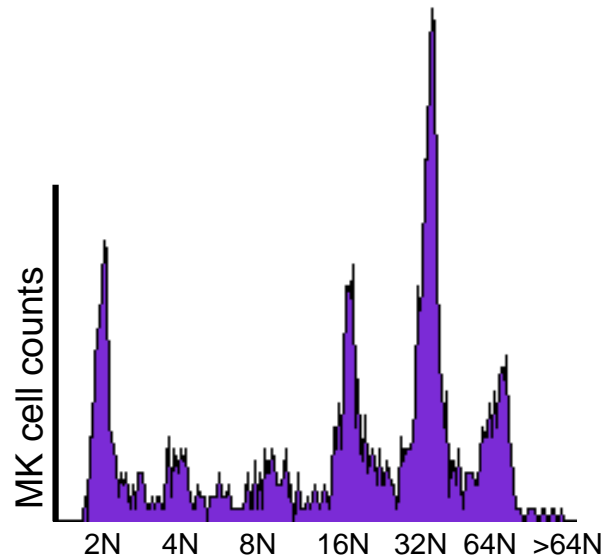
---

**Figure 29. LOX-PP inhibits polyploidization of murine Megakaryocytes in a dose related manner.**

Bone marrow cells were cultured in reduced serum conditions for 3 days and LOX-PP was used in two concentrations of 6  $\mu\text{g}$  and 10  $\mu\text{g}$  per ml respectively. As vehicle dH<sub>2</sub>O was used. Cells were fixed in 70% ethanol and subject to FACS. Panel A) Treatment with 10  $\mu\text{g}/\text{ml}$  LOX-PP inhibited polyploidization of high ploidy Megakaryocytes (<8N); N = 5. Panel B) A concomitant decrease in size of Megakaryocytes as assayed by the mean FSC was also noted. A similar, but less pronounced, pattern in reduction of ploidy was noted with 6  $\mu\text{g}$  treatment. The percentage of CD41<sup>+</sup> cells and viability as assayed by trypan blue or subdiploid content was not different between LOX-PP and vehicle treated cells.

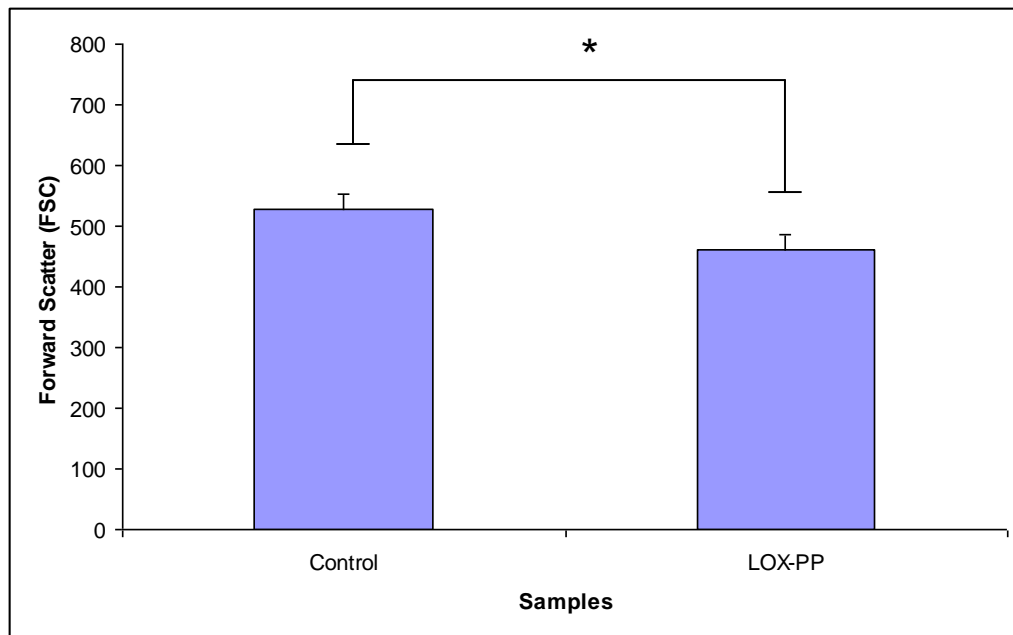


LOX-PP 10 µg/ml

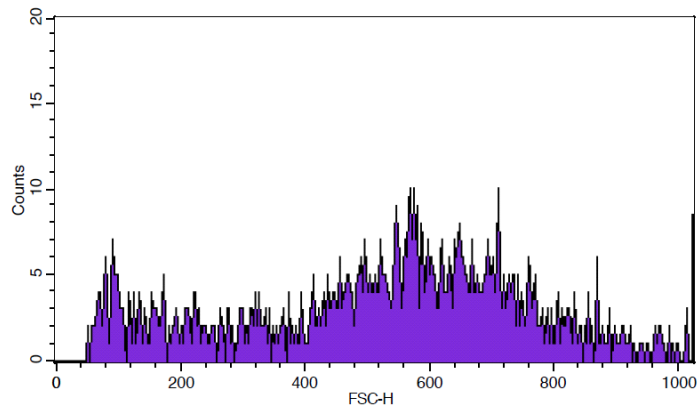


Control

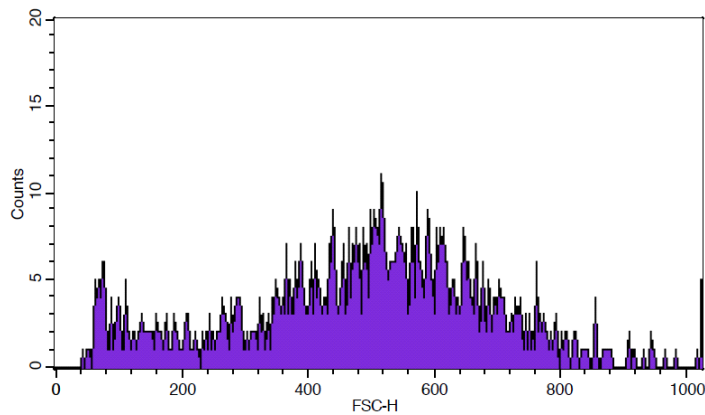
A



Control



LOX-PP

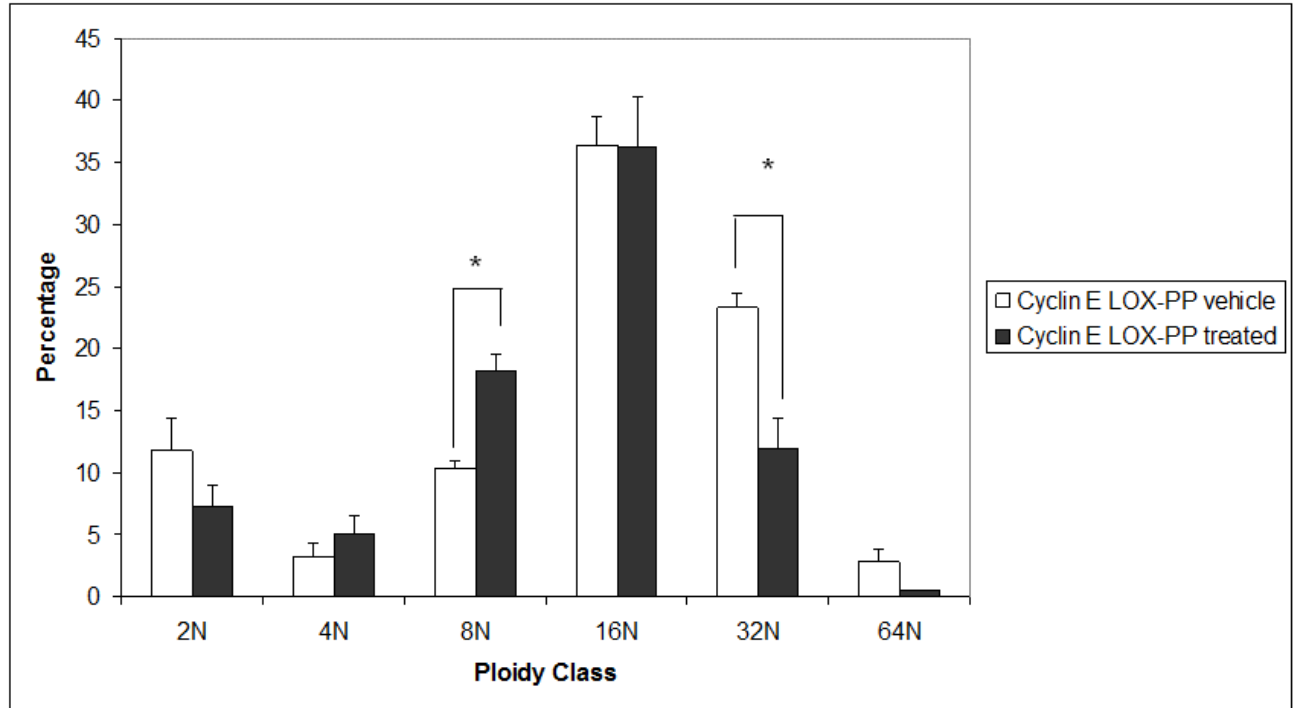


**B**

**Figure 30. LOX-PP inhibits polyploidization of Cyclin E transgenic mouse model bone cultures.**

Results are from an experiment involving 3 male, 7 week heterozygote Cyclin E mice. Samples ( $13 \times 10^6$  cells) were treated with 10  $\mu\text{g/ml}$  LOX-PP or vehicle and cells were fixed 3 days later. No wild type mice were included. No statistical difference between LOX-PP treated and vehicle treated groups regarding total number of BM cells or viability prior to fixation was noted. No statistical difference between LOX-PP treated and vehicle treated samples regarding percentage of CD41 or 2N,4N,16N as well as 64 N modal class (P value is 0.055 for the later).

Of note, in all samples ~ 1400 Megakaryocytes were analyzed apart from a Cyclin E mouse that 1600 Megakaryocytes were collected.



N=3

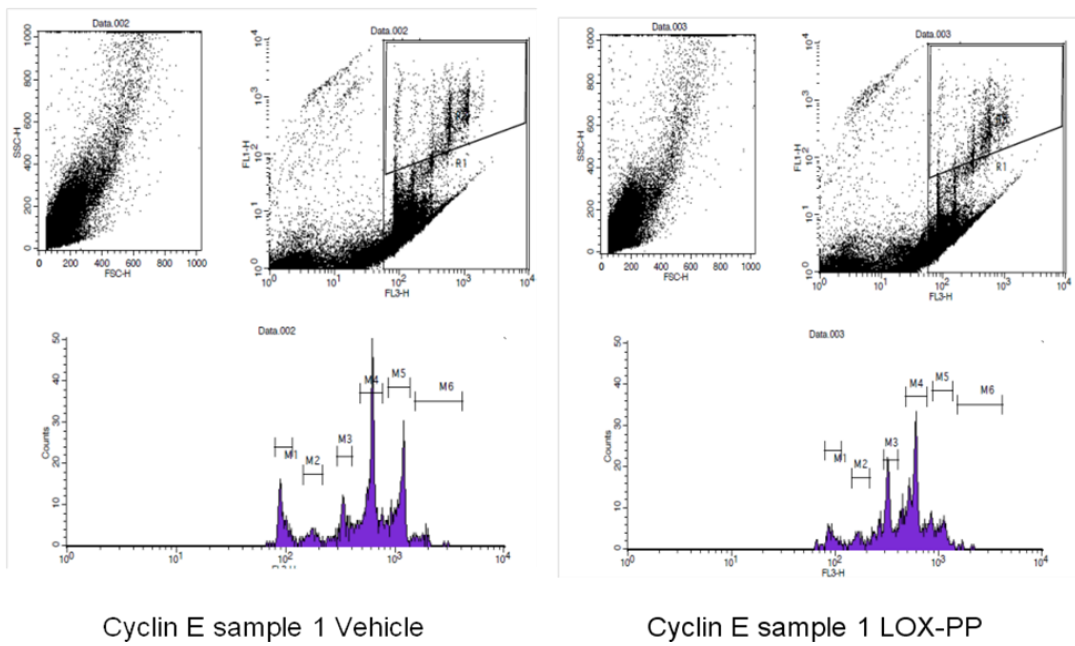
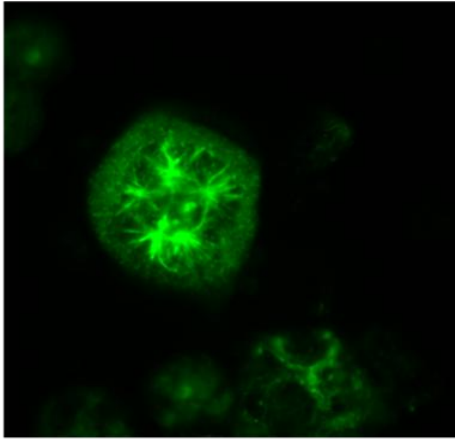
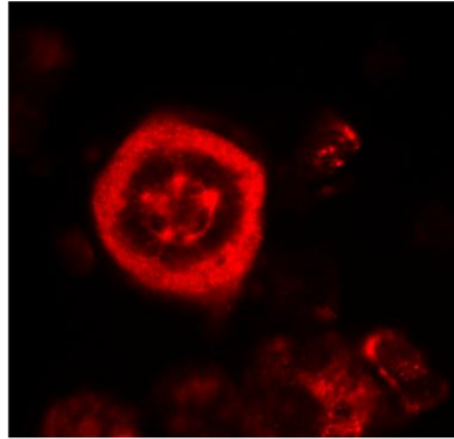


**Figure 31. Immunofluorescence studies of Bone marrow cells focusing on Megalaryocytes using anti LOX-PP and anti tubulin antibodies.**

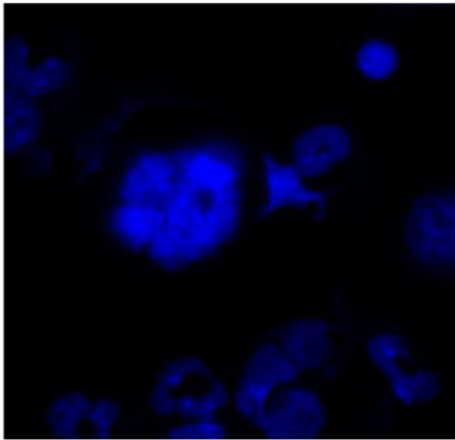
Bone marrow cells were cultured in the presence of TPO and were subject to immunofluorescence studies using the anti LOX-PP antibody and anti a tubulin antibodies. MKs were recognized based on their size relative to other diploid cells and from the presence of multiple spindle poles that is a unique characteristic of MKs among bone marrow cells. LOX-PP moiety appears to co-localize with microtubules. Panels A depict double immunostaining experiments and B depict LOX-PP only staining. Panel C depicts isotype staining.



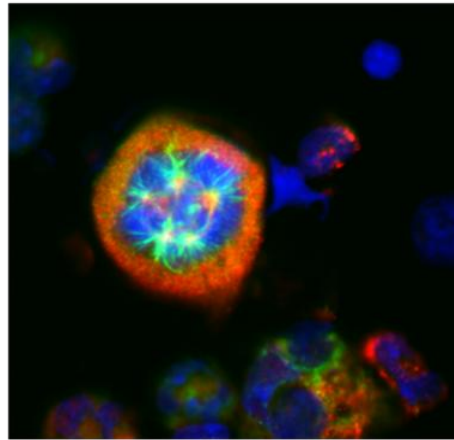
Microtubule staining



LOX-PP staining



DAPI



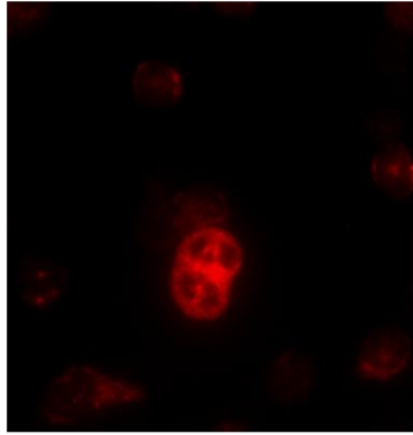
Composite

60X

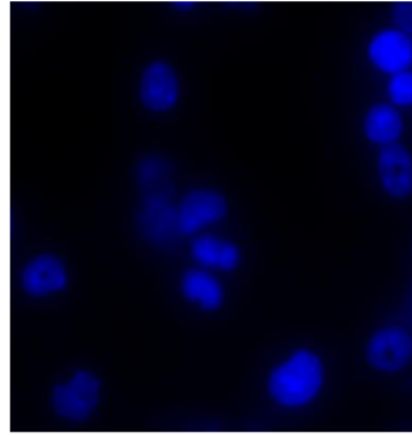
---

A

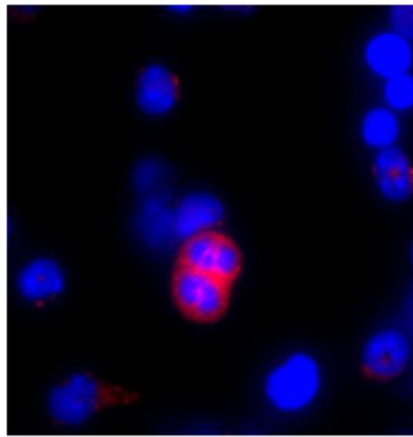




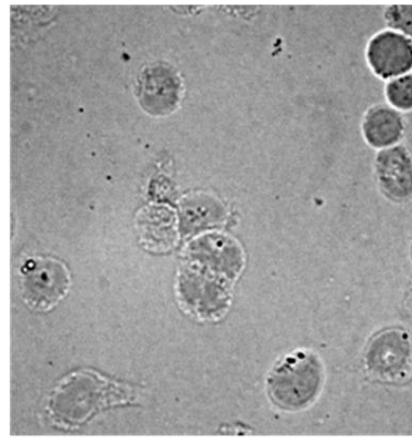
LOX-PP staining



DAPI



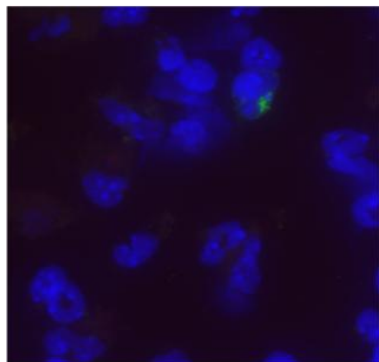
Composite



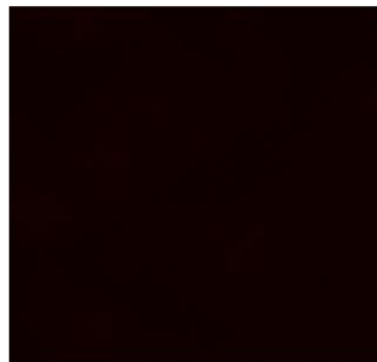
Phase

60X

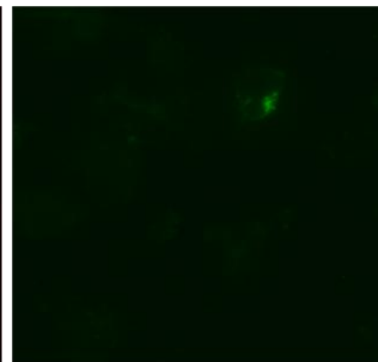
**B**



Composite (including DAPI)



Red



GFP

**C**

## **Chapter IV. Discussion**

Our current attempt to visualize microtubules is based on a transgenic construct that PF4 promoter drives expression of the EMTB fused in frame with 3 GFP moieties. This mouse model by the 3GFP moieties fused to EMTB provides a very bright fluorescent signal that would be ideal for living imaging of MKs.

The new approach is different because the GFP moieties are not fused with tubulin but with EMTB and thus provide indirect visualization of the microtubule network. Another advantage of this approach is that 3GFP moieties provide a strong signal, minimizing exposure time and photo-bleaching; attributes favorable for live imaging applications. In addition, the same construct was successfully used to visualize microtubules of skin cells, in a recently reported transgenic mouse line.

We are currently, screening founders for the presence of fluorescence by FACS analysis and microscopy.

On the other hand, the generation of PF4 Cyclin E transgenic model is an important tool for the study of endomitosis. This model would reveal whether Cyclin E could promote polyploidy and in what extent. Moreover, this mouse model could be used to investigate if overexpression of Cyclin E could overcome the effect of ploidy inhibitors. Indeed, the use of PF4 Cyclin E mouse model was used to study the effect of ROS inhibitors and was able to partially restore the ploidy compared to wild type induced by ..inhibitors.

## AIM I

We utilized Megakaryocytes of our transgenic mouse model to visualize DNA content in a subnuclear scale and to study endomitosis in vivo. The in vivo cell imaging approach has key advantages compared to studies of endomitosis based on immunocytochemistry. Studies based on fixed Megakaryocytes are hampered by low yield of isolated Megakaryocytes in anaphase and antibody specificity and sensitivity problems producing conflicting results. Another drawback is that immunocytochemistry studies can not discern if a Megakaryocyte with 4N content is undergoing or has already completed endomitosis. Furthermore, static images obtained by immunocytochemistry studies can not capture the details of chromosome / microtubule dynamics during endomitosis.

In our model, in vivo imaging is performed at subnuclear level. Higher magnifications have the disadvantages that only few megakaryocytes are visualized per optical field and image clarity can be affected by subtle movement of cells. However, our strategy had the advantage of visualizing in greater detail the phases of endomitosis. In addition, the use of high magnification was crucial for the demonstration that in high ploidy Megakaryocytes territories resembling midzone are formed.

This novel in vivo cell imaging model permitted tracking of chromosomal segregation during all phases of endomitosis including anaphase in Megakaryocytes of both low and high ploidy. This approach has the key advantage that the chromosomal dynamics were directly visualized in contrast to previous reports<sup>187</sup> where ploidy status was indirectly inferred. In low ploidy Megakaryocytes chromosomes were segregated into two groups and midzone formation was evident. The two chromosomal groups were subsequently merged in the last

steps of mitosis without cellular division. The whole process occurred rapidly and is in agreement with previous estimations<sup>188</sup>. The formation of midzone is important for the assembly of chromosomal passenger proteins. Midzone formation also heralds the site of cleavage furrow an important step for the assembly of factors regulating cytokinesis and cytoskeleton rearrangements. Our data are in agreement with recent reports of cleavage furrows that ingress considerably before regressing at the last steps of endomitosis<sup>187</sup>.

However images obtained from high ploidy megakaryocytes did not follow the above pattern. The first steps of mitosis were also retained intact but the condensed chromosomes formed ring type alignments followed by separation of uneven amounts of DNA to form territories resembling midzones. The subsequent steps included chromosomal pulling to one side without the events associated with cytokinesis.

In addition our approach of in vivo imaging utilizing histone tagging can serve as an essential primer for the future study in vivo of endomitotic aspects that remain enigmatic such as the localization of Chromosome Passenger complex proteins.

Hence, we documented that chromosomal segregation patterns during anaphase A are different in low and high ploidy MKs. Based on these findings we envision that in low ploidy cells there is a deregulated expression of a cell cycle protein(s), which leads to lack of cytokinesis. The mitotic regulator is still elusive, although studies in cultured primary MKs implicated PLK downregulation<sup>86</sup>, survivin mislocalization<sup>100</sup> and furrowing/cytokinesis modulators.<sup>87</sup> The, now higher ploidy cell re-enters endomitosis, likely promoted by cyclins D3 and E as shown by studies of Zimmet<sup>89,189</sup> and Geng<sup>95</sup>. At this cell cycle stage anaphase is different, as illustrated in our current study, likely also due to the effect of high DNA content on the segregation process or its regulation. Since visualization of chromosomal dynamics in

living MKs provides a platform for deciphering the molecular mechanisms that power endomitosis, our new mouse line could be cross bred to other lines with modified mitotic regulators, when they are identified and the mice become available, to estimate effects on the dynamics of endomitosis in vivo. In this study we try to address how megakaryocytes divide their DNA during their complex cycle of endomitosis.

Another study that was published following that of ours and was based on a *in vitro* culture of human Megakaryocytes derived from CD34<sup>+</sup> cells<sup>88</sup>. CD34<sup>+</sup> cells were incubated with a serum medium (based on TPO) that induced differentiation to Megakaryocytic lineage. Cells were transduced (twice in a sequential manner) using lentiviruses that expressed EF1a-H2BGFP to visualize DNA and identification of Megakaryocytes was further validated by using a CD41 APC monoclonal antibody. Live imaging of the above human Megakaryocytes demonstrated a normal mitosis occurring in the 2N to 4N transition throughout the cell cycle apart from Anaphase. Two daughter cells were formed and were only connected by a small cytoplasmic bridge for a prolonged period (of approximately 30 minutes) prior to rejoining to a single cell. In addition, nuclear division was studied and it was found the percentage of Megakaryocytes with two separated nucleus could be up to 46.6%. Another important observation regarding low ploidy Megakaryocytes was that the internuclear distance was shorter in the endomitotic Megakaryocytes compared to those that underwent complete division to generate two diploid megakaryocytes.

The Megakaryocytes of higher ploidy followed a different pattern of endomitosis compared to that of low ploidy megakaryocytes. The Megakaryocytes formed in the last steps of mitotic cycle 4 daughter cells that authors describe as “exactly like a flower with 4 petals”. The daughter cells reunified in a sequential manner and the authors of the study observed a

marked decrease in the degree of furrowing that correlate with the degree of polyploidy. Through immunofluorescence studies it was demonstrated that Aurora B, Survivin were correctly localized and present in the spindling complex. By contrast, less F-actin was noted to accumulate in the central contractile ring and it was shown that RhoA was incompletely activated during endomitosis. PLK-1 may play an important role in orchestrating the accumulation and activation of RhoA in the central spindle assembly as it was shown before.

In different publication<sup>190</sup> study of endomitosis was based on cord blood derived Megakaryocytes which differ from their counterparts of bone marrow in that their ploidy levels are extremely low and their potential for division is much less restricted<sup>191</sup>. Cord blood cells were again induced to differentiate- through use of TPO containing medium- to Megakaryocytes. The percentage of Megakaryocytes in the cultures increased steadily from a 44% to 87% when day 5 to Day 10 were compared. Since clearly as a significant percentage of cells was not belonging to megakaryocytic lineage the authors of the study used diverse approaches to identify Megakaryocytes undergoing endomitosis. For example, they followed the size of a cell and its morphological changes associated with its life cycle as well as its ancestors. A second approach was visualization of the DNA content using Hoechst DNA abd then determination of DNA content based on number of lobes. Finally, based on the well established correlation between ploidy and concomitant increase in cell size the authors of the study extrapolated the ploidy status of the Megakaryocytes under observation. Based on the above described strategies the authors concluded that only a small minority of CK-MB attained a level of ploidy above 4N ( 7% for 8N and only 3% for 16N without any Megakaryocytes attaining higher level of ploidy). A strength of this study was that the length of endomitosis was studied in a large number of cells and was found to exhibit a trend towards decrease as the

ploidy increased. Namely, transition to 4N lasted 33 minutes with a SD of 28.5 minutes while transition to 8N lasted 28.1 minutes with a standard deviation of 21 minutes.

However, in this study it was reported the occurrence of both asymmetric as well as symmetric division of polyploid Megakaryocytes. Namely, polyploid Megakaryocytes could give rise to polyploid Megakaryocytes which could undergo further endomitosis. Another provocative finding was the presence of megakaryocyte with hexaploid DNA content that was generated by an octaploid Megakaryocyte with asymmetrical division. Use of human bone marrow cell derived Megakaryocytes showed similar findings albeit to a much less extent. More specifically, although 27 % and 8 % of the cord derived Megakaryocytes with ploidy of 4N and 8N respectively underwent mitosis in their counterparts derived from bone marrow occurred only in 6% and 1%.

A strength of the particular study was the great number of Megakaryocytes that was observed as well as the ability to track Megakaryocytes back to their ancestry line or follow simultaneously the fate of daughter cells.

However, one key difference between our work and the work published from others is that our work is based in the mouse transgenic model that has constant and the same amount of fluorescence in its DNA. The study from the other groups was performed using CD34 human stem cells requiring the use of high titer lentiviruses viruses to infect the cells which could lead - due to stochastic reasons- to variable level of fluorescence . Moreover, although the overall viability or ploidy status of the population may not be affected by the lentiviral treatment it is important to note that it is not possible to determine if the particular cell under observation might have been affected detrimentally by the transduction.

Another important fact that should be highlighted is that Megakaryocytes derived from human stem cells do not attain high ploidy states. The usual upper limit of ploidy for this system is 16-32N and while in our system it has been documented by prior studies that the level of ploidy can reach 126- 256 N therefore closely mimicking what occurs under physiological conditions in the human bone marrow. Overall though, the two studies showed for the first time under live conditions that the megakaryocytic process of DNA replication has distinct pathways between low and high ploidy Megakaryocytes.

The other study using cord blood stem cells that were induced to become Megakaryocytes reported findings that do not conform to the regular pathway of DNA replication. Critics of this study point to the fact that the cells used do not typically attain high levels of ploidy and also in this study the viability of the cells was significantly affected. Hence, it remains a question whether the results of this study describe phenomena occurring exclusively in the cord blood derived Megakaryocytes or they might be affected by culture conditions and media used. These intriguing results have not been previously reported especially the presence of aneuploid Megakaryocytes.

Our study also showed and provided conclusive evidence that the endomitosis is a process closely resembling the model which was originally proposed based on immunohistochemistry studies. Although the immunohistochemistry studies provide static images and they cannot capture the dynamic process of the DNA content separation, they were correct in predicting the key steps of endomitosis. An evolving theory that a key component of endomitosis is the failure of cytokinesis<sup>192,193</sup> likely linked to lack of activation of the Rho protein and defect in myosin localization<sup>194</sup> in the contractile ring between daughter cells<sup>195</sup>. A recent report



demonstrated that most multipolar Megakaryocytes undergoing endomitosis had a thin extension of laminin between chromosomes that persisted till the end of endomitosis<sup>195</sup>.

## **AIM II**

Visualization of Megakaryocyte cytoskeleton or microtubal architecture during the complex cell-division cycle of the MK ex vivo or in vivo was not successful so far. There has been attempts using lentiviral vehicles to deliver fluorescently tagged tubulin to cells in order to provide direct visualization of the microtubule/actin network at different cell cycle stages<sup>70</sup>. studies employing this strategy were successful in allowing the tracking of endomitosis and reaffirmed prior studies based on immunohistochemistry. However potential drawbacks of this approach are that lentiviral integration can lead to cell toxicity and over accumulation of the over expressed fluorescent protein.

In fact, tubulin is a crucial protein that the level of it needs to be tightly regulated. Overabundance of this protein can cause formation of aggregates leading to cell death, artifactual cell size and shape changes or even destruction of the elaborate cell cycle timeframe. Therefore a system that allows precise visualization of the cell cycle, but at the same time resembling as close as possible the physiological conditions, is needed. This approach in a transgenic mouse model is a formidable challenge.

Expression of the transgenic tubulin is also going to be regulated by a complex cascade of mechanisms said to prevent expression of foreign DNA in cells. These mechanisms become more difficult to understand and interpret in the context of megakaryocytes. It has been known

and it has published before that expression of transgenic proteins in megakaryocytes do not follow the same rules as in other diploid cells. Seminal studies have shown that only a subset of megakaryocytes express the protein of interest<sup>126</sup>. The question why cells that they have exactly the same genetic component present with a viable level of expression of a transgenic protein is not well understood. This has been observed both in proteins that do not interfere or they are not directly responsible for cell cycle-associated steps but also it has been shown to occur in proteins that are grossly intact. A possible mechanism is postulated to occur through methylation of the promoter of the foreign DNA<sup>196</sup>. How megakaryocytes can recognize and attenuate expression of foreign DNA may be of interest in other future studies.

Integration of DNA in the Megakaryocyte genome is random in the fact that different founders were produced with the same results of none or very limited fluorescents points towards a mechanism that is not site and transgene copy specific but rather follows a sequence-specific attenuation. Given this complexity, we decided to employ a new transgenic approach composed by a very bright fluorescent that protein does not integrate in the microtubal network but rather it attached it decodes the cytoskeleton. This has been successfully used in another transgenic mouse model which visualized the cells of the skin. Was based on Ensconsin fused to GFP.

Ensconsin is a microtubule (MT) associated protein (MAP) with a molecular weight of 84 KDa. Ensconsin was extensively studied by Dr Bulinski and the name of the protein derived from the word 'Ensconce' denotes that a) binds tenaciously to MTs b) covers and protects MTs from depolymerization caused by calcium of cold temperature<sup>156</sup>.

Ensconsin was demonstrated to bind all polymerized MTs during all phases of the cell cycle. Ensconsin does not affect MT dynamics and does not modulate their function. The

microtubule binding domain of Ensconsin that includes its C-terminus is designated as EMTB (Ensconsin Microtubule Binding domain). EMTB exhibits the same characteristics as Ensconsin. Ensconsin or EMTB was fused to GFP but these constructs required high levels of expression in order to perform in vivo satisfactory visualization of microtubules<sup>157</sup>. A significant problem was that these high levels of expression caused formation of MT bundles (threshold > 200 molecules/ $\mu\text{m}$  MT) and also affected mitotic index. However when EMTB or Ensconsin were fused with up to 5 tandem GFP moieties the level of construct expression was reduced correlating with the number of GFP moieties fused to EMTB or Ensconsin (reviewed in <sup>157</sup>). Namely, the EMTB/ $\mu\text{m}$  MT ratio was reduced from 399 in GFP-EMTB to 107 in 3XGFP-EMTB. The lower expression of constructs with multiple GFP moieties linked to EMTB was beneficial because these constructs were not associated with disruption of the mitotic cycle or MT dynamics. The fluorescent intensity of the 2XGFP-EMTB up to 5XGFP-EMTB were comparable and brighter than the GFP-EMTB constructs. An additional benefit was that the extra GFP moieties reduced photo bleaching. The 5XGFP-EMTB appears to be the upper limit because the ratio of EMTB/ $\mu\text{M}$  MT of this molecule is very low and the bulky size of 5XGFP-EMTB may affect MT stability or MT dynamics<sup>154</sup>.

We propose to use 3XGFP-EMTB construct to generate a transgenic mouse that expression of 3xGFP-EMTB is targeted specifically to MKs. The 3XGFP-EMTB was used successfully in the generation of transgenic mouse model that visualized microtubules in keratinocytes<sup>147</sup>. The notion here is that even if the transgene is expressed in the low amounts the fluorescence should be strong enough to visualize megakarocyte.

We used the variant of 3 molecules attached to the protein decoding the reason being that studies showed that four and above can have a detrimental effect given the large molecular

size of the construct. Visualizing Megakarocytes using this approach and the attempts described before had to overcome the problem of identifying the living founders that not only have integrated DNA in their genome but also have functional expression. However identifying functional expression in Megakarocytes would necessitate the sacrifice of the founder and harvesting of the bone marrow and visualization of the Megakarocytes.

In order to avoid such a problem, and given the fact that tubulin from Megakarocytes is a key structural component of the platelets we devised a strategy which was described in materials and metals. In this strategy founders were retro-orbital bled and the small amount of blood was centrifuged and the platelets that constituted the supernatant were either visualized in the microscope or they were subject to FACS sorting and the level of GFP expression was compared against platelets derived from white-type mice that were bled at the same time and their blood was processed concurrently with the blood of the founders. By that way we were able to potentially detect which founders were expressing GFP tagged microtubules without sacrificing the founders. This approach may be used to screen for proteins that can be found in megakarocytes or are known to be packed into the platelets in other models without sacrificing the founders.

Given the diminished fluorescence of the 3XGFP-EMTB as manifested by platelet FACS and bone marrow a completely different strategy was employed and was based on the work of Kawamoto and colleagues<sup>197</sup>.

This research group has designated a transgenic mouse model where EGFP expression can be tissue specific based on an ingenious strategy employing the Cre recombinase promoter. There strategy was based on a transgenic mouse line that harbors the a construct where the powerful modified chicken B- actin promoter coupled with CMV-IE enhancer (CAG

promoter) drives the expression of Chlorophenicol reporter gene (CAT). Moreover, the CAT sequence is flanked by LoxP elements and is followed by the sequence of EGFP sequence. The construct denoted as CAG-CAT-EGFP was shown to express CAT gene in all tissues without detectable expression of EGFP. However, when this transgenic mouse line was crossed with a mouse line where CAG drives expression of Cre the excision of the LoxP element flanked CAT had as result the ubiquitous expression of EGFP apart from red blood cells and hair. Authors did not investigate the mechanism behind these findings or if there was expression in Megakaryocytes or platelets. A potential explanation of the above findings is that melanin and hemoglobin were masking the GFP fluorescence. Furthermore, the group succeeded in targeted expression of EGFP only in cells of epidermis by crossing the transgenic mouse line CAG-CAT-EGFP with the K5-Cre transgenic mouse line ( K5 is keratinocyte specific promoter). The construct has been used by other groups successfully. <sup>198</sup>

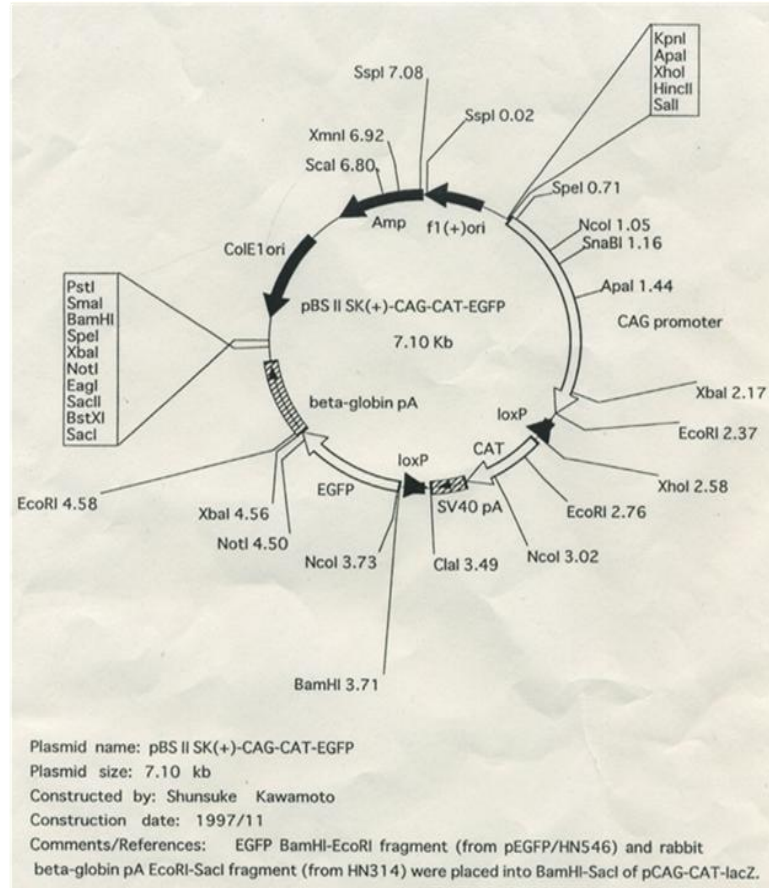
**Figure 32. Schematic representation of the CAG-CAT-EGFP plasmid.**

Panel A) Schematic representation of the plasmid that CAT is flanked by LoxP sites and is followed by EGFP gene sequence. The chicken beta actin promoter coupled with CMV iE enhancer drives expression of CAT or EGFP (the latter after recombination).

Panel B) Schematic representation of the construct following effect of Cre recombinase.

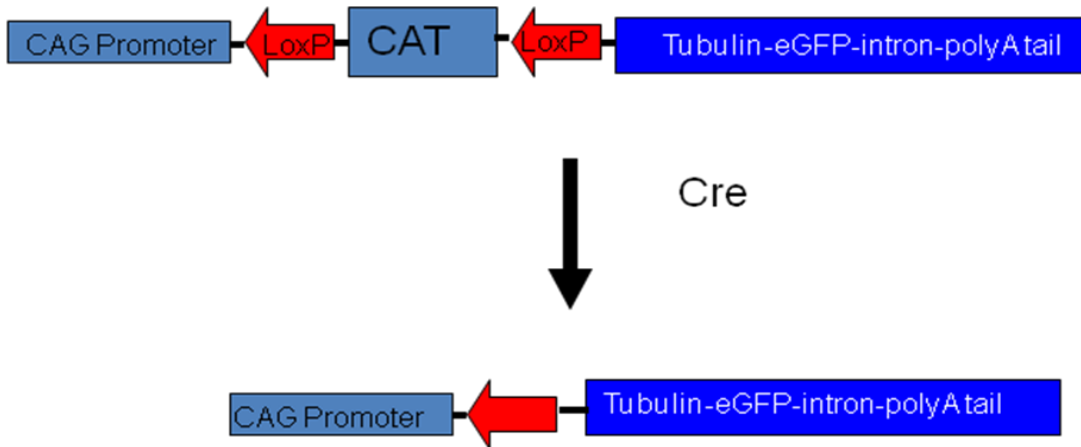
CAG stands for chicken  $\beta$ -actin promoter with CMV-IE enhancer.

CAT stands for Chlorophenicol Acetyltransferase gene.



Kawamoto et al, FEBS, vol 470 (2000)

A



B

Our proposed strategy is to create a transgenic mouse line which the above EGFP sequence will be replaced by a DNA sequence encoding EGFP-tubulin resulting in the generation of CAG-CAT-EGFP-tubulin. This transgenic mouse line is anticipated to express in all tissues Chloraphenicol including tail tissue. To this end identified founders harboring the construct can be easily screened for CAT expression by employing one of the several commercial assays that are available.

Founders of interest then can be crossed with the well characterized and commercially available PF4-Cre mouse in which PF4 drives expression of Cre. Tail DNA screening can be performed to identify mice that co express PF4-Cre and CAG-CAT-EGFP-tubulin. These mice will be expected to undergo excision of the LoxP flanked CAT only in Megakaryocytes and thus expression of EGFP tubulin will be promoted.

In viable mice that EGFP tubulin expression is not detrimental to the Megakaryocytes platelets could be screened for the presence of fluorescence.

Our model will be significant to delineate aspects of megakaryocyte life cycle and especially the biogenesis of platelets. There are several aspects of platelet ultrastructure and biogenesis that have not been elucidated and visualized and a mouse model offering this ability would be invaluable.



**Figure 33. Overview of the strategy to generate transgenic mice that expresses Tubulin –EGFP only on Megakaryocytes using a Cre recombinase approach.**

A schematic outline of the proposed strategy to create a transgenic mouse line with expression of tubulin EGFP targeted to Megakaryocytes.

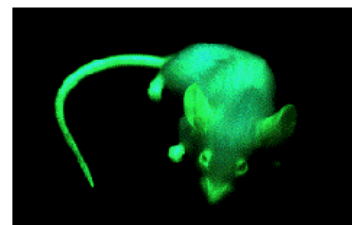
Inject construct → Pups are born → PCR Screening of founders → Founders determined → Screen tail tissue or MKs (F1) for CAT activity.



PF4-Cre

X Crossing with PF4-Cre mouse

→ PCR screening for double transgenic mouse



MK specific expression of EGFP-B1 tubulin

### **AIM III**

The pathways controlling endomitosis including cyclins in the study of megakaryocytes, as was summarized in the introduction, have been difficult to study. Cell lines that become endomitotic although they exist have abrogated the regulatory mechanisms that strictly control mitosis and as described it could lead to extrapolations that are not relevant to the wild type Megakaryocyte. It is important to select a system that would allow study of a Cyclin in the least disruptive manner for molecular mechanisms.

The generation of a transgenic mouse model where human Cyclin E is overexpressed in Megakaryocytes was instrumental for the study of Cyclin E in the context of polyploidy.

For example, it was known that in a knock out mice that both cyclins are abrogated only a very limited repertoire tissues are affected including megakaryocytes. However, the study of overexpression of Cyclin E was not pursued in hematopoietic primary cells. The available Cyclin E transgenic mice are tissue restricted and were studied in the context of malignancies. In our mouse model we present data that provide insight in the role of Cyclin E overexpression. As this project was divided here will discuss specific aspects of the project.

The use of Real time PCR to establish homogeneity is not common. Usually identification is based on the very laborious and time consuming Southern Blotting technique.

We used an approach where the Delta Delta approach to detect homozygotes versus heterozygotes or wild type mice. This approach was based on the calculation of transgene copies (in this case human Cyclin E) compared against a gene that is present as a single copy in the genome (we used A2b murine gene). The ease of an automated process such as Real time PCR led to identification of progeny in few hours compared to days. Although our

approach could identify wild type mice and heterozygotes from homozygotes it can not provide the exact number of copies of transgene in the genome of the transgenic mouse line. This approach has been adopted by our lab and has led to identification of homozygotes that were further validated by protein/functional assays.

BrdU assay also indicated that a higher fraction of cells are in the S phase in the unstimulated bone marrow of our transgenic megakaryocyte mouse line compared to that of wild type Megakaryocytes. The technical aspect of the experiment were challenging; too short the administration of BrdU suboptimal staining could occur. The more prolonged the incubation with BrdU the more cells would be stained but at the same time it could stain megakaryocytes that have undergone already S phase. These results support the finding that in freshly isolated bone marrow CyclinE overexpression leads to higher ploidy.

#### **AIM IV**

The majority of Megakaryocytes are cell cycle arrested and the mechanism that drives them from Go back to cycling are not well understood. The family of Polo-Like-Kinase (PLK) proteins has attracted attention in modulation of cell cycle but data regarding Megakaryocytes are scant. Interestingly, PLK1<sup>84,105</sup> has attracted attention in the context of Megakaryocytic endomitosis based on a study which demonstrated that PLK1 expression was decreased in mouse primary polyploid Megakaryocytes<sup>86</sup>. We focused our efforts on PLK3 as a previous study demonstrated that PLK3 modulates Cyclin E levels. Furthermore, it was detected in several megakaryocytic lines following stimulation with TPO or polyploidizing agents.

We also detected PLK3 expression in the megakaryocytic cell line Y-10 and also in enriched fractions of bone marrow cells selected for expression of CD41. We have shown in different studies that the purity of Megakaryocytes in the enriched fractions are high (~80%)<sup>11</sup>. Our data indicated that PLK3 is expressed on Megakaryocytes and that the gene expression is enhanced upon stimulation of TPO. Furthermore, we detected PLK3 expression in the vascular smooth muscle cells that become polyploidy as they age. These data support the notion that PLK3 is a gene affected by the endomitotic process.

PLK3 KO mice were reported to be viable, but they have a propensity to develop tumors at lung, kidney and liver after the first year of life<sup>116</sup>. PLK3 was shown in the same publication to act as tumor suppressor. However, PLK3 KO mice were shown in our preliminary studies and then published by others that they have no significant difference in ploidy compared to controls<sup>185</sup>. This points towards mechanisms that are redundant for entrance in the polyploidy. Intriguingly, the study of the other group demonstrated that the percentage of CD41 cells in the bone marrow of PLK3 mice is less compared to wild type and that the tail bleeding time is prolonged<sup>185</sup>.

## **AIM V**

We seek to elucidate the role of LOX-PP in the megakaryopoiesis. Using an antibody that recognizes the LOX-PP moiety we could detect LOX-PP in Megakaryocytes regardless of ploidy and the LOX-PP appeared to co-localize with microtubules. This co-localization may be important for mechanisms governing endomitosis. This was manifested by the reduction in ploidy of Megakaryocytes derived from bone marrow cell cultures treated with LOX-PP. The

mechanisms that could lead to inhibition of ploidy have not been elucidated but could include modulation of the ERK pathway<sup>199</sup> that has been shown to be important in Megakaryopoiesis<sup>200</sup>. An important element of this study was the finding that LOX-PP does not affect viability of bone marrow cultures or number of Megakaryocytes. Furthermore, in our pilot experiments overexpression of Cyclin E1 in megakaryocytes was not able to overcome the effect of LOX-PP in Polyploidization. This effect in polyploidy is reminiscent of Anagrelide<sup>201</sup> a medication used to treat Myeloproliferative neoplasms<sup>202,203</sup>.

Large clinical trials focusing on the treatment of Myeloproliferative neoplasms are limited, and treatments based on empirical reasoning are not uncommon. For ET and PV, the modalities currently in use<sup>202</sup>, which include Aspirin, Hydroxyurea, Busulphan, Chlorambucil and <sup>32</sup>P, lack a specific molecular target. The management of myelofibrosis is a clinical challenge with grim prognosis<sup>204</sup>. Stem cell transplantation, although potentially curative, is accompanied by significant mortality and morbidity.

Hence, it is not surprising that research is focused on modified/mutated genes in myelofibrosis patients. The discovery of the JAK2V617F mutation, although not fitting the BCR-ABL paradigm of the CML, drew attention to the development of targeted inhibitors of JAK2V617F. Several inhibitors are now in clinical trials with encouraging results, although myelosuppression and gastrointestinal side effects occur (recently reviewed in<sup>205</sup>). Other approaches include inhibition of the mTOR/AKT pathway<sup>206</sup> or Histone Deacetylase Complex<sup>207</sup>. In addition, inhibitors of the BCL-2<sup>208</sup>, BCL-XL, HSP90 and telomerase are under development..

An important study relating to JAK2 inhibitors is the Controlled Myelofibrosis Study with Oral JAK inhibitor Treatment (COMFORT)<sup>209,210</sup>. However, JAK2 inhibitors have been shown to

effective only as palliative agents<sup>205</sup> and therefore need to find other agents with little toxicity is needed in order to treat the Myeloproliferative Neoplasms associated with megakaryocytic proliferation<sup>211,212</sup>.

Our group has recently published<sup>213</sup> that LOX is produced in low ploidy Megakaryocytes and is absent in high ploidy and that although a specific inhibitor of LOX does not alter ploidy levels in Megakaryocytes induced a significant reduction in Myelofibrosis in a mouse model that recapitulates key aspects of myelofibrosis.

Taken together, LOX-PP and LOX may have an important therapeutic role in the context of Myeloproliferative Neoplasms<sup>214</sup>.

## Acknowledgments

I would like to thank of all members of Dr Ravid's lab for the help and assistance all this time. Especially, I would like to thank Alexia Aeliades and Shannon Carroll for their collaboration especially in real time PCR studies. Figures 9 and 16 were generated with the help of Shannon Carroll.

*Parts of the thesis are based on excerpts of the following publications. Original Copyright to the journals below.*

The JBC and Blood journal grant automatic permission to use articles in a thesis/dissertation. Permission to use material from Cell Cycle Journal was also granted for Ph.D thesis.

1. *Eliades A, Papadantonakis N, Ravid K. New roles for cyclin E in megakaryocytic polyploidization. J Biol Chem;285:18909-18917.*
2. *Papadantonakis N, Matsuura S, Ravid K. Megakaryocyte pathology and bone marrow fibrosis: the lysyl oxidase connection. Blood;120:1774-1781.*
3. *McCCrann DJ, Yezefski T, Nguyen HG, et al. Survivin overexpression alone does not alter megakaryocyte ploidy nor interfere with erythroid/megakaryocytic lineage development in transgenic mice. Blood. 2008;111:4092-4095.*
4. *Papadantonakis N, Makitalo M, McCrann DJ, et al. Direct visualization of the endomitotic cell cycle in living megakaryocytes: differential patterns in low and high ploidy cells. Cell Cycle. 2008;7:2352-2356.*
5. *Eliades A, Papadantonakis N, Bhupatiraju A, et al. Control of megakaryocyte expansion and bone marrow fibrosis by lysyl oxidase. J Biol Chem. 2011;286:27630-27638.*



## References

1. Ebbe. Biology of Megakaryocytes. *Progress in Hemost Thromb.* 1976;3:211-217.
2. Levine RF. Isolation and characterization of normal human megakaryocytes. *British Journal of Haematology.* 1980;45:487-497.
3. Levine RF, Hazzard KC, Lamberg JD. The significance of megakaryocyte size. *Blood.* 1982;60:1122-1131.
4. Szalai G LA, Watson DK. Molecular mechanisms of megakaryopoiesis. *Cell Mol Life Sci.* 2006;63:2460-2476.
5. Deutsch VR, Tomer A. Megakaryocyte development and platelet production. *British Journal of Haematology.* 2006;134:453-466.
6. Ravid K, Lu J, Zimmet JM, Jones MR. Roads to polyploidy: the megakaryocyte example. *J Cell Physiol.* 2002;190:7-20.
7. Goyannes-Villaescuca V. Ultrastructure of endomitosis in megakaryocytes. *Cell and Tissue Kinetics.* 1969;2:165.
8. Kuter DJ, Greenberg SM, Rosenberg RD. Analysis of megakaryocyte ploidy in rat bone marrow cultures. *Blood.* 1989;74:1952-1962.
9. McDonald TP, Sullivan PS. Megakaryocytic and erythrocytic cell lines share a common precursor cell. *Experimental Hematology.* 1993;21:1316-1320.
10. Goldfarb AN. Transcriptional control of megakaryocyte development. *Oncogene.* 2007;26:6795-6802.
11. Eliades A, Papadantonakis N, Ravid K. New roles for cyclin E in megakaryocytic polyploidization. *J Biol Chem;*285:18909-18917.
12. Wang Z, Zhang Y, Kamen D, Lees E, Ravid K. Cyclin D3 is essential for megakaryocytopoiesis. *Blood.* 1995;86:3783-3788.
13. McCrann DJ, Eliades A, Makitalo M, Matsuno K, Ravid K. Differential expression of NADPH oxidases in megakaryocytes and their role in polyploidy. *Blood.* 2009;114:1243-1249.
14. Bluteau D, Lordier L, Di Stefano A, et al. Regulation of megakaryocyte maturation and platelet formation. *J Thromb Haemost.* 2009;7 Suppl 1:227-234.
15. Geddis AE. Megakaryopoiesis. *Semin Hematol.* 2010;47:212-219.
16. Zheng C, Yang R, Han Z, Zhou B, Liang L, Lu M. TPO-independent megakaryocytopoiesis. *Crit Rev Oncol Hematol.* 2008;65:212-222.
17. Kuter DJ, Gminski DM, Rosenberg RD. Transforming growth factor beta inhibits megakaryocyte growth and endomitosis. *Blood.* 1992;79:619-626.
18. Long MW. Cyclins and cell division kinases in megakaryocytic endomitosis. *Comptes Rendus de l Academie des Sciences - Serie Iii, Sciences de la Vie.* 1995;318:649-654.
19. Takada M, Morii N, Kumagai S, Ryo R. The involvement of the rho gene product, a small molecular weight GTP-binding protein, in polyploidization of a human megakaryocytic cell line, CMK. *Experimental Hematology.* 1996;24:524-530.
20. Iancu-Rubin C, Nasrallah CA, Atweh GF. Stathmin prevents the transition from a normal to an endomitotic cell cycle during megakaryocytic differentiation. *Cell Cycle.* 2005;4:1774-1782.
21. Gurney AL, Wong SC, Henzel WJ, de Sauvage FJ. Distinct regions of c-Mpl cytoplasmic domain are coupled to the JAK-STAT signal transduction pathway and Shc

phosphorylation. *Proceedings of the National Academy of Sciences of the United States of America*. 1995;92:5292-5296.

22. Schulze H, Shivdasani RA. Mechanisms of thrombopoiesis. *Journal of Thrombosis and Haemostasis*. 2005;3:1717-1724.
23. Tajika K, Nakamura H, Nakayama K, Dan K. Thrombopoietin can influence mature megakaryocytes to undergo further nuclear and cytoplasmic maturation. *Exp Hematol*. 2000;28:203-209.
24. Wang Q, Miyakawa Y, Fox N, Kaushansky K. Interferon-alpha directly represses megakaryopoiesis by inhibiting thrombopoietin-induced signaling through induction of SOCS-1. *Blood*. 2000;96:2093-2099.
25. Hama A, Muramatsu H, Makishima H, et al. Molecular lesions in childhood and adult acute megakaryoblastic leukaemia. *Br J Haematol*;156:316-325.
26. Lippert E, Boissinot M, Kralovics R, et al. The JAK2-V617F mutation is frequently present at diagnosis in patients with essential thrombocythemia and polycythemia vera. *Blood*. 2006;108:1865-1867.
27. Mercher T, Wernig G, Moore SA, et al. JAK2T875N is a novel activating mutation that results in myeloproliferative disease with features of megakaryoblastic leukemia in a murine bone marrow transplantation model. *Blood*. 2006;108:2770-2779.
28. Vainchenker W, Dusa A, Constantinescu SN. JAKs in pathology: role of Janus kinases in hematopoietic malignancies and immunodeficiencies. *Semin Cell Dev Biol*. 2008;19:385-393.
29. Raslova H, Baccini V, Loussaief L, et al. Mammalian target of rapamycin (mTOR) regulates both proliferation of megakaryocyte progenitors and late stages of megakaryocyte differentiation. *Blood*. 2006;107:2303-2310.
30. Hitchcock IS, Fox NE, Prevost N, Sear K, Shattil SJ, Kaushansky K. Roles of focal adhesion kinase (FAK) in megakaryopoiesis and platelet function: studies using a megakaryocyte lineage specific FAK knockout. *Blood*. 2008;111:596-604.
31. McInerney JM, Nemeth MJ, Lowrey CH. Erythropoiesis: Review Article: Slow and Steady Wins The Race? Progress in the Development of Vectors for Gene Therapy of beta-Thalassemia and Sickle Cell Disease. *Hematology*. 2000;4:437-455.
32. Gold P. The control of erythropoiesis: a review. *McGill Med J*. 1960;29:129-140.
33. Keerthivasan G, Liu H, Gump JM, Dowdy SF, Wickrema A, Crispino JD. A novel role for survivin in erythroblast enucleation. *Haematologica*.
34. Leung CG, Xu Y, Mularski B, Liu H, Gurbuxani S, Crispino JD. Requirements for survivin in terminal differentiation of erythroid cells and maintenance of hematopoietic stem and progenitor cells. *J Exp Med*. 2007;204:1603-1611.
35. Brass LF. Did dinosaurs have megakaryocytes? New ideas about platelets and their progenitors. *J Clin Invest*. 2005;115:3329-3331.
36. Klement GL, Yip TT, Cassiola F, et al. Platelets actively sequester angiogenesis regulators. *Blood*. 2009;113:2835-2842.
37. Patel-Hett S, Richardson JL, Schulze H, et al. Visualization of microtubule growth in living platelets reveals a dynamic marginal band with multiple microtubules. *Blood*. 2008;111:4605-4616.
38. Forestier F, Daffos F, Catherine N, Renard M, Andreux JP. Developmental hematopoiesis in normal human fetal blood. *Blood*. 1991;77:2360-2363.

39. Debili N, Coulombel L, Croisille L, et al. Characterization of a bipotent erythromegakaryocytic progenitor in human bone marrow. *Blood*. 1996;88:1284-1296.
40. Jackson H, Williams N, Bertocello I, Green R. Classes of primitive murine megakaryocytic progenitor cells. *Exp Hematol*. 1994;22:954-958.
41. Bruno E, Murray LJ, DiGiusto R, Mandich D, Tsukamoto A, Hoffman R. Detection of a primitive megakaryocyte progenitor cell in human fetal bone marrow. *Exp Hematol*. 1996;24:552-558.
42. Briddell RA, Brandt JE, Straneva JE, Srouf EF, Hoffman R. Characterization of the human burst-forming unit-megakaryocyte. *Blood*. 1989;74:145-151.
43. Yu M, Cantor AB. Megakaryopoiesis and thrombopoiesis: an update on cytokines and lineage surface markers. *Methods Mol Biol*;788:291-303.
44. Tomer A. Human marrow megakaryocyte differentiation: multiparameter correlative analysis identifies von Willebrand factor as a sensitive and distinctive marker for early (2N and 4N) megakaryocytes. *Blood*. 2004;104:2722-2727.
45. Pronk CJ, Rossi DJ, Mansson R, et al. Elucidation of the phenotypic, functional, and molecular topography of a myeloerythroid progenitor cell hierarchy. *Cell Stem Cell*. 2007;1:428-442.
46. Kuter DJ, Begley CG. Recombinant human thrombopoietin: basic biology and evaluation of clinical studies. *Blood*. 2002;100:3457-3469.
47. Kaushansky K, Drachman JG. The molecular and cellular biology of thrombopoietin: the primary regulator of platelet production. *Oncogene*. 2002;21:3359-3367.
48. Solar GP, Kerr WG, Zeigler FC, et al. Role of c-mpl in early hematopoiesis. *Blood*. 1998;92:4-10.
49. Stoffel R, Wiestner A, Skoda RC. Thrombopoietin in thrombocytopenic mice: evidence against regulation at the mRNA level and for a direct regulatory role of platelets. *Blood*. 1996;87:567-573.
50. Wolber EM, Fandrey J, Frackowski U, Jelkmann W. Hepatic thrombopoietin mRNA is increased in acute inflammation. *Thromb Haemost*. 2001;86:1421-1424.
51. Peck-Radosavljevic M, Wichlas M, Zacherl J, et al. Thrombopoietin induces rapid resolution of thrombocytopenia after orthotopic liver transplantation through increased platelet production. *Blood*. 2000;95:795-801.
52. Kaushansky K. Molecular mechanisms of thrombopoietin signaling. *J Thromb Haemost*. 2009;7 Suppl 1:235-238.
53. Alexander WS, Dunn AR. Structure and transcription of the genomic locus encoding murine c-Mpl, a receptor for thrombopoietin. *Oncogene*. 1995;10:795-803.
54. Wendling F, Maraskovsky E, Debili N, et al. cMpl ligand is a humoral regulator of megakaryocytopoiesis. *Nature*. 1994;369:571-574.
55. Bartley TD, Bogenberger J, Hunt P, et al. Identification and cloning of a megakaryocyte growth and development factor that is a ligand for the cytokine receptor Mpl. *Cell*. 1994;77:1117-1124.
56. Kuter DJ. New thrombopoietic growth factors. *Blood*. 2007;109:4607-4616.
57. Feese MD, Tamada T, Kato Y, et al. Structure of the receptor-binding domain of human thrombopoietin determined by complexation with a neutralizing antibody fragment. *Proc Natl Acad Sci U S A*. 2004;101:1816-1821.

58. Fox N, Priestley G, Papayannopoulou T, Kaushansky K. Thrombopoietin expands hematopoietic stem cells after transplantation. *J Clin Invest.* 2002;110:389-394.
59. Goncalves F, Lacout C, Villeval JL, Wendling F, Vainchenker W, Dumenil D. Thrombopoietin does not induce lineage-restricted commitment of Mpl-R expressing pluripotent progenitors but permits their complete erythroid and megakaryocytic differentiation. *Blood.* 1997;89:3544-3553.
60. Ito T, Ishida Y, Kashiwagi R, Kuriya S. Recombinant human c-Mpl ligand is not a direct stimulator of proplatelet formation in mature human megakaryocytes. *Br J Haematol.* 1996;94:387-390.
61. Jackson CW, Steward SA, Chenaille PJ, Ashmun RA, McDonald TP. An analysis of megakaryocytopoiesis in the C3H mouse: an animal model whose megakaryocytes have 32N as the modal DNA class. *Blood.* 1990;76:690-696.
62. Song C, Liu S, Xiao J, et al. Polyploid organisms. *Sci China Life Sci;*55:301-311.
63. Comai L. The advantages and disadvantages of being polyploid. *Nat Rev Genet.* 2005;6:836-846.
64. MacAuley A, Cross JC, Werb Z. Reprogramming the cell cycle for endoreduplication in rodent trophoblast cells. *Molecular Biology of the Cell.* 1998;9:795-807.
65. Jones MR, Ravid K. Vascular smooth muscle polyploidization as a biomarker for aging and its impact on differential gene expression. *J Biol Chem.* 2004;279:5306-5313.
66. McCrann DJ, Nguyen HG, Jones MR, Ravid K. Vascular smooth muscle cell polyploidy: An adaptive or maladaptive response? *J Cell Physiol.* 2008.
67. Vitrat NS, Le Couedic JP, Pique C, Debili N, Vainchenker W. Megakaryocyte endomitosis are really abortive mitosis. *Blood.* 1996;88:abst. 1135.
68. Roy L, Coullin P, Vitrat N, et al. Asymmetrical segregation of chromosomes with a normal metaphase/anaphase checkpoint in polyploid megakaryocytes. *Blood.* 2001;97:2238-2247.
69. Zhang Y, Wang Z, Ravid K. The cell cycle in polyploid megakaryocytes is associated with reduced activity of cyclin B1-dependent cdc2 kinase. *Journal of Biological Chemistry.* 1996;271:4266-4272.
70. Geddis AE, Kaushansky K. Endomitotic megakaryocytes form a midzone in anaphase but have a deficiency in cleavage furrow formation. *Cell Cycle.* 2006;5:538-545.
71. Odell TT, Jackson CW, Reiter RS. Generation cycle of rat megakaryocytes. *Experimental Cell Research.* 1968;53:3231-3238.
72. Crow CE, Fox NE, Kaushansky K. Kinetics of endomitosis in primary murine megakaryocytes. *J Cell Physiol.* 2001;188:291-303.
73. Hook SS, Lin JJ, Dutta A. Mechanisms to control rereplication and implications for cancer. *Curr Opin Cell Biol.* 2007;19:663-671.
74. Machida YJ, Dutta A. Cellular checkpoint mechanisms monitoring proper initiation of DNA replication. *J Biol Chem.* 2005;280:6253-6256.
75. L MR. Tetraploidy and tumor development. *Cancer Cell.* 2005;8:353-354.
76. Coqueret O. Linking cyclins to transcriptional control. *GENE.* 2002;299:35-55.
77. Kato JY. Control of G1 progression by D-type cyclins: key event for cell proliferation. *Leukemia.* 1997;11 Suppl 3:347-351.

78. Prosperi E, Stivala LA, Scovassi AI, Bianchi L. Cyclins: relevance of subcellular localization in cell cycle control. *Eur J Histochem*. 1997;41:161-168.
79. Grana X, Reddy EP. Cell cycle control in mammalian cells: role of cyclins, cyclin dependent kinases (CDKs), growth suppressor genes and cyclin-dependent kinase inhibitors (CKIs). *Oncogene*. 1995;11:211-219.
80. Wang Z, Zimmet J, Sasaki H, Ravid L. Transcriptional activity of the cyclin D3 gene is upregulated by thrombopoietin. *Blood*. 1996;88:195a.
81. Sun S, Zimmet M, Toselli P, Thompson A, Jackson W, Ravid K. Overexpression of cyclin D1 moderately increases ploidy in megakaryocytes. *Hematologica*. 2001;86:17-23.
82. Zhang Y, Wang Z, Liu DX, Pagano M, Ravid K. Ubiquitin-dependent degradation of cyclin B is accelerated in polyploid megakaryocytes. *Journal of Biological Chemistry*. 1998;273:1387-1392.
83. Takai N, Hamanaka R, Yoshimatsu J, Miyakawa I. Polo-like kinases (Plks) and cancer. *Oncogene*. 2005;24:287-291.
84. Petronczki M, Lenart P, Peters JM. Polo on the Rise-from Mitotic Entry to Cytokinesis with Plk1. *Dev Cell*. 2008;14:646-659.
85. Hansen DV, Loktev AV, Ban KH, Jackson PK. Plk1 regulates activation of the anaphase promoting complex by phosphorylating and triggering SCFbetaTrCP-dependent destruction of the APC Inhibitor Emi1. *Mol Biol Cell*. 2004;15:5623-5634.
86. Yagi M, Roth GJ. Megakaryocyte polyploidization is associated with decreased expression of polo-like kinase (PLK). *J Thromb Haemost*. 2006;4:2028-2034.
87. Geddis AE, Fox NE, Tkachenko E, Kaushansky K. Endomitotic megakaryocytes that form a bipolar spindle exhibit cleavage furrow ingression followed by furrow regression. *Cell Cycle*. 2007;6:455-460.
88. Lordier L, Jalil A, Aurade F, et al. Megakaryocyte endomitosis is a failure of late cytokinesis related to defects in the contractile ring and Rho/Rock signaling. *Blood*. 2008.
89. Zimmet J, Toselli P, Ravid K. Cyclin D3 and megakaryocyte development: exploration of a transgenic phenotype. *Stem Cells*. 1998;16:97-106.
90. Knoblich JA, Sauer K, Jones L, Richardson H, Saint R, Lehner CF. Cyclin E controls S phase progression and its down-regulation during *Drosophila* embryogenesis is required for the arrest of cell proliferation. *Cell*. 1994;77:107-120.
91. Duronio RJ, Brook A, Dyson N, O'Farrell PH. E2F-induced S phase requires cyclin E. *Genes Dev*. 1996;10:2505-2513.
92. Ohtsubo M, Theodoras AM, Schumacher J, Roberts JM, Pagano M. Human cyclin E, a nuclear protein essential for the G1-to-S phase transition. *Mol Cell Biol*. 1995;15:2612-2624.
93. Moroy T, Geisen C. Cyclin E. *Int J Biochem Cell Biol*. 2004;36:1424-1439.
94. Zhang HS, Gavin M, Dahiya A, et al. Exit from G1 and S phase of the cell cycle is regulated by repressor complexes containing HDAC-Rb-hSWI/SNF and Rb-hSWI/SNF. *Cell*. 2000;101:79-89.
95. Geng Y, Yu Q, Sicinska E, et al. Cyclin E Ablation in the Mouse. *Cell*. 2003;114:431-443.
96. Keck JM, Summers MK, Tedesco D, et al. Cyclin E overexpression impairs progression through mitosis by inhibiting APCCdh1. *J Cell Biol*. 2007;178:371-385.

97. Bortner DM, Rosenberg MP. Induction of mammary gland hyperplasia and carcinomas in transgenic mice expressing human cyclin E. *Mol Cell Biol.* 1997;17:453-459.
98. Freemantle SJ, Dmitrovsky E. Cyclin E transgenic mice: discovery tools for lung cancer biology, therapy, and prevention. *Cancer Prev Res (Phila)*;3:1513-1518.
99. Nguyen HG, Ravid K. Tetraploidy/aneuploidy and stem cells in cancer promotion: The role of chromosome passenger proteins. *J Cell Physiol.* 2006;208:12-22.
100. Zhang Y, Nagata Y, Yu G, et al. Aberrant quantity and localization of Aurora-B/AIM-1 and survivin during megakaryocyte polyploidization and the consequences of Aurora-B/AIM-1-deregulated expression. *Blood.* 2004;103:3717-3726.
101. McCrann DJ, Yezefski T, Nguyen HG, et al. Survivin overexpression alone does not alter megakaryocyte ploidy nor interfere with erythroid/megakaryocytic lineage development in transgenic mice. *Blood.* 2008;111:4092-4095.
102. Wen Q, Leung C, Huang Z, et al. Survivin is not required for the endomitotic cell cycle of megakaryocytes. *Blood.* 2009;114:153-156.
103. Cox BD, Natarajan M, Stettner MR, Gladson CL. New concepts regarding focal adhesion kinase promotion of cell migration and proliferation. *J Cell Biochem.* 2006;99:35-52.
104. Patel SR, Hartwig JH, Italiano JE, Jr. The biogenesis of platelets from megakaryocyte proplatelets. *J Clin Invest.* 2005;115:3348-3354.
105. van Vugt MA, van de Weerd BC, Vader G, et al. Polo-like kinase-1 is required for bipolar spindle formation but is dispensable for anaphase promoting complex/Cdc20 activation and initiation of cytokinesis. *J Biol Chem.* 2004;279:36841-36854.
106. van de Weerd BC, Medema RH. Polo-like kinases: a team in control of the division. *Cell Cycle.* 2006;5:853-864.
107. Li B, Ouyang B, Pan H, et al. Prk, a cytokine-inducible human protein serine/threonine kinase whose expression appears to be down-regulated in lung carcinomas. *J Biol Chem.* 1996;271:19402-19408.
108. Huang X, Ruan Q, Fang Y, Traganos F, Darzynkiewicz Z, Dai W. Physical and functional interactions between mitotic kinases during polyploidization and megakaryocytic differentiation. *Cell Cycle.* 2004;3:946-951.
109. Holtrich U, Wolf G, Yuan J, et al. Adhesion induced expression of the serine/threonine kinase Fnk in human macrophages. *Oncogene.* 2000;19:4832-4839.
110. Kauselmann G, Weiler, M., Wulff, P., Jessberger, S., Konietzko, U., Scafidi, J., Stabubli, U., Bereiter-Hahn, J., Strebhardt, K., Kuhl, D. The polo-like protein kinases Fnk and Snk associate with a Ca(2+)-and integrin-binding protein and are regulated dynamically with a synaptic plasticity. *EMBO J.* 1999;18:5528-5539.
111. Zimmerman WC, Erikson RL. Finding Plk3. *Cell Cycle.* 2007;6:1314-1318.
112. Zimmerman WC, Erikson RL. Polo-like kinase 3 is required for entry into S phase. *Proc Natl Acad Sci U S A.* 2007;104:1847-1852.
113. Grim JE, Gustafson MP, Hirata RK, et al. Isoform- and cell cycle-dependent substrate degradation by the Fbw7 ubiquitin ligase. *J Cell Biol.* 2008;181:913-920.
114. Welcker M, Clurman BE. FBW7 ubiquitin ligase: a tumour suppressor at the crossroads of cell division, growth and differentiation. *Nat Rev Cancer.* 2008;8:83-93.
115. Singer JD, Gurian-West M, Clurman B, Roberts JM. Cullin-3 targets cyclin E for ubiquitination and controls S phase in mammalian cells. *Genes Dev.* 1999;13:2375-2387.

116. Yang Y, Bai J, Shen R, et al. Polo-like kinase 3 functions as a tumor suppressor and is a negative regulator of hypoxia-inducible factor-1 alpha under hypoxic conditions. *Cancer Res.* 2008;68:4077-4085.
117. Straight AF, Field CM. Microtubules, membranes and cytokinesis. *Curr Biol.* 2000;10:R760-770.
118. Machida YJ, Hamlin JL, Dutta A. Right place, right time, and only once: replication initiation in metazoans. *Cell.* 2005;123:13-24.
119. C. Kotwaliwale SB. Microtubule Capture: A Concerted Effort. . *Cell.* 2006;127:1105-1108.
120. Hoffmann I. Protein kinases involved in mitotic spindle checkpoint regulation. *Results Probl Cell Differ.* 2006;42:93-109.
121. Khmelinskii A, Schiebel E. Assembling the spindle midzone in the right place at the right time. *Cell Cycle.* 2008;7:283-286.
122. Musacchio A. Spindle assembly checkpoint: the third decade. *Philos Trans R Soc Lond B Biol Sci;*366:3595-3604.
123. Geddis AE, Linden HM, Kaushansky K. Thrombopoietin: a pan-hematopoietic cytokine. *Cytokine Growth Factor Rev.* 2002;13:61-73.
124. Schmitt A, Guichard J, Masse JM, Debili N, Cramer EM. Of mice and men: comparison of the ultrastructure of megakaryocytes and platelets. *Exp Hematol.* 2001;29:1295-1302.
125. Mattia G, Vulcano F, Milazzo L, et al. Different ploidy levels of megakaryocytes generated from peripheral or cord blood CD34+ cells are correlated with different levels of platelet release. *Blood.* 2002;99:888-897.
126. Zhang J, Varas F, Stadtfeld M, Heck S, Faust N, Graf T. CD41-YFP mice allow in vivo labeling of megakaryocytic cells and reveal a subset of platelets hyperreactive to thrombin stimulation. *Exp Hematol.* 2007;35:490-499.
127. Maione TE, Gray GS, Petro J, et al. Inhibition of angiogenesis by recombinant human platelet factor-4 and related peptides. *Science.* 1990;247:77-79.
128. Deuel TF, Senior RM, Chang D, Griffin GL, Heinrikson RL, Kaiser ET. Platelet factor 4 is chemotactic for neutrophils and monocytes. *Proc Natl Acad Sci U S A.* 1981;78:4584-4587.
129. Ryo R, Nakeff A, Huang SS, Ginsberg M, Deuel TF. New synthesis of a platelet-specific protein: platelet factor 4 synthesis in a megakaryocyte-enriched rabbit bone marrow culture system. *J Cell Biol.* 1983;96:515-520.
130. Ravid K, Beeler DL, Rabin MS, Ruley HE, Rosenberg RD. Selective Targeting of Gene Products with the Megakaryocyte Platelet Factor 4 Promoter. *PNAS.* 1991;88:1521-1525.
131. Nguyen HG, Yu G, Makitalo M, et al. Conditional overexpression of transgenes in megakaryocytes and platelets in vivo. *Blood.* 2005;106:1559-1564.
132. Gutierrez-Herrero S, Maia V, Gutierrez-Berzal J, et al. C3G transgenic mouse models with specific expression in platelets reveal a new role for C3G in platelet clotting through its GEF activity. *Biochim Biophys Acta;*1823:1366-1377.
133. Tabilio A, Pelicci PG, Vinci G, et al. Myeloid and megakaryocytic properties of K-562 cell lines. *Cancer Res.* 1983;43:4569-4574.

134. Ogura M, Morishima Y, Ohno R, et al. Establishment of a novel human megakaryoblastic leukemia cell line, MEG-01, with positive Philadelphia chromosome. *Blood*. 1985;66:1384-1392.
135. Datta NS, Williams JL, Caldwell J, Curry AM, Ashcraft EK, Long MW. Novel alterations in CDK1/cyclin B1 kinase complex formation occur during the acquisition of a polyploid DNA content. *Molecular Biology of the Cell*. 1996;7:209-223.
136. Hudson KM, Denko NC, Schwab E, Oswald E, Weiss A, Lieberman MA. Megakaryocytic cell line-specific hyperploidy by cytotoxic necrotizing factor bacterial toxins. *Blood*. 1996;88:3465-3473.
137. Conde I, Pabon D, Jayo A, Lastres P, Gonzalez-Manchon C. Involvement of ERK1/2, p38 and PI3K in megakaryocytic differentiation of K562 cells. *Eur J Haematol*;84:430-440.
138. Kaushansky K. The mpl ligand: molecular and cellular biology of the critical regulator of megakaryocyte development. *Stem Cells*. 1994;12:91-96; discussion 96-97.
139. Zeigler FC, de Sauvage F, Widmer HR, et al. In vitro megakaryocytopoietic and thrombopoietic activity of c-mpl ligand (TPO) on purified murine hematopoietic stem cells. *Blood*. 1994;84:4045-4052.
140. Banu N, Wang JF, Deng B, Groopman JE, Avraham H. Modulation of megakaryocytopoiesis by thrombopoietin: the c-Mpl ligand. *Blood*. 1995;86:1331-1338.
141. Nagata Y, Yoshinao M, Todokoro K. Thrombopoietin-induced polyploidization of bone marrow megakaryocytes is due to a unique regulatory mechanism in late mitosis. *The Journal of Cell Biology*. 1997;139:449-457.
142. T. K. Chromatin modifications and their function. *Cell*. 2007;128:693-705.
143. Nguyen HG, Yu G, Makitalo M, et al. Conditional overexpression of transgenes in megakaryocytes and platelets in vivo. *Blood*. 2005;106:1559-1564.
144. Kanda T SK, Wahl GM. Histone-GFP fusion protein enables sensitive analysis of chromosome dynamics in living mammalian cells. *Curr Biol*. 1998;8:377-385.
145. Stuart T. Fraser A-KHKESWOGKEAVJMEDMHB. Using a histone yellow fluorescent protein fusion for tagging and tracking endothelial cells in ES cells and mice. *genesis*. 2005;42:162-171.
146. Shaner NC, Steinbach PA, Tsien RY. A guide to choosing fluorescent proteins. *Nat Methods*. 2005;2:905-909.
147. Lechler T, Fuchs E. Desmoplakin: an unexpected regulator of microtubule organization in the epidermis. *J Cell Biol*. 2007;176:147-154.
148. Nowotschin S, Eakin GS, Hadjantonakis AK. Live-imaging fluorescent proteins in mouse embryos: multi-dimensional, multi-spectral perspectives. *Trends Biotechnol*. 2009;27:266-276.
149. Pratt T, Sharp L, Nichols J, Price DJ, Mason JO. Embryonic stem cells and transgenic mice ubiquitously expressing a tau-tagged green fluorescent protein. *Dev Biol*. 2000;228:19-28.
150. Papadantonakis N, Makitalo M, McCrann DJ, et al. Direct visualization of the endomitotic cell cycle in living megakaryocytes: differential patterns in low and high ploidy cells. *Cell Cycle*. 2008;7:2352-2356.
151. Nowotschin S, Hadjantonakis AK. Cellular dynamics in the early mouse embryo: from axis formation to gastrulation. *Curr Opin Genet Dev*;20:420-427.



152. Viotti M, Nowotschin S, Hadjantonakis AK. Afp::mCherry, a red fluorescent transgenic reporter of the mouse visceral endoderm. *genesis*;49:124-133.
153. Kimble M, Kuzmiak C, McGovern KN, de Hostos EL. Microtubule organization and the effects of GFP-tubulin expression in dictyostelium discoideum. *Cell Motil Cytoskeleton*. 2000;47:48-62.
154. Bulinski JC, Gruber D, Faire K, Prasad P, Chang W. GFP chimeras of E-MAP-115 (ensconsin) domains mimic behavior of the endogenous protein in vitro and in vivo. *Cell Struct Funct*. 1999;24:313-320.
155. Masson D, Kreis TE. Identification and molecular characterization of E-MAP-115, a novel microtubule-associated protein predominantly expressed in epithelial cells. *J Cell Biol*. 1993;123:357-371.
156. Bulinski JC, Bossler A. Purification and characterization of ensconsin, a novel microtubule stabilizing protein. *J Cell Sci*. 1994;107 ( Pt 10):2839-2849.
157. Faire K, Waterman-Storer CM, Gruber D, Masson D, Salmon ED, Bulinski JC. E-MAP-115 (ensconsin) associates dynamically with microtubules in vivo and is not a physiological modulator of microtubule dynamics. *J Cell Sci*. 1999;112 ( Pt 23):4243-4255.
158. Wuhr M, Obholzer ND, Megason SG, Detrich HW, 3rd, Mitchison TJ. Live imaging of the cytoskeleton in early cleavage-stage zebrafish embryos. *Methods Cell Biol*;101:1-18.
159. Kagan HM, Li W. Lysyl oxidase: properties, specificity, and biological roles inside and outside of the cell. *J Cell Biochem*. 2003;88:660-672.
160. Uzel MI, Scott IC, Babakhanlou-Chase H, et al. Multiple bone morphogenetic protein 1-related mammalian metalloproteinases process pro-lysyl oxidase at the correct physiological site and control lysyl oxidase activation in mouse embryo fibroblast cultures. *J Biol Chem*. 2001;276:22537-22543.
161. Bondareva A, Downey CM, Ayres F, et al. The lysyl oxidase inhibitor, beta-aminopropionitrile, diminishes the metastatic colonization potential of circulating breast cancer cells. *PLoS ONE*. 2009;4:e5620.
162. Kenyon NJ, Ward RW, Last JA. Airway fibrosis in a mouse model of airway inflammation. *Toxicol Appl Pharmacol*. 2003;186:90-100.
163. Keles G, Basoglu T, Yapici O, Cetinkaya BO, Acikgoz G, Firatli E. Periodontal & systemic bone changes in rats with experimental lathyrism. *Indian J Med Res*. 2006;123:541-546.
164. Gao S, Zhao Y, Kong L, et al. Cloning and characterization of the rat lysyl oxidase gene promoter: identification of core promoter elements and functional nuclear factor I-binding sites. *J Biol Chem*. 2007;282:25322-25337.
165. Lucero HA, Ravid K, Grimsby JL, et al. Lysyl oxidase oxidizes cell membrane proteins and enhances the chemotactic response of vascular smooth muscle cells. *J Biol Chem*. 2008;283:24103-24117.
166. Li PA, He Q, Cao T, et al. Up-regulation and altered distribution of lysyl oxidase in the central nervous system of mutant SOD1 transgenic mouse model of amyotrophic lateral sclerosis. *Brain Res Mol Brain Res*. 2004;120:115-122.
167. Erler JT, Giaccia AJ. Lysyl oxidase mediates hypoxic control of metastasis. *Cancer Res*. 2006;66:10238-10241.

168. Payne SL, Hendrix MJ, Kirschmann DA. Paradoxical roles for lysyl oxidases in cancer--a prospect. *J Cell Biochem.* 2007;101:1338-1354.
169. Payne SL, Fogelgren B, Hess AR, et al. Lysyl oxidase regulates breast cancer cell migration and adhesion through a hydrogen peroxide-mediated mechanism. *Cancer Res.* 2005;65:11429-11436.
170. Contente S, Yeh TJ, Friedman RM. Tumor suppressive effect of lysyl oxidase proenzyme. *Biochim Biophys Acta.* 2009;1793:1272-1278.
171. Palamakumbura AH, Jeay S, Guo Y, et al. The propeptide domain of lysyl oxidase induces phenotypic reversion of ras-transformed cells. *J Biol Chem.* 2004;279:40593-40600.
172. Csiszar K. Lysyl oxidases: a novel multifunctional amine oxidase family. *Prog Nucleic Acid Res Mol Biol.* 2001;70:1-32.
173. Hurtado PA, Vora S, Sume SS, et al. Lysyl oxidase propeptide inhibits smooth muscle cell signaling and proliferation. *Biochem Biophys Res Commun.* 2008;366:156-161.
174. Min C, Yu Z, Kirsch KH, et al. A loss-of-function polymorphism in the propeptide domain of the LOX gene and breast cancer. *Cancer Res.* 2009;69:6685-6693.
175. Zhao Y, Min C, Vora SR, Trackman PC, Sonenshein GE, Kirsch KH. The lysyl oxidase pro-peptide attenuates fibronectin-mediated activation of focal adhesion kinase and p130Cas in breast cancer cells. *J Biol Chem.* 2009;284:1385-1393.
176. Palamakumbura AH, Vora SR, Nugent MA, Kirsch KH, Sonenshein GE, Trackman PC. Lysyl oxidase propeptide inhibits prostate cancer cell growth by mechanisms that target FGF-2-cell binding and signaling. *Oncogene.* 2009.
177. Hayashi K, Fong KS, Mercier F, Boyd CD, Csiszar K, Hayashi M. Comparative immunocytochemical localization of lysyl oxidase (LOX) and the lysyl oxidase-like (LOXL) proteins: changes in the expression of LOXL during development and growth of mouse tissues. *J Mol Histol.* 2004;35:845-855.
178. Liu X, Zhao Y, Gao J, et al. Elastic fiber homeostasis requires lysyl oxidase-like 1 protein. *Nat Genet.* 2004;36:178-182.
179. Peinado H, Del Carmen Iglesias-de la Cruz M, Olmeda D, et al. A molecular role for lysyl oxidase-like 2 enzyme in snail regulation and tumor progression. *Embo J.* 2005;24:3446-3458.
180. Maki JM. Lysyl oxidases in mammalian development and certain pathological conditions. *Histol Histopathol.* 2009;24:651-660.
181. Raslova H, Kauffmann A, Sekkai D, et al. Interrelation between polyploidization and megakaryocyte differentiation: a gene profiling approach. *Blood.* 2007;109:3225-3234.
182. Piersma SR, Broxterman HJ, Kapci M, et al. Proteomics of the TRAP-induced platelet releasate. *J Proteomics.* 2009;72:91-109.
183. Zhu LJ, Altmann SW. mRNA and 18S-RNA coapplication-reverse transcription for quantitative gene expression analysis. *Anal Biochem.* 2005;345:102-109.
184. Myer DL, Bahassi el M, Stambrook PJ. The Plk3-Cdc25 circuit. *Oncogene.* 2005;24:299-305.
185. Kostyak J. CIB1 regulates Megakaryopoiesis. 2011.
186. Vora SR, Guo Y, Stephens DN, et al. Characterization of recombinant lysyl oxidase propeptide. *Biochemistry.* 49:2962-2972.

187. Geddis AE FN, Tkachenko E, Kaushansky K. Endomitotic megakaryocytes that form a bipolar spindle exhibit cleavage furrow ingression followed by furrow regression. *Cell Cycle*. 2007;6:455-460.
188. Vitrat N, Cohen-Solal K, Pique C, et al. Endomitosis of Human Megakaryocytes Are Due to Abortive Mitosis. *Blood*. 1998;91:3711-3723.
189. Zimmet JM, Ladd D, Jackson CW, Stenberg PE, Ravid K. A role for cyclin D3 in the endomitotic cell cycle. *Molecular and Cellular Biology*. 1997;17:7248-7259.
190. Leysi-Derilou Y, Robert A, Duchesne C, Garnier A, Boyer L, Pineault N. Polyploid megakaryocytes can complete cytokinesis. *Cell Cycle*;9:2589-2599.
191. Bornstein R, Garcia-Vela J, Gilsanz F, Auray C, Cales C. Cord blood megakaryocytes do not complete maturation, as indicated by impaired establishment of endomitosis and low expression of G1/S cyclins upon thrombopoietin-induced differentiation. *Br J Haematol*. 2001;114:458-465.
192. Lordier L, Jalil A, Aurade F, et al. Megakaryocyte endomitosis is a failure of late cytokinesis related to defects in the contractile ring and Rho/Rock signaling. *Blood*. 2008;112:3164-3174.
193. Gao Y, Smith E, Ker E, et al. Role of RhoA-specific guanine exchange factors in regulation of endomitosis in megakaryocytes. *Dev Cell*;22:573-584.
194. Lordier L, Bluteau D, Jalil A, et al. RUNX1-induced silencing of non-muscle myosin heavy chain IIB contributes to megakaryocyte polyploidization. *Nat Commun*;3:717.
195. Lordier L, Pan J, Naim V, et al. Presence of a defect in karyokinesis during megakaryocyte endomitosis. *Cell Cycle*;11:4385-4389.
196. Park CW, Kren BT, Largaespada DA, Steer CJ. DNA methylation of Sleeping Beauty with transposition into the mouse genome. *Genes Cells*. 2005;10:763-776.
197. Kawamoto S, Niwa H, Tashiro F, et al. A novel reporter mouse strain that expresses enhanced green fluorescent protein upon Cre-mediated recombination. *FEBS Lett*. 2000;470:263-268.
198. Nishikawa Y, Hirota F, Yano M, et al. Biphasic Aire expression in early embryos and in medullary thymic epithelial cells before end-stage terminal differentiation. *J Exp Med*;207:963-971.
199. Sato S, Trackman PC, Maki JM, Myllyharju J, Kirsch KH, Sonenshein GE. The Ras signaling inhibitor LOX-PP interacts with Hsp70 and c-Raf to reduce Erk activation and transformed phenotype of breast cancer cells. *Mol Cell Biol*;31:2683-2695.
200. Rojnuckarin P, Drachman JG, Kaushansky K. Thrombopoietin-induced activation of the mitogen-activated protein kinase (MAPK) pathway in normal megakaryocytes: role in endomitosis. *Blood*. 1999;94:1273-1282.
201. Mazur EM, Rosmarin AG, Sohl PA, Newton JL, Narendran A. Analysis of the mechanism of anagrelide-induced thrombocytopenia in humans. *Blood*. 1992;79:1931-1937.
202. Barosi G, Lupo L, Rosti V. Management of Myeloproliferative Neoplasms: From Academic Guidelines to Clinical Practice. *Curr Hematol Malig Rep*. 2012;7:50-56.
203. Vannucchi AM, Guglielmelli P, Tefferi A. Advances in understanding and management of myeloproliferative neoplasms. *CA Cancer J Clin*. 2009;59:171-191.
204. Vannucchi AM. Management of myelofibrosis. *Hematology Am Soc Hematol Educ Program*;2011:222-230.

205. Stein BL, Crispino JD, Moliterno AR. Janus kinase inhibitors: an update on the progress and promise of targeted therapy in the myeloproliferative neoplasms. *Curr Opin Oncol.* 2011;23:609-616.
206. Guglielmelli P, Barosi G, Rambaldi A, et al. Safety and efficacy of everolimus, a mTOR inhibitor, as single agent in a phase 1/2 study in patients with myelofibrosis. *Blood.* 2011;118:2069-2076.
207. Rambaldi A, Dellacasa CM, Finazzi G, et al. A pilot study of the Histone-Deacetylase inhibitor Givinostat in patients with JAK2V617F positive chronic myeloproliferative neoplasms. *Br J Haematol.* 2010;150:446-455.
208. Parikh SA, Kantarjian H, Schimmer A, et al. Phase II study of obatoclox mesylate (GX15-070), a small-molecule BCL-2 family antagonist, for patients with myelofibrosis. *Clin Lymphoma Myeloma Leuk.* 2010;10:285-289.
209. Harrison C, Kiladjian JJ, Al-Ali HK, et al. JAK inhibition with ruxolitinib versus best available therapy for myelofibrosis. *N Engl J Med.* 2012;366:787-798.
210. Verstovsek S, Mesa RA, Gotlib J, et al. A double-blind, placebo-controlled trial of ruxolitinib for myelofibrosis. *N Engl J Med.* 2012;366:799-807.
211. Ostojic A, Vrhovac R, Verstovsek S. Ruxolitinib for the treatment of myelofibrosis: its clinical potential. *Ther Clin Risk Manag;*8:95-103.
212. Pardanani A. Ruxolitinib for myelofibrosis therapy: current context, pros and cons. *Leukemia;*26:1449-1451.
213. Eliades A, Papadantonakis N, Bhupatiraju A, et al. Control of megakaryocyte expansion and bone marrow fibrosis by lysyl oxidase. *J Biol Chem.* 2011;286:27630-27638.
214. Papadantonakis N, Matsuura S, Ravid K. Megakaryocyte pathology and bone marrow fibrosis: the lysyl oxidase connection. *Blood;*120:1774-1781.